

Bremsstrahlung photon contributions to parton energy loss at high virtuality (Q^2) : a perturbative calculation at $\mathcal{O}(\alpha_s\alpha_{em})$

Amit Kumar^{1,*} and Gojko Vujanovic^{1,†}

¹*Department of Physics, University of Regina, Regina, SK S4S 0A2, Canada*

(Dated: February 11, 2025)

In this work, real photon production scattering rates from jet-medium interactions in the quark-gluon plasma (QGP) is perturbatively calculated using the higher-twist (HT) formalism. Focus is given towards real photon production from a highly virtual (and highly energetic) quark, taking into account heavy-quark mass scales [Phys. Rev. C 94, 054902 (2016)], fermion-boson conversion processes [Nucl. Phys. A 793, 128–170 (2007)], as well as coherence effects [Phys. Rev. C 105, 024908 (2022)]. A generalized factorization procedure, such as that used in e - A deep-inelastic scattering, is employed to derive an improved single-scattering medium-induced photon emission kernel that goes beyond the traditional in-medium gluon exchange approximation. Diagrams are classified based on the final state particles, and include four types of scattering kernels at $\mathcal{O}(\alpha_{em}\alpha_s)$ giving the following final states: (i) real photon and real quark, (ii) real photon and real gluon (iii) virtual photon corrections to quark-antiquark pair-production and (iv) virtual photon correction to quark-quark production. The collision-kernel, thus derived, includes full phase factors from all non-vanishing diagrams and complete second-order derivative terms in the transverse momentum gradient expansion. Moreover, the calculation includes heavy-quark mass effects, thus exploring heavy-quark energy loss. The in-medium parton distribution functions, and the related jet transport coefficients, have a hard transverse momentum dependence (of the emitted gluon or photon) present within the phase factor. It is observed that the jet transport coefficients resemble the transverse-momentum-dependent parton distribution functions.

I. INTRODUCTION

Ultra-relativistic heavy-ions collisions performed at the Relativistic Heavy-Ion Collider (RHIC) and the Large Hadron Collider (LHC) produce a deconfined state of quarks and gluons, called quark-gluon plasma (QGP). One of the primary goals of these collisions is to constrain properties of QGP, through, e.g., the modifications it imparts on high-energy jets and photons. In past decades, many observables have been proposed to constrain the parton energy loss, including high- p_T hadrons [1–5], single-inclusive jets [6–9], γ -triggered jets [10–12], γ -hadron correlation [13, 14], flow observables [15–17] and so on. The challenge is to describe multiple observables simultaneously. The JETSCAPE framework [18, 19] has emerged as a unified and modular framework comprehensively and simultaneously studying multiple observables, allowing to obtain novel constraints on parton energy loss. Parton energy-loss models, such as MATTER [20], LBT [20], and MARTINI [21] are based on medium-induced gluon bremsstrahlung kernel and have been implemented in the JETSCAPE framework. However, a comprehensive implementation of the multi-scale dynamics responsible for medium-induced photon bremsstrahlung computed in parton energy loss simulations is still lacking. This paper focuses on providing a comprehensive calculation of photon production from highly virtual quarks of all flavors.

As the electromagnetic coupling is much smaller than the strong coupling, electromagnetic radiation can leave the QGP as soon as it is produced and with negligible rescattering, thus carrying detailed information on the QGP state at production time. So far, two approaches have been considered for the real-photon production. Perturbative calculations at low virtualities require extensive resummations, to account for infrared behavior composed of Hard Thermal Loops [22] as well as the Landau-Pomeranchuk-Migdal effect [23, 24]. Electromagnetic radiation from the QGP has shown a remarkable convergence when going from leading [24] to next to leading order in perturbative QCD (pQCD) corrections [25], an observation that is not universal across all QGP-related observables. Indeed, perturbative calculations of the transport coefficient \hat{q} [26], encapsulating transverse momentum broadening of the high-energy partons traversing the QGP, show significant corrections when comparing leading order and next-to-leading order pQCD calculations, at typical QGP temperature scales reached in heavy-ion collisions. A recent comparison of the electromagnetic spectral function in perturbative, i.e. next-to-leading order (NLO) pQCD calculations [27], and non-perturbative [28] approaches shows remarkable reliability of thermal photon perturbative calculations, especially when higher temperatures are considered.

* Corresponding author: amit.kumar@uregina.ca

† Corresponding author: gojko.vujanovic@uregina.ca

Given this behavior of perturbative calculations of electromagnetic radiation, this work focuses on extending photon production rates by including additional sources of jet-medium real photon production. To date, phenomenological calculations of jet-medium photons [29, 30] only include electromagnetic production from nearly on-shell light mass partons. Of course, other photon sources, such as prompt photons [31], photons from the hydrodynamical evolution [32] and hadronic transport emissions [33] have been considered. In this contribution, focus is given towards calculating real photon production rates from highly virtual partons, specifically obtaining a photon production rate from highly virtual quarks of light and heavy flavors, through the higher-twist formalism, thus giving an in-medium correction to prompt photon production.¹

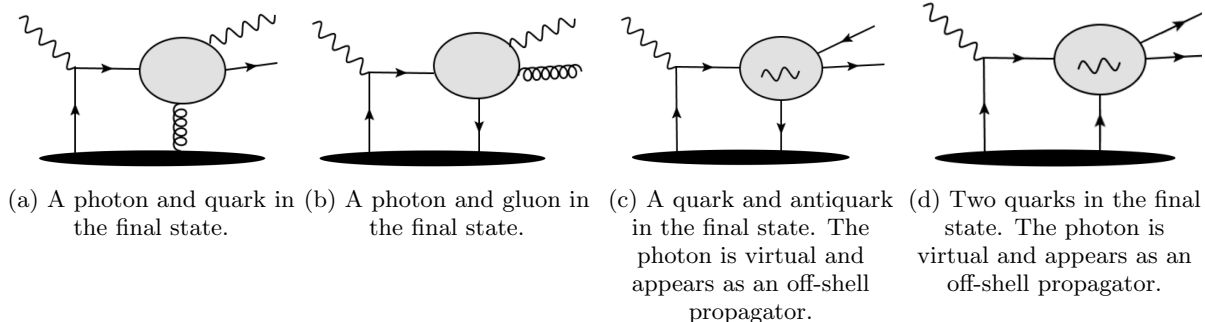


FIG. 1: Single scattering induced photon emission processes at next-to-leading order (NLO).

Schematically, photon production investigated herein stems from processes illustrated in Fig. 1. Using the higher-twist (HT) formalism in the single-scattering-induced radiation limit, real photon emission is present in Fig. 1 (a) and (b), while virtual photon corrections contributing the HT scattering kernel are considered for completeness in Fig. 1 (c,d). In addition to including photon emissions from heavy quarks, attention will also be given towards coherence effects [37] that were recently included in the context of gluon emissions from highly virtual quarks. The calculation herein will extend the results in Ref. [37, 38] by including additional interactions with in-medium partons depicted in Fig. 1 (b), (c) and (d). These will be referred to as Kumar-Vujanovic (KV) kernels.

II. HADRONIC TENSOR IN DEEP INELASTIC SCATTERING

The goal of this paper is to study the hadronic tensor in the context of deep-inelastic scattering between the energetic electron and the nucleus carrying mass number A . This study involves semi-inclusive production of photon (γ) together with scattered electron, along with the underlying remnant X , encapsulated in the equation below

$$e^-(\ell_{\text{in}}) + A(P) \rightarrow e^-(\ell_{\text{out}}) + \gamma(\ell_2) + X. \quad (1)$$

The difference of the outgoing (ℓ_{out}) and incoming (ℓ_{in}) electron momenta allows to define the virtual photon momentum q^μ — as illustrated in Fig. 2 — which is both highly energetic (i.e. a hard photon) and highly virtual. The study presented herein is carried out in the Breit frame, where the momentum of the virtual photon has the following form

$$\begin{aligned} q^\mu &\equiv \ell_{\text{out}}^\mu - \ell_{\text{in}}^\mu \\ &= [q^+, q^-, \mathbf{q}_\perp = \mathbf{0}_\perp] \\ &= \left[\frac{-Q^2}{2q^-}, q^-, 0, 0 \right], \end{aligned} \quad (2)$$

where $-Q^2 = q^2 = q^\mu q_\mu$. The connection between the light-cone coordinates and Cartesian coordinates is

$$[q^+, q^-, \mathbf{q}_\perp] = \left[\frac{q^0 + q^z}{\sqrt{2}}, \frac{q^0 - q^z}{\sqrt{2}}, \mathbf{q}_\perp \right], \quad (3)$$

¹ Note the Arnold-Moore-Yaffe (AMY) formalism [23, 34, 35], upon which jet-medium photon simulations [29, 30] were devised, has yet to be extended to include the mass scales of heavy quark flavors. A similar statement holds true for the next-to-leading order extension of the AMY formalism [25]. In the higher-twist formalism, heavy-quark mass scales have been taken into account only in the context of gluon radiation from a massive quark [36].

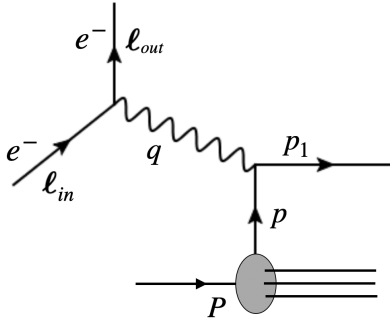


FIG. 2: A schematic diagram of deep-inelastic scattering between electron and a nucleon inside the nucleus. The virtual photon carries momentum q , whereas the struck quark carries momentum p . The nucleus momentum is $\mathcal{P} = AP$, where P is the momentum of the nucleon.

thus giving the expected $q^2 = 2q^+q^- - \mathbf{q}_\perp \cdot \mathbf{q}_\perp$.

In Fig. 2 the incoming virtual photon can strike light and heavy-quark flavors alike, both of which are considered herein. The nucleus momentum is labeled by \mathcal{P}^μ , the average momentum of the nucleon momentum is P^μ such that $\mathcal{P}^\mu = AP^\mu$, while the quark momentum is p^μ . The semi-inclusive cross section can be separated in a QED portion of the scattering and a QCD portion as

$$\ell_{\text{out}}^0 \frac{d^4\sigma}{d^3\ell_{\text{out}}dy} = \frac{\alpha_{\text{EM}}^2}{2\pi s} \frac{L_{\mu\nu}}{Q^4} \frac{dW^{\mu\nu}}{dy}. \quad (4)$$

The interesting QCD portion is encoded in $\frac{dW^{\mu\nu}}{dy}$, where $W^{\mu\nu}$ is the hadronic tensor. The rest of the expression consists of QED interaction and kinematics. More specifically, ℓ_{out}^0 is the energy of the outgoing electron, $s = (P + \ell_{\text{in}})^2$ is the usual Mandelstam variable, the QED leptonic tensor is given by $L^{\mu\nu} = \frac{1}{2} \text{Tr} [\ell_{\text{in}} \gamma^\mu \ell_{\text{out}} \gamma^\nu]$, while $\ell = \ell_\mu \gamma^\mu$ with γ^μ being the usual Dirac matrices. In the differential hadronic tensor, $\frac{dW^{\mu\nu}}{dy}$, y is the momentum fraction of the momentum of p_1 that will be carried away by the final-state photon produced within the reaction given in Eq. 1. The photon is involved in many mechanisms studied in subsequent sections, all of which follow a perturbative expansion scheme. The hard scale is given by $Q = \sqrt{-q^2} \gg \Lambda_{\text{QCD}}$ such that the q^+ and q^- components of the incoming virtual momentum are large — i.e. $\mathcal{O}(1)$ — giving $q^\mu \sim [\mathcal{O}(1), \mathcal{O}(1), \mathbf{0}_\perp]Q$. In this setup, the struck nucleon is traveling in positive z -direction and hence the struck quark has a very small $p^- \sim \lambda^2 Q$ momentum — where the dimensionless parameter λ is a small quantity $\lambda^2 \ll 1$ — while the large component is $p^+ \sim Q$, thus $p^\mu \sim [\mathcal{O}(1), \mathcal{O}(\lambda^2), \mathbf{0}_\perp]Q$. The momentum components of the quark after the scattering are organized as $p_1^\mu \sim [\mathcal{O}(\lambda^2), \mathcal{O}(1), \mathbf{0}_\perp]Q$.² Thus, λ is used to establish a perturbation series expansion.

Following the original deep inelastic scattering vertex depicted in Fig. 2, the produced quark with momentum p_1 is highly virtual and radiates regardless of whether a medium is present. In general, that radiation is included in the hadronic tensor ($W^{\mu\nu}$) given by

$$\begin{aligned} \frac{dW^{\mu\nu}}{dy} &= \frac{dW_0^{\mu\nu}}{dy} + \sum_{i=1,2} \frac{dW_i^{\mu\nu}}{dy} \\ &= \sum_q \int dx f_q^A(x) \mathcal{H}_0^{\mu\nu} \mathcal{K}_0 \\ &\quad + \sum_{i=1,2} \sum_q \int dx f_q^A(x) \mathcal{H}_i^{\mu\nu} \mathcal{K}_i, \end{aligned} \quad (5)$$

where $\frac{dW_0^{\mu\nu}}{dy}$ is the vacuum contribution to photon radiation, while the in-medium correction is encapsulated by $\sum_i \frac{dW_i^{\mu\nu}}{dy}$ and is depicted in Fig. 1.³ The first common factor for both vacuum and in-medium contributions is the

² Note that, $p_1^\mu = \left[\frac{M^2 - Q^2 + 2(p^+q^- - \frac{M^2}{2p^+} \frac{Q^2}{2q^-})}{2p_1^-}, p_1^-, \mathbf{0}_\perp \right]$, where M is the mass of the quark which is not neglected herein as $\frac{M}{Q} \sim \mathcal{O}(\lambda)$.

³ Only kernels 1 and 2 contribute to photon emission in Eq. (5), while kernel 3 and 4 are solely virtual corrections at $\mathcal{O}(\alpha_{\text{EM}}\alpha_s)$.

parton distribution function (PDF)

$$f_q^A(x) = A \int \frac{dy^-}{2\pi} \frac{e^{-ixp^+y^-}}{2} \langle P | \bar{\psi}(y^-) \gamma^+ \psi(0) | P \rangle, \quad (6)$$

giving the probability to find a quark of given flavor in the nucleus A with which the virtual photon can collide. The momentum fraction x carried by the struck quark is $x = p^+/P^+$, where p^+ is the first component of its momentum in light-cone coordinates, with P^+ is the corresponding momentum of the nucleon in the nucleus. The y^- variable in the PDF definition keeps track of the spacetime information of the $\langle P | \bar{\psi}(y^-) \gamma^+ \psi(0) | P \rangle$ expectation value in light-cone coordinates, and will play a more important role later.

The interaction between the quark from the PDF and the incoming virtual photon (with momentum q) is given by

$$\mathcal{H}_0^{\mu\nu} = \frac{e_q^2}{2} (2\pi) \delta[(q + xp)^2] \text{Tr} [\not{p} \gamma^\mu (\not{q} + xp) \gamma^\nu], \quad (7)$$

where $e_q = 2/3$ for up, charm, and top quarks, while being $e_q = -1/3$ for down, strange, and bottom quarks. The goal of the subsequent sections is to explore the functions \mathcal{K}_i , where \mathcal{K}_0 describes vacuum contributions, while $\mathcal{K}_{i=1,2,3,4}$ correspond to the in-medium interactions described in Fig. 1 (a) through (d), respectively.

Following the creation of the virtual quark with momentum p_1 , there is an emission of a photon with momentum ℓ_2 both in the vacuum (c.f. Fig. 3) as well as in the medium (c.f. Figs. 4, 6, 8, and 10). As can be seen in the latter figures, many possible gluon scatterings can affect photon radiation in a strongly interacting nuclear medium, each explored in a dedicated section. Therefore, our discussion is separated into two categories: vacuum photon radiation and medium-modified photon emission.

A. Single photon emission without in-medium scattering: the vacuum contribution

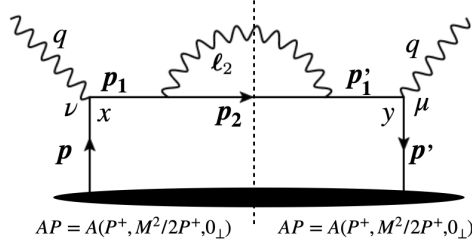


FIG. 3: Forward scattering diagram of leading order photon production. The cut-line (i.e. dashed line) represents the final state.

In the case where no medium is present, as shown in Fig. 3, the hadronic tensor is given by

$$\frac{dW_0^{\mu\nu}}{dy} = \sum_q \int dx f_q^A(x) \mathcal{H}_0^{\mu\nu} \mathcal{K}_0(\ell_{2,\perp}, y), \quad (8)$$

$$\mathcal{K}_0(\ell_{2,\perp}, y) = \int \frac{d\ell_{2,\perp}^2}{\ell_{2,\perp}^2} \frac{\alpha_{\text{EM}}}{2\pi} e_q^2 \left[\frac{1 + (1-y)^2}{y} \right], \quad (9)$$

a result which can be inferred from Refs. [39, 40], where the momentum fraction y is given by $y = \ell_2^-/p_1^-$. Any calculation of $W^{\mu\nu}$ proceeds by first obtaining the full T -matrix amplitude $T^{\mu\nu}$ of a given process before extracting the forward scattering limit using

$$W^{\mu\nu} = \frac{1}{2\pi} \text{Disc} [T^{\mu\nu}],$$

$$\text{Disc} [T^{\mu\nu}] \equiv -2\text{Im} [T^{\mu\nu}]. \quad (10)$$

The various components of the momentum $\ell_2^\mu = \left[\frac{\ell_1^2}{2yp_1^-}, yp_1^-, \ell_{\perp} \right]$ have different powers of the small scale λ , specifically $\ell_2^\mu \sim [\mathcal{O}(\lambda^2), \mathcal{O}(1), \mathcal{O}(\lambda), \mathcal{O}(\lambda)] Q$.⁴ The outgoing quark $p_2^\mu = \left[\frac{\ell_1^2 + M^2}{2(1-y)p_1^-}, (1-y)p^-, -\ell_{\perp} \right]$ scales as $p_2^\mu \sim [\mathcal{O}(\lambda^2), \mathcal{O}(1), \mathcal{O}(\lambda), \mathcal{O}(\lambda)] Q$ and takes into account that $p_2^2 = M^2$. Having established the result in the vacuum, along with providing details about the size of different contributions relative to the scale λ , the manner in which the nuclear environment affects the vacuum result is considered next.

B. Classification of in-medium single-scattering induced photon emission diagrams

The in-medium scattering kernels that contribute at $\mathcal{O}(\alpha_s \alpha_{em})$ are classified based on the identity of the particles in the final state. The first kind of kernel (\mathcal{K}_1) contains a real photon and a quark in the final state shown in Fig. 1 (a). In this kernel, the hard quark undergoes real photon emission and in-medium Glauber gluon scattering. There are a total of eight possible diagrams for this process and are shown in Fig. 4. Their calculation is discussed in Section III.

The second kind of kernel (\mathcal{K}_2) of interest consists of a real photon and real gluon emission with an in-medium Glauber quark exchange with the medium, as depicted in Fig. 1 (b). There are a total of six possible central cut diagrams, shown in Fig. 6 contributing to this kernel, which are discussed in Section IV.

The third kernel (\mathcal{K}_3) represents virtual photon corrections to single emission and single scattering kernel shown in Fig. 1 (c), comprising eight central cut diagrams illustrated in Fig. 8. Details of this calculation are presented in Section V.

The fourth kernel (\mathcal{K}_4) also represent virtual photon corrections but contains two quarks in the final state, see Fig. 1 (d). There are a total of four possible diagrams and they are discussed in Section VI.

III. SINGLE-SCATTERING INDUCED EMISSION: ONE PHOTON AND ONE QUARK IN THE FINAL STATE

Considered below are solely cases where the hard quark produced in the primary hard scattering undergoes a single photon emission and single Glauber gluon scattering with the nuclear medium, as depicted in Fig. 4. The (dashed) cut-line represents the final state and gives rise to a total of 8 diagrams. The full analytic calculation considering all possible diagrams is now presented, including complete phase factors and quark-mass effects. We performed the calculation in light-cone gauge $n \cdot A = A^- = 0$, where light-cone vector $n = [1, 0, \mathbf{0}_{\perp}]$, and the photon with four momentum X has a polarization tensor

$$d_{\mu\nu}^{(X)} = -g_{\mu\nu} + \frac{X_{\mu}n_{\nu} + n_{\mu}X_{\nu}}{n \cdot X}. \quad (11)$$

To illustrate the manner in which our results are obtained, we will present one calculation in great detail corresponding to the top left diagram in Fig. 4. All other diagrams are shown in Appendix A.

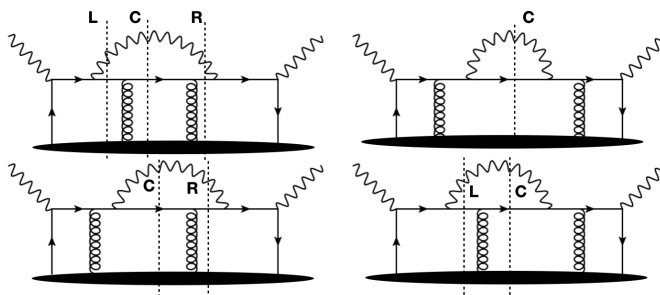


FIG. 4: Forward scattering diagrams for single photon emission with a single Glauber gluon scattering, giving a final state consisting of a real photon and a quark. These diagrams contribute to kernel-1. The cut-lines L, C, R represent the left-cut, the center-cut, and the right-cut, respectively.

⁴ The ℓ_2 photon is on-shell $\ell_2^2 = 0$ after the imaginary part of the T -matrix amplitude has been taken via Eq. 10.

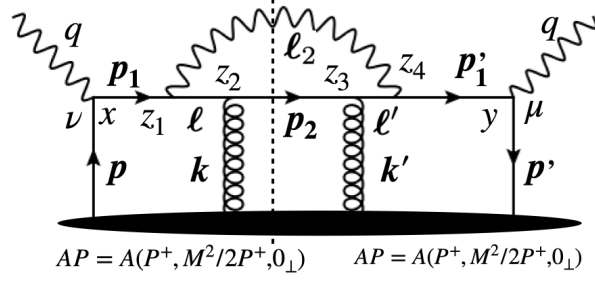


FIG. 5: A single scattering induced photon emission process at next-to-leading order for kernel-1.

The process shown in Fig. 5, where the hard quark undergoes bremsstrahlung photon radiation followed by in-medium Glauber gluon scattering, is now considered. The amplitude ($T_{1,c}^{\mu\nu}$) of the central-cut forward scattering diagram in Fig. 5 is

$$\begin{aligned}
T_{1,c}^{\mu\nu} &= e^2 e_q^2 g_s^2 \int d^4 y d^4 x d^4 z_1 d^4 z_2 d^4 z_3 d^4 z_4 e^{iq(y-x)} \langle AP | \bar{\psi}(y) \gamma^\mu \int \frac{d^4 p'_1}{(2\pi)^4} \frac{i(\not{p}'_1 + M)}{(p'^2_1 - M^2 + i\epsilon)} e^{-ip'_1(y-z_4)} \gamma^{\sigma_4} \\
&\times \int \frac{d^4 \ell'}{(2\pi)^4} \frac{i(\not{\ell}' + M)}{(\ell'^2 - M^2 + i\epsilon)} e^{-i\ell'(z_4-z_3)} \gamma^{\sigma_2} A_{\sigma_3}(z_3) \int \frac{d^4 p_2}{(2\pi)^4} \frac{i(\not{p}_2 + M)}{(p^2_2 - M^2 + i\epsilon)} e^{-ip_2(z_3-z_2)} \gamma^{\sigma_2} A_{\sigma_2}(z_2) \\
&\times \int \frac{d^4 \ell}{(2\pi)^4} \frac{i(\not{\ell} + M)}{(\ell^2 - M^2 + i\epsilon)} e^{-i\ell(z_2-z_1)} \gamma^{\sigma_1} \int \frac{d^4 p_1}{(2\pi)^4} \frac{i(\not{p}_1 + M)}{(p^2_1 - M^2 + i\epsilon)} e^{-ip_1(z_1-x)} \gamma^\nu \psi(x) | AP \rangle \\
&\times \int \frac{d^4 \ell_2}{(2\pi)^4} \frac{id_{\sigma_1 \sigma_4}^{(\ell_2)}}{(\ell_2^2 + i\epsilon)} e^{-i\ell_2(z_4-z_1)}.
\end{aligned} \tag{12}$$

The above equation is rearranged below to better highlight the operator structure. That is,

$$\begin{aligned}
T_{1,c}^{\mu\nu} &= e^2 e_q^2 g_s^2 \int d^4 x d^4 y d^4 z_1 d^4 z_2 d^4 z_3 d^4 z_4 \int \frac{d^4 p_1}{(2\pi)^4} \frac{d^4 p'_1}{(2\pi)^4} \frac{d^4 \ell}{(2\pi)^4} \frac{d^4 \ell'}{(2\pi)^4} \frac{d^4 \ell_2}{(2\pi)^4} \frac{d^4 p_2}{(2\pi)^4} \\
&\times e^{iy(q-p'_1)} e^{-ix(q-p_1)} e^{iz_1(\ell-p_1+\ell_2)} e^{iz_2(-\ell+p_2)} e^{iz_3(\ell'-p_2)} e^{iz_4(p'_1-\ell'-\ell_2)} \\
&\times \left\langle AP \left| \text{Tr} \left[\psi(x) \bar{\psi}(y) \gamma^\mu \frac{(\not{p}'_1 + M)}{(p'^2_1 - M^2 + i\epsilon)} \gamma^{\sigma_4} \frac{(\not{\ell}' + M)}{(\ell'^2 - M^2 + i\epsilon)} \gamma^{\sigma_3} A_{\sigma_3}(z_3) \right. \right. \right. \\
&\times \left. \frac{(\not{p}_2 + M)}{(p^2_2 - M^2 + i\epsilon)} \gamma^{\sigma_2} A_{\sigma_2}(z_2) \frac{(\not{\ell} + M)}{(\ell^2 - M^2 + i\epsilon)} \gamma^{\sigma_1} \frac{(\not{p}_1 + M)}{(p^2_1 - M^2 + i\epsilon)} \gamma^\nu \right] \left. \left. \right| AP \right\rangle \\
&\times \frac{d_{\sigma_4 \sigma_1}^{(\ell_2)}}{(\ell_2^2 + i\epsilon)}.
\end{aligned} \tag{13}$$

In order to separate out the perturbative and non-perturbative portions of this calculation, a power counting scheme is established. The incoming quark before primary scattering is moving in (+)-ve direction, i.e. $p = [p^+, M^2/2p^+, \mathbf{0}_\perp]$, and thus $p^\mu \sim [\mathcal{O}(1), \mathcal{O}(\lambda), \mathbf{0}_\perp] Q$. The same λ -scales also hold for p' since $p'^+/Q \sim 1$ and $p' = [p'^+, M^2/2p'^+, \mathbf{0}_\perp]$. Isolating the leading non-perturbative component, which is $\psi(x)\bar{\psi}(y)$ for the first scattering correlator herein, allows to write $\psi(x)\bar{\psi}(y)$ in terms of a scalar function $T(x, y)$:

$$\psi(x)\bar{\psi}(y) = \not{p} T(x, y) = p^+ \gamma^- T(x, y) \implies \text{Tr}[\gamma^+ \psi(x)\bar{\psi}(y)] = p^+ \text{Tr}[\gamma^+ \gamma^-] T(x, y) \implies \psi(x)\bar{\psi}(y) = \gamma^- \text{Tr} \left[\bar{\psi}(y) \frac{\gamma^+}{4} \psi(x) \right]. \tag{14}$$

In the light-cone gauge $A^- = 0$, the Glauber gluon emanating from the medium has $A^+ \gg A_\perp$, and thus $\gamma^{\sigma_3} A_{\sigma_3}(z_3) \approx \gamma^- A^+(z_3)$ and $\gamma^{\sigma_2} A_{\sigma_2}(z_2) \approx \gamma^- A^+(z_2)$. In addition, we assume that the hard quark produced from the primary hard scattering with the nucleon struck by the virtual photon, will undergo further re-scatterings while traversing the remaining $A - 1$ nucleons. As $Q \gg 1$, any scatterings following the first one are assumed independent, and thus the correlators are factorized

$$\left\langle AP \left| \text{Tr} \left[\bar{\psi}(y) \frac{\gamma^+}{4} \psi(x) \right] A^+(z_3) A^+(z_2) \right| AP \right\rangle \approx \left\langle P \left| \text{Tr} \left[\bar{\psi}(y) \frac{\gamma^+}{4} \psi(x) \right] \right| P \right\rangle \langle P_{A-1} | A^+(z_3) A^+(z_2) | P_{A-1} \rangle, \tag{15}$$

where the first term will be absorbed in the definition of the nuclear parton distribution function, while the second term will be included in the scattering kernel. The resulting $T^{\mu\nu}$ is

$$\begin{aligned}
T_{1,c}^{\mu\nu} &= e^2 e_q^2 g_s^2 \int d^4x d^4y d^4z_1 d^4z_2 d^4z_3 d^4z_4 \int \frac{d^4p_1}{(2\pi)^4} \frac{d^4p'_1}{(2\pi)^4} \frac{d^4\ell}{(2\pi)^4} \frac{d^4\ell'}{(2\pi)^4} \frac{d^4\ell_2}{(2\pi)^4} \frac{d^4p_2}{(2\pi)^4} e^{iy(q-p'_1)} e^{-ix(q-p_1)} \\
&\times \left\langle P \left| \bar{\psi}(y) \frac{\gamma^+}{4} \psi(x) \right| P \right\rangle e^{iz_1(\ell-p_1+\ell_2)} e^{iz_2(-\ell+p_2)} e^{iz_3(\ell'-p_2)} \langle P_{A-1} | A^+(z_3) A^+(z_2) | P_{A-1} \rangle e^{iz_4(p'_1-\ell'-\ell_2)} \\
&\times \text{Tr} \left[\gamma^- \gamma^\mu \frac{(\not{p}'_1 + M)}{(p_1'^2 - M^2 + i\epsilon)} \gamma^{\sigma_4} \frac{(\not{\ell}' + M)}{(\ell'^2 - M^2 + i\epsilon)} \gamma^- \frac{(\not{p}_2 + M)}{(p_2^2 - M^2 + i\epsilon)} \gamma^- \frac{(\not{\ell} + M)}{(\ell^2 - M^2 + i\epsilon)} \gamma^{\sigma_1} \frac{(\not{p}_1 + M)}{(p_1^2 - M^2 + i\epsilon)} \gamma^\nu \right] \\
&\times \frac{d_{\sigma_4 \sigma_1}^{(\ell_2)}}{(\ell_2^2 + i\epsilon)}. \tag{16}
\end{aligned}$$

After performing the change of variable $p'_1 = q + p'$ and $p_1 = q + p$ in Eq. 13 (see also Fig. 5), which stem from energy and momentum conservation, the integration measure $d^4p'_1$ transforms as $d^4p'_1 \rightarrow d^4p'$, while $d^4p_1 \rightarrow d^4p$. Combining these results yields

$$\begin{aligned}
T_{1,c}^{\mu\nu} &= e^2 e_q^2 g_s^2 \int d^4x d^4y d^4z_1 d^4z_2 d^4z_3 d^4z_4 \int \frac{d^4p}{(2\pi)^4} \frac{d^4p'}{(2\pi)^4} \frac{d^4\ell}{(2\pi)^4} \frac{d^4\ell'}{(2\pi)^4} \frac{d^4\ell_2}{(2\pi)^4} \frac{d^4p_2}{(2\pi)^4} \\
&\times e^{-iy p'} e^{ix p} \left\langle P \left| \bar{\psi}(y) \frac{\gamma^+}{4} \psi(x) \right| P \right\rangle e^{iz_1(\ell-q-p+\ell_2)} e^{iz_2(-\ell+p_2)} e^{iz_3(\ell'-p_2)} \langle P_{A-1} | A^+(z_3) A^+(z_2) | P_{A-1} \rangle e^{iz_4(p'+q-\ell'-\ell_2)} \\
&\times \text{Tr} \left[\frac{\gamma^- \gamma^\mu (\not{q} + \not{p}' + M)}{[(q+p')^2 - M^2 + i\epsilon]} \gamma^{\sigma_4} \frac{(\not{\ell}' + M)}{(\ell'^2 - M^2 + i\epsilon)} \frac{\gamma^- (\not{p}_2 + M)}{(p_2^2 - M^2 + i\epsilon)} \frac{\gamma^- (\not{\ell} + M)}{(\ell^2 - M^2 + i\epsilon)} \gamma^{\sigma_1} \frac{(\not{q} + \not{p} + M)}{((q+p)^2 - M^2 + i\epsilon)} \gamma^\nu \right] \\
&\times \frac{d_{\sigma_4 \sigma_1}^{(\ell_2)}}{(\ell_2^2 + i\epsilon)}. \tag{17}
\end{aligned}$$

Performing the integrals over d^4z_1 and d^4z_4 gives

$$(2\pi)^4 \delta^{(4)}(-q-p+\ell+\ell_2) (2\pi)^4 \delta^{(4)}(q+p'-\ell'-\ell_2), \tag{18}$$

which allows for the $d^4\ell$ and $d^4\ell'$ integration in Eq. 17 to be performed generating

$$\begin{aligned}
T_{1,c}^{\mu\nu} &= e^2 e_q^2 g_s^2 \int d^4x d^4y d^4z_2 d^4z_3 \int \frac{d^4p}{(2\pi)^4} \frac{d^4p'}{(2\pi)^4} \frac{d^4\ell_2}{(2\pi)^4} \frac{d^4p_2}{(2\pi)^4} \\
&\times e^{-iy p'} e^{ix p} \left\langle P \left| \bar{\psi}(y) \frac{\gamma^+}{4} \psi(x) \right| P \right\rangle e^{iz_2(\ell_2-p-q+p_2)} e^{iz_3(p'+q-\ell_2-p_2)} \langle P_{A-1} | A^+(z_3) A^+(z_2) | P_{A-1} \rangle \\
&\times \text{Tr} \left[\frac{\gamma^- \gamma^\mu (\not{q} + \not{p}' + M)}{[(q+p')^2 - M^2 + i\epsilon]} \frac{\gamma^{\sigma_4} (\not{q} + \not{p}' - \not{\ell}_2 + M)}{[(q+p'-\ell_2)^2 - M^2 + i\epsilon]} \frac{\gamma^- (\not{p}_2 + M)}{(p_2^2 - M^2 + i\epsilon)} \frac{\gamma^- (\not{q} + \not{p} - \not{\ell}_2 + M) \gamma^{\sigma_1}}{[(q+p-\ell_2)^2 - M^2 + i\epsilon]} \frac{(\not{q} + \not{p} + M) \gamma^\nu}{[(q+p)^2 - M^2 + i\epsilon]} \right] \\
&\times \frac{d_{\sigma_4 \sigma_1}^{(\ell_2)}}{(\ell_2^2 + i\epsilon)}. \tag{19}
\end{aligned}$$

Applying Cutkosky's [41] procedure to obtain the hadronic tensor yields

$$\begin{aligned}
W_{1,c}^{\mu\nu} &= e^2 e_q^2 g_s^2 \int d^4x d^4y d^4z_2 d^4z_3 \int \frac{d^4p}{(2\pi)^4} \frac{d^4p'}{(2\pi)^4} \frac{d^4\ell_2}{(2\pi)^4} \frac{d^4p_2}{(2\pi)^4} e^{ip'(z_3-y)} e^{ip(x-z_2)} \left\langle P \left| \bar{\psi}(y) \frac{\gamma^+}{4} \psi(x) \right| P \right\rangle \\
&\times e^{iz_3(q-p_2-\ell_2)} e^{iz_2(\ell_2+p_2-q)} \langle P_{A-1} | A^+(z_3) A^+(z_2) | P_{A-1} \rangle (2\pi) \delta(\ell_2^2) (2\pi) \delta(p_2^2 - M^2) d_{\sigma_1 \sigma_4}^{(\ell_2)} \\
&\times \frac{\text{Tr} \left[\gamma^- \gamma^\mu (\not{q} + \not{p}' + M) \gamma^{\sigma_4} (\not{q} + \not{p}' - \not{\ell}_2 + M) \gamma^- (\not{p}_2 + M) \gamma^- (\not{q} + \not{p} - \not{\ell}_2 + M) \gamma^{\sigma_1} (\not{q} + \not{p} + M) \gamma^\nu \right]}{\left[(q+p')^2 - M^2 - i\epsilon \right] \left[(q+p'-\ell_2)^2 - M^2 - i\epsilon \right] \left[(q+p-\ell_2)^2 - M^2 + i\epsilon \right] \left[(q+p)^2 - M^2 + i\epsilon \right]}, \tag{20}
\end{aligned}$$

where the discontinuity in the photon and quark propagators has been applied, namely:

$$\begin{aligned}
\text{Disc} \left[\frac{1}{\ell_2^2 + i\epsilon} \right] &= 2\pi \delta(\ell_2^2), \\
\text{Disc} \left[\frac{1}{p_2^2 - M^2 + i\epsilon} \right] &= 2\pi \delta(p_2^2 - M^2). \tag{21}
\end{aligned}$$

The expression in Eq. 20 becomes singular when the denominator of the quark propagator for p_1 , ℓ , ℓ' and p'_1 vanishes. Computing this integral is easiest in the complex plane of p^+ and p'^+ , where both p^+ and p'^+ have two simple poles.⁵ The contour integration for p^+ can be carried out as

$$\begin{aligned}
C_1 &= \oint \frac{dp^+}{(2\pi)} \frac{e^{ip^+(x^- - z_2^-)}}{[(q+p)^2 - M^2 + i\epsilon][(q+p-\ell_2)^2 - M^2 + i\epsilon]} \\
&= \oint \frac{dp^+}{(2\pi)} \frac{e^{ip^+(x^- - z_2^-)}}{2q^- \left[q^+ + p^+ - \frac{M^2}{2q^-} + i\epsilon \right] 2(q^- - \ell_2^-) \left[q^+ + p^+ - \ell_2^+ - \frac{\ell_{2\perp}^2 + M^2}{2(q^- - \ell_2^-)} + i\epsilon \right]} \\
&= \frac{(2\pi i)}{2\pi} \frac{\theta(x^- - z_2^-)}{4q^-(q^- - \ell_2^-)} \left[\frac{e^{i(-q^+ + \frac{M^2}{2q^-})(x^- - z_2^-)}}{\left\{ \frac{M^2}{2q^-} - \ell_2^+ - \frac{\ell_{2\perp}^2 + M^2}{2(q^- - \ell_2^-)} \right\}} + \frac{e^{i(-q^+ + \ell_2^+ + \frac{\ell_{2\perp}^2 + M^2}{2(q^- - \ell_2^-)})(x^- - z_2^-)}}{\left\{ \ell_2^+ + \frac{\ell_{2\perp}^2 + M^2}{2(q^- - \ell_2^-)} - \frac{M^2}{2q^-} \right\}} \right] \\
&= \frac{(2\pi i)}{2\pi} \frac{\theta(x^- - z_2^-)}{4q^-(q^- - \ell_2^-)} e^{i(-q^+ + \frac{M^2}{2q^-})(x^- - z_2^-)} \left[\frac{-1 + e^{i\mathcal{G}_M^{(\ell_2)}(x^- - z_2^-)}}{\mathcal{G}_M^{(\ell_2)}} \right],
\end{aligned} \tag{23}$$

where

$$\mathcal{G}_M^{(\ell_2)} = \ell_2^+ + \frac{\ell_{2\perp}^2 + M^2}{2(q^- - \ell_2^-)} - \frac{M^2}{2q^-}. \tag{24}$$

The contour integration for p'^+ proceeds analogously giving

$$\begin{aligned}
C_2 &= \oint \frac{dp'^+}{(2\pi)} \frac{e^{-ip'^+(y^- - z_3^-)}}{[(q+p')^2 - M^2 - i\epsilon][(q+p'-\ell_2)^2 - M^2 - i\epsilon]} \\
&= \oint \frac{dp'^+}{(2\pi)} \frac{e^{-ip'^+(y^- - z_3^-)}}{2q^- \left[q^+ + p'^+ - \frac{M^2}{2q^-} - i\epsilon \right] 2(q^- - \ell_2^-) \left[q^+ + p'^+ - \ell_2^+ - \frac{\ell_{2\perp}^2 + M^2}{2(q^- - \ell_2^-)} - i\epsilon \right]} \\
&= \frac{(-2\pi i)}{2\pi} \frac{\theta(y^- - z_3^-)}{4q^-(q^- - \ell_2^-)} e^{-i(-q^+ + \frac{M^2}{2q^-})(y^- - z_3^-)} \left[\frac{-1 + e^{-i\mathcal{G}_M^{(\ell_2)}(y^- - z_3^-)}}{\mathcal{G}_M^{(\ell_2)}} \right].
\end{aligned} \tag{25}$$

As the final expression for C_1 and C_2 is independent of p and p' , respectively, the dependence on these variables in Eq. 20 remains within $e^{ip(x-z_2)}$ and $e^{ip'(z_3-y)}$ as well as the trace over γ -matrices. While our λ -power counting scheme constrains the size of momentum variables, the same cannot be said about position variables. Thus, the $e^{ip(x-z_2)}$ and $e^{ip'(z_3-y)}$ phase factors must remain intact. As the trace in Eq. 20 only contributes at $\mathcal{O}(\lambda^2)$ in p and p' , the only non-trivial contribution remaining to the p and p' integrals stems solely from $e^{ip(x-z_2)}$ and $e^{ip'(z_3-y)}$ phase factors. To perform the remaining integrals for p and p' , the following substitutions are used $p = [p^+, p^-, \mathbf{0}_\perp] = [p^+, \frac{M^2}{2p^+} + \delta p^-, \mathbf{0}_\perp]$ and $p' = [p'^+, p'^-, \mathbf{0}_\perp] = [p'^+, \frac{M^2}{2p'^+} + \delta p'^-, \mathbf{0}_\perp]$, where $\delta p^- \sim \mathcal{O}(\lambda^2)$ and $\delta p'^- \sim \mathcal{O}(\lambda^2)$. Thus, the integrals over $dp^- d^2 p_\perp dp'^- d^2 p'_\perp$ simply become integrals over $d(\delta p^-) d^2 p_\perp d(\delta p'^-) d^2 p'_\perp$ yielding

$$(2\pi)^3 \delta(x^+ - z_2^+) \delta^2(\mathbf{x}_\perp - \mathbf{z}_{2\perp}) (2\pi)^3 \delta(-y^+ + z_3^+) \delta^2(-\mathbf{y}_\perp + \mathbf{z}_{3\perp}). \tag{26}$$

⁵ One of the propagators takes the form

$$\begin{aligned}
[(q+p)^2 - M^2 + i\epsilon]^{-1} &= \left[2(q^+ + p^+)(q^- + p^-) - |\mathbf{q}_\perp + \mathbf{p}_\perp|^2 - M^2 + i\epsilon \right]^{-1} \\
&\approx \left[2(q^+ + p^+)q^- [1 + \mathcal{O}(\lambda^2)] - M^2 + i\epsilon \right]^{-1} \\
&\approx 2q^- \left[q^+ + p^+ - \frac{M^2}{2q^-} + i\epsilon \right]^{-1}
\end{aligned} \tag{22}$$

where the established power counting $p^-/q^- \sim \lambda^2$ together with $\mathbf{p}_\perp = \mathbf{0}_\perp$ was used to simplify the full propagator to the expression above. A similar procedure is used for $[(q+p-\ell_2)^2 - M^2 + i\epsilon]$.

Performing the integral over spacetime variables (x^+, \mathbf{x}_\perp) and (y^+, \mathbf{y}_\perp) using δ -functions in Eq. 26 yields

$$\begin{aligned}
W_{1,c}^{\mu\nu} &= e^2 e_q^2 g_s^2 \int dx^- dy^- d^4 z_2 d^4 z_3 \int \frac{d^4 \ell_2}{(2\pi)^4} \frac{d^4 p_2}{(2\pi)^4} \left\langle P \left| \bar{\psi}(z_3^+, y^-, \mathbf{z}_{3\perp}) \frac{\gamma^+}{4} \psi(z_2^+, x^-, \mathbf{z}_{2\perp}) \right| P \right\rangle \\
&\times \frac{\theta(x^- - z_2^-) \theta(y^- - z_3^-)}{(2q^-)^2 [2(q^- - \ell_2^-)]^2} \frac{1}{[\mathcal{G}_M^{(\ell_2)}]^2} e^{i(q^+ - \frac{M^2}{2q^-})(y^- - x^- - z_3^- + z_2^-)} \left[-1 + e^{i\mathcal{G}_M^{(\ell_2)}(x^- - z_2^-)} \right] \left[-1 + e^{-i\mathcal{G}_M^{(\ell_2)}(y^- - z_3^-)} \right] \\
&\times e^{iz_3(q - p_2 - \ell_2)} e^{iz_2(\ell_2 + p_2 - q)} \langle P_{A-1} | A^+(z_3) A^+(z_2) | P_{A-1} \rangle (2\pi) \delta(\ell_2^2) (2\pi) \delta(p_2^2 - M^2) d_{\sigma_1 \sigma_4}^{(\ell_2)} \\
&\times \text{Tr} \left[\gamma^- \gamma^\mu (\not{q} + \not{p}' + M) \gamma^{\sigma_4} (\not{q} + \not{p}' - \not{\ell}_2 + M) \gamma^- (\not{p}_2 + M) \gamma^- (\not{q} + \not{p} - \not{\ell}_2 + M) \gamma^{\sigma_1} (\not{q} + \not{p} + M) \gamma^\nu \right], \tag{27}
\end{aligned}$$

where $x^+ = z_2^+$, $y^+ = z_3^+$, $\mathbf{x}_\perp = \mathbf{z}_{2\perp}$, and $\mathbf{y}_\perp = \mathbf{z}_{3\perp}$ was used to simplify the expression for $W^{\mu\nu}$. Note that the trace inside $W^{\mu\nu}$ has been left intact owing to power counting. The next step is to perform the $d\ell_2^+$ as well as the $dp_2^+ dp_2^-$ integrals aided by the presence of the $\delta(\ell_2^2)$ and $\delta(p_2^2 - M^2)$ and λ -power counting. Indeed,

$$\begin{aligned}
\delta(\ell_2^2) &= \delta(2\ell_2^+ \ell_2^- - \ell_{2\perp}^2) = \frac{1}{2\ell_2^-} \delta\left(\ell_2^+ - \frac{\ell_{2\perp}^2}{2\ell_2^-}\right) \\
\delta(p_2^2 - M^2) &= \delta(2p_2^+ p_2^- - \mathbf{p}_{2\perp}^2 - M^2) = \frac{1}{2p_2^-} \delta\left(p_2^+ - \frac{\mathbf{p}_{2\perp}^2 + M^2}{2p_2^-}\right), \tag{28}
\end{aligned}$$

which, when inserted in $W^{\mu\nu}$, gives

$$\begin{aligned}
W_{1,c}^{\mu\nu} &= e^2 e_q^2 g_s^2 \int dx^- dy^- d^4 z_2 d^4 z_3 \int \frac{d^4 \ell_2}{(2\pi)^3} \frac{d^4 p_2}{(2\pi)^3} \left\langle P \left| \bar{\psi}(z_3^+, y^-, \mathbf{z}_{3\perp}) \frac{\gamma^+}{4} \psi(z_2^+, x^-, \mathbf{z}_{2\perp}) \right| P \right\rangle \\
&\times \frac{\theta(x^- - z_2^-) \theta(y^- - z_3^-)}{(2q^-)^2 [2(q^- - \ell_2^-)]^2} \frac{1}{[\mathcal{G}_M^{(\ell_2)}]^2} e^{i(q^+ - \frac{M^2}{2q^-})(y^- - x^- - z_3^- + z_2^-)} \left[-1 + e^{i\mathcal{G}_M^{(\ell_2)}(x^- - z_2^-)} \right] \left[-1 + e^{-i\mathcal{G}_M^{(\ell_2)}(y^- - z_3^-)} \right] \\
&\times e^{i(p_2 + \ell_2)(z_2 - z_3)} e^{iq(z_3 - z_2)} \frac{1}{2\ell_2^-} \delta\left(\ell_2^+ - \frac{\ell_{2\perp}^2}{2\ell_2^-}\right) \frac{1}{2p_2^-} \delta\left(p_2^+ - \frac{\mathbf{p}_{2\perp}^2 + M^2}{2p_2^-}\right) \langle P_{A-1} | A^+(z_3) A^+(z_2) | P_{A-1} \rangle d_{\sigma_1 \sigma_4}^{(\ell_2)} \\
&\times \text{Tr} \left[\gamma^- \gamma^\mu (\not{q} + \not{p}' + M) \gamma^{\sigma_4} (\not{q} + \not{p}' - \not{\ell}_2 + M) \gamma^- (\not{p}_2 + M) \gamma^- (\not{q} + \not{p} - \not{\ell}_2 + M) \gamma^{\sigma_1} (\not{q} + \not{p} + M) \gamma^\nu \right]. \tag{29}
\end{aligned}$$

Defining the momentum fraction y as $\ell_2^- = yq^-$, allows to rewrite $d\ell_2^- = q^- dy$. Furthermore, energy and momentum conservation in Fig. 5 implies that

$$q + p = p_1 = \ell_2 + \ell = \ell_2 + (p_2 - k) \iff q + p - \ell_2 - p_2 + k = 0. \tag{30}$$

While the δ -functions can be used to perform the ℓ_2^+ and p_2^+ integrals, p_2^- can also be performed using λ -power counting. Indeed, as $k^\mu \sim [\mathcal{O}(\lambda^2), \mathcal{O}(\lambda^2), \mathcal{O}(\lambda), \mathcal{O}(\lambda)] Q$, while $\ell_2^\mu \sim [\mathcal{O}(\lambda^2), \mathcal{O}(1), \mathcal{O}(\lambda), \mathcal{O}(\lambda)] Q$ and $p_2^\mu \sim [\mathcal{O}(\lambda^2), \mathcal{O}(1), \mathcal{O}(\lambda), \mathcal{O}(\lambda)] Q$, using energy and momentum conservation implies

$$\begin{aligned}
0 &= q^- + p^- - \ell_2^- - p_2^- + k^- \\
0 &= q^- + \mathcal{O}(\lambda^2) - \ell_2^- - p_2^- + \mathcal{O}(\lambda), \tag{31}
\end{aligned}$$

and thus the following change of variable $p_2^- = q^- - \ell_2^- + k^- + \delta p_2^-$, where $\delta p_2^- \sim \mathcal{O}(\lambda^2)$ is a small quantity, induces a change in the integration measure $dp_2^- = d(\delta p_2^-)$. Thus, the integration over dp_2^- yields a $\delta(z_2^+ - z_3^+)$, as the only function in Eq. 29 that is not small is $e^{ip_2^-(z_3^+ - z_2^+)}$, since $(z_3^+ - z_2^+)$ is not subject to the power counting in λ . Any other dependence on p_2^- seen in Eq. 29 can simply be set to $q^- - \ell_2^- + k^-$. Thus,

$$\begin{aligned}
W_{1,c}^{\mu\nu} &= e^2 e_q^2 g_s^2 \int dx^- dy^- d^4 z_2 d^4 z_3 \int \frac{dy d^2 \ell_{2\perp}}{(2\pi)^3} \frac{d^2 p_{2\perp}}{(2\pi)^2} \delta(z_2^+ - z_3^+) \left\langle P \left| \bar{\psi}(z_3^+, y^-, \mathbf{z}_{3\perp}) \frac{\gamma^+}{4} \psi(z_2^+, x^-, \mathbf{z}_{2\perp}) \right| P \right\rangle \\
&\times \frac{\theta(x^- - z_2^-) \theta(y^- - z_3^-)}{(2q^-)^2 [2q^- (1 - y)]^2} \frac{1}{[\mathcal{G}_M^{(\ell_2)}]^2} e^{i(q^+ - \frac{M^2}{2q^-})(y^- - x^-)} \left[-1 + e^{i\mathcal{G}_M^{(\ell_2)}(x^- - z_2^-)} \right] \left[-1 + e^{-i\mathcal{G}_M^{(\ell_2)}(y^- - z_3^-)} \right] \\
&\times e^{i(z_2^- - z_3^-) \mathcal{H}_M^{(\ell_2, p_2)}} e^{-i(\mathbf{p}_{2\perp} + \ell_{2\perp}) \cdot (\mathbf{z}_{2\perp} - \mathbf{z}_{3\perp})} e^{-ik^-(z_3^+ - z_2^+)} \frac{1}{2y 2q^- (1 - y + \eta y)} \langle P_{A-1} | A^+(z_3) A^+(z_2) | P_{A-1} \rangle \\
&\times d_{\sigma_1 \sigma_4}^{(\ell_2)} \text{Tr} \left[\gamma^- \gamma^\mu (\not{q} + \not{p}' + M) \gamma^{\sigma_4} (\not{q} + \not{p}' - \not{\ell}_2 + M) \gamma^- (\not{p}_2 + M) \gamma^- (\not{q} + \not{p} - \not{\ell}_2 + M) \gamma^{\sigma_1} (\not{q} + \not{p} + M) \gamma^\nu \right], \tag{32}
\end{aligned}$$

where

$$\eta = \frac{k^-}{\ell_2^-} = \frac{k^-}{yq^-}, \quad (33)$$

and

$$\mathcal{G}_M^{(\ell_2)} = \frac{\ell_{2\perp}^2 + y^2 M^2}{2y(1-y)q^-}, \quad (34)$$

$$\mathcal{H}_M^{(\ell_2, p_2)} = \ell_2^+ + p_2^+ - \frac{M^2}{2q^-} = \frac{\ell_{2\perp}^2}{2yq^-} + \frac{\mathbf{p}_{2\perp}^2 + M^2}{2q^-(1-y+\eta y)} - \frac{M^2}{2q^-}. \quad (35)$$

Applying the following transformation $\mathbf{p}_{2\perp} + \ell_{2\perp} = \mathbf{k}_\perp$ allows to express $d^2 p_{2\perp} \rightarrow d^2 k_{2\perp}$, for a fixed ℓ_2 . Furthermore, the following transformation of coordinates is useful

$$\begin{aligned} z &= \frac{z_3 + z_2}{2}, \\ \Delta z &= z_3 - z_2, \end{aligned} \quad (36)$$

as the integration measure remains unchanged, i.e. $d^4 z_3 d^4 z_2 = d^4 z d^4(\Delta z)$. The resulting hadronic tensor has the following form:

$$\begin{aligned} W_{1,c}^{\mu\nu} &= e^2 e_q^2 g_s^2 \int dx^- dy^- d^4 z d^4(\Delta z) \int \frac{dy}{2\pi} \frac{d^2 \ell_{2\perp}}{(2\pi)^2} \frac{d^2 k_\perp}{(2\pi)^2} \delta(\Delta z^+) e^{-i\Delta z^+ k^-} \\ &\times \left\langle P_{A-1} \left| A^+ \left(z + \frac{\Delta z}{2} \right) A^+ \left(z - \frac{\Delta z}{2} \right) \right| P_{A-1} \right\rangle \\ &\times e^{i\left(q^+ - \frac{M^2}{2q^-}\right)(y^- - x^-)} \left\langle P \left| \bar{\psi} \left(z^+ + \frac{\Delta z^+}{2}, y^-, \mathbf{z}_\perp + \frac{\Delta \mathbf{z}_\perp}{2} \right) \frac{\gamma^+}{4} \psi \left(z^+ - \frac{\Delta z^+}{2}, x^-, \mathbf{z}_\perp - \frac{\Delta \mathbf{z}_\perp}{2} \right) \right| P \right\rangle \\ &\times \left[-1 + e^{i\mathcal{G}_M^{(\ell_2)}(x^- - z_2^-)} \right] \left[-1 + e^{-i\mathcal{G}_M^{(\ell_2)}(y^- - z_3^-)} \right] e^{-i\Delta z^- \mathcal{H}_M^{(\ell_2, p_2)}} e^{i\mathbf{k}_\perp \cdot \Delta \mathbf{z}_\perp} \\ &\times \frac{\theta(x^- - z_2^-) \theta(y^- - z_3^-)}{(2q^-)^2 [2(1-y)q^-]^2} \left[\mathcal{G}_M^{(\ell_2)} \right]^{-2} \frac{1}{2y} \frac{1}{2(1-y+\eta y)q^-} \\ &\times d_{\sigma_1 \sigma_4}^{(\ell_2)} \text{Tr} \left[\gamma^- \gamma^\mu (\not{q} + \not{p}' + M) \gamma^{\sigma_4} (\not{q} + \not{p}' - \not{\ell}_2 + M) \gamma^- (\not{p}_2 + M) \gamma^- (\not{q} + \not{p} - \not{\ell}_2 + M) \gamma^{\sigma_1} (\not{q} + \not{p} + M) \gamma^\nu \right]. \end{aligned} \quad (37)$$

Note that the two-point gauge field operator $\langle P_{A-1} | A^+(z + \Delta z/2) A^+(z - \Delta z/2) | P_{A-1} \rangle$ is invariant under translation by four-vector z . This is primarily true owing to the fact that the incoming state $|P_{A-1}\rangle$ and the outgoing state $\langle P_{A-1}|$ are identical. Therefore, any dependence on z seen in that operator expectation value is not physical.⁶

The phases that depend on the relative distances $\Delta X^- = y^- - x^-$ such as $e^{i\left(q^+ - \frac{M^2}{2q^-}\right)(y^- - x^-)}$ are absorbed in the definition of the quark PDF, and phases $e^{-i\Delta z^- \mathcal{H}_M^{(\ell_2, p_2)}} e^{i\mathbf{k}_\perp \cdot \Delta \mathbf{z}_\perp}$ are included within the nuclear medium's distribution function.

While translational invariance was helpful for dealing with expectation values of operator products, quantum coherence (or interference) effects are more sensitive to positional information, as seen in the phase factor $\left[-1 + e^{i\mathcal{G}_M^{(\ell_2)}(x^- - z_2^-)} \right]$ and $\left[-1 + e^{-i\mathcal{G}_M^{(\ell_2)}(y^- - z_3^-)} \right]$. Since the process (Fig. 5) in the amplitude is identical to the process on the complex conjugate, the $W^{\mu\nu}$ is required to be a real number. Therefore, the remaining phase factors must be real-valued:

$$\begin{aligned} \mathcal{R} &= \left[-1 + e^{i\mathcal{G}_M^{(\ell_2)}(x^- - z_2^-)} \right] \left[-1 + e^{-i\mathcal{G}_M^{(\ell_2)}(y^- - z_3^-)} \right] \\ \mathcal{R} &= \left[1 - e^{i\mathcal{G}_M^{(\ell_2)}(x^- - z_2^-)} - e^{-i\mathcal{G}_M^{(\ell_2)}(y^- - z_3^-)} + e^{i\mathcal{G}_M^{(\ell_2)}(x^- - z_2^- - y^- + z_3^-)} \right] \in \mathbb{R} \\ &\implies \mathcal{G}_M^{(\ell_2)}(x^- - z_2^- - y^- + z_3^-) = 2n\pi, \text{ where } n \in \mathbb{Z} \\ &\implies \mathcal{G}_M^{(\ell_2)}(x^- - z_2^-) = \mathcal{G}_M^{(\ell_2)}(y^- - z_3^-) + 2n\pi, \\ &\implies \mathcal{R} = \left[2 - 2 \cos \left\{ \mathcal{G}_M^{(\ell_2)}(y^- - z_3^-) \right\} \right] = \left[2 - 2 \cos \left\{ \mathcal{G}_M^{(\ell_2)}(x^- - z_2^-) \right\} \right]. \end{aligned} \quad (38)$$

⁶ A similar statement can be made to hold true for the z^+ and \mathbf{z}_\perp dependence within the $\langle \bar{\psi} \gamma^+ \psi \rangle$ operator in Eq. 37, by undoing the spacetime integrals associated with the δ -functions in Eq. 26.

The above derivation entails that $y^- - z_3^- = x^- - z_2^-$, which is expected as $x^- - z_2^-$ represents the distance between first scattering and second scattering on the amplitude side, while $y^- - z_3^-$ is the same distance on the complex conjugate side. As $\theta(x^- - z_2^-)$ suggests that $x^- - z_2^- > 0$, while $\theta(y^- - z_3^-)$ implies $y^- - z_3^- > 0$, a new length integration variable $\zeta^- = y^- - z_3^- = x^- - z_2^-$ is defined to encapsulate that spacetime distance, and ensure that the scattering probability is real-valued. Introducing new variables for distance:

$$\begin{aligned}\Delta X^- &= y^- - x^-, \\ X^- &= \frac{y^- + x^-}{2}, \\ \zeta^- &= y^- - z_3^- = x^- - z_2^- = X^- - z^-, \end{aligned} \quad (39)$$

and incorporating them in $W^{\mu\nu}$, allows to perform the integrals over d^4z ,⁷ Δz^+ , and X^- ,⁸ giving

$$\begin{aligned}W_{1,c}^{\mu\nu} &= e^2 e_q^2 g_s^2 \int d(\Delta X^-) d\zeta^- d(\Delta z^-) d^2 \Delta z_\perp \int \frac{dy}{2\pi} \frac{d^2 \ell_{2\perp}}{(2\pi)^2} \frac{d^2 k_\perp}{(2\pi)^2} e^{i\Delta X^- (q^+ - \frac{M^2}{2q^-})} \left\langle P \left| \bar{\psi}(\Delta X^-) \frac{\gamma^+}{4} \psi(0) \right| P \right\rangle \\ &\times \left[2 - 2 \cos \left\{ \mathcal{G}_M^{(\ell_2)} \zeta^- \right\} \right] e^{-i\Delta z^- \mathcal{H}_M^{(\ell_2, p_2)}} e^{i\mathbf{k}_\perp \cdot \Delta \mathbf{z}_\perp} \\ &\times \frac{\theta(\zeta^-)}{(2q^-)^2 [2(1-y)q^-]^2} \left[\mathcal{G}_M^{(\ell_2)} \right]^{-2} \left[\frac{1}{2y} \frac{1}{2(1-y+\eta y)q^-} \right] \langle P_{A-1} | A^+(\zeta^-, \Delta z^-, \Delta z_\perp) A^+(\zeta^-, 0) | P_{A-1} \rangle \\ &\times d_{\sigma_1 \sigma_4}^{(\ell_2)} \text{Tr} \left[\gamma^- \gamma^\mu (\not{q} + \not{p}' + M) \gamma^{\sigma_4} (\not{q} + \not{p}' - \not{\ell}_2 + M) \gamma^- (\not{p}_2 + M) \gamma^- (\not{q} + \not{p} - \not{\ell}_2 + M) \gamma^{\sigma_1} (\not{q} + \not{p} + M) \gamma^\nu \right]. \end{aligned} \quad (40)$$

The trace in the above equation can be simplified to get

$$\begin{aligned}\text{Tr} &\left[\gamma^- \gamma^\mu (\not{q} + \not{p}' + M) \gamma^{\sigma_4} (\not{q} + \not{p}' - \not{\ell}_2 + M) \gamma^- (\not{p}_2 + M) \gamma^- (\not{q} + \not{p} - \not{\ell}_2 + M) \gamma^{\sigma_1} (\not{q} + \not{p} + M) \gamma^\nu \right] d_{\sigma_1 \sigma_4}^{(\ell_2)} \\ &= \text{Tr} \left[\gamma^- \gamma^\mu (\not{q} + \not{p}' + M) \gamma^{\sigma_4} (\not{q} + \not{p}' - \not{\ell}_2 + M) \gamma^- (\not{p}_2 + M) \gamma^- (\not{q} + \not{p} - \not{\ell}_2 + M) \gamma^{\sigma_1} (\not{q} + \not{p} + M) \gamma^\nu \right] \\ &\times \left[-g_{\sigma_1 \sigma_4} + \frac{n_{\sigma_1} \ell_{2\sigma_4} + n_{\sigma_4} \ell_{2\sigma_1}}{n \cdot \ell_2} \right] \\ &= 32(q^-)^3 [-g_{\perp\perp}^{\mu\nu}] \left[\frac{1-y+\eta y}{y} \right] \left[\frac{1+(1-y)^2}{y} \right] [\ell_{2\perp}^2 + M^2 y^4 \kappa], \end{aligned} \quad (41)$$

where

$$\kappa = \left[1 + (1-y)^2 \right]^{-1}. \quad (42)$$

Using the expression in Eq. 41, the hadronic tensor becomes

$$\begin{aligned}W_{1,c}^{\mu\nu} &= 2 [-g_{\perp\perp}^{\mu\nu}] e^2 e_q^2 g_s^2 \int d(\Delta X^-) e^{i\Delta X^- (q^+ - \frac{M^2}{2q^-})} \left\langle P \left| \bar{\psi}(\Delta X^-) \frac{\gamma^+}{4} \psi(0) \right| P \right\rangle \\ &\times \int d(\Delta z^-) d^2 \Delta z_\perp \frac{dy}{2\pi} \frac{d^2 \ell_{2\perp}}{(2\pi)^2} \frac{d^2 k_\perp}{(2\pi)^2} \left[\frac{1+(1-y)^2}{y} \right] e^{-i\Delta z^- \mathcal{H}_M^{(\ell_2, p_2)}} e^{i\mathbf{k}_\perp \cdot \Delta \mathbf{z}_\perp} \\ &\times \int d\zeta^- \theta(\zeta^-) \left[2 - 2 \cos \left\{ \mathcal{G}_M^{(\ell_2)} \zeta^- \right\} \right] \frac{[\ell_{2\perp}^2 + M^2 y^4 \kappa]}{[\ell_{2\perp}^2 + y^2 M^2]^2} \langle P_{A-1} | A^+(\zeta^-, \Delta z^-, \Delta z_\perp) A^+(\zeta^-, 0) | P_{A-1} \rangle, \end{aligned} \quad (43)$$

where κ is defined in Eq. 42, while, for completeness,

$$\begin{aligned}\mathcal{G}_M^{(\ell_2)} &= \ell_2^+ + \frac{\ell_{2\perp}^2 + M^2}{2(q^- - \ell_2^-)} - \frac{M^2}{2q^-} = \frac{\ell_{2\perp}^2 + y^2 M^2}{2y(1-y)q^-}, \\ \mathcal{H}_M^{(\ell_2, p_2)} &= \ell_2^+ + p_2^+ - \frac{M^2}{2q^-} = \frac{\ell_{2\perp}^2 - yM^2}{2yq^-} + \frac{(\ell_{2\perp} - \mathbf{k}_\perp)^2 + M^2}{2q^- (1-y+\eta y)}. \end{aligned} \quad (44)$$

There are seven other diagrams, including non-central-cut diagrams, present in kernel-1, whose contributions to the hadronic tensor $W_1^{\mu\nu}$ is in Appendix A.

⁷ The integral over d^4z just gives an overall normalization factor, which is absorbed in the redefinition of the operator product expectation value.

⁸ In Eq. 43, the expectation value $\langle \bar{\psi} \gamma^+ \psi \rangle$ was translated by a different amount than $\langle A^+ A^+ \rangle$.

IV. SINGLE-SCATTERING INDUCED EMISSION: ONE PHOTON AND ONE GLUON IN THE FINAL STATE

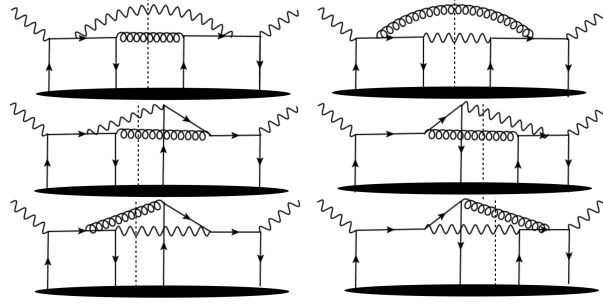


FIG. 6: Diagrams in kernel-2 giving a real photon and a gluon final states. The 2nd scattering with the nuclear medium is mediated by the exchange of a Glauber quark.

The possible diagrams that give rise to the photon-gluon final state are illustrated in Fig. 6. There are a total of 6 central-cut diagrams. These diagrams are referred to as kernel-2 in the remainder of the paper. As in the previous section, the calculation of the central cut with the most salient information is given before the final hadronic tensor $W_2^{\mu\nu}$ is quoted.

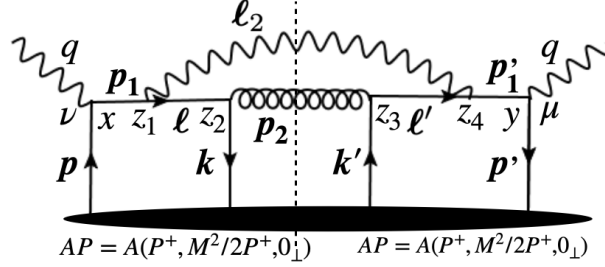


FIG. 7: A forward scattering diagram in kernel-2. It consists of fermion-to-boson conversion process, giving a real photon and a gluon final states.

The diagram under consideration is shown in Fig. 7. In that diagram, the hard quark produced from the initial-state hard scattering undergoes collinear emission followed by in-medium fermion-to-boson conversion. The forward scattering amplitude of this process is given as

$$\begin{aligned}
T_{2,c}^{\mu\nu} &= e^2 e_q^2 g_s^2 \int d^4x d^4y d^4z_1 d^4z_2 d^4z_3 d^4z_4 \int \frac{d^4p_1}{(2\pi)^4} \frac{d^4p'_1}{(2\pi)^4} \frac{d^4\ell}{(2\pi)^4} \frac{d^4\ell'}{(2\pi)^4} \frac{d^4\ell_2}{(2\pi)^4} \frac{d^4p_2}{(2\pi)^4} \\
&\times e^{iy(q-p'_1)} e^{-ix(q-p_1)} e^{iz_1(\ell-p_1+\ell_2)} e^{iz_2(-\ell+p_2)} e^{iz_3(\ell'-p_2)} e^{iz_4(p'_1-\ell'-\ell_2)} \\
&\times \left\langle AP \left| \text{Tr} \left[\psi(x) \bar{\psi}(y) \gamma^\mu \frac{\not{p}'_1}{(p'^2_1 + i\epsilon)} \gamma^{\sigma_4} \frac{\not{\ell}'}{(\ell'^2 + i\epsilon)} \gamma^{\sigma_3} \psi(z_3) \bar{\psi}(z_2) \gamma^{\sigma_2} \frac{\not{\ell}}{(\ell^2 + i\epsilon)} \gamma^{\sigma_1} \frac{\not{p}_1}{(p^2_1 + i\epsilon)} \gamma^\nu \right] \right| AP \right\rangle \\
&\times \frac{d_{\sigma_4 \sigma_1}^{(\ell_2)}}{\ell_2^2 + i\epsilon} \frac{d_{\sigma_3 \sigma_2}^{(p_2)}}{p_2^2 + i\epsilon} \text{Tr} [t^a t^b] \delta^{ab},
\end{aligned} \tag{45}$$

where $d_{\sigma_4 \sigma_1}^{(\ell_2)}$ and $d_{\sigma_3 \sigma_2}^{(p_2)}$ are defined as in Eq. 11, while the color algebra can be simplified to

$$\text{Tr} [t^a t^b] \delta^{ab} = \frac{\delta^{ab}}{2} \delta^{ab} = \frac{1}{2} \sum_{i=1}^8 \delta^{ii} = \frac{N_c^2 - 1}{2} = C_f N_c. \tag{46}$$

The integral over d^4z_1 and d^4z_4 can be carried out to yield $(2\pi)^{(4)} \delta^4(\ell - p_1 + \ell_2) (2\pi)^4 \delta^{(4)}(p'_1 - \ell' - \ell_2)$, allowing the integration over $d^4\ell$ and $d^4\ell'$ to be performed. Moreover, instituting the change of variable $p'_1 = q + p'$ and $p_1 = q + p$ in Eq. 45 modifies the integration $d^4p'_1 \rightarrow d^4p'$, while $d^4p_1 \rightarrow d^4p$. Applying Cutkosky's rule [41], the hadronic tensor

for the central-cut diagram is

$$\begin{aligned}
W_{2,c}^{\mu\nu} &= e^2 e_q^2 g_s^2 C_f N_c \int d^4 x d^4 y d^4 z_2 d^4 z_3 \int \frac{d^4 p}{(2\pi)^4} \frac{d^4 p'}{(2\pi)^4} \frac{d^4 \ell_2}{(2\pi)^4} \frac{d^4 p_2}{(2\pi)^4} e^{-iy p'} e^{ipx} \left\langle P \left| \bar{\psi}(y) \frac{\gamma^+}{4} \psi(x) \right| P \right\rangle \\
&\times (2\pi) \delta(\ell_2^2) (2\pi) \delta(p_2^2) \times e^{iz_2(p_2 + \ell_2 - q - p)} e^{iz_3(q + p' - \ell_2 - p_2)} \left\langle P_{A-1} \left| \bar{\psi}(z_2) \frac{\gamma^+}{4} \psi(z_3) \right| P_{A-1} \right\rangle \\
&\times \frac{\text{Tr} [\gamma^- \gamma^\mu (\not{q} + \not{p}') \gamma^{\sigma_4} (\not{q} + \not{p}' - \not{\ell}_2) \gamma^{\sigma_3} \gamma^- \gamma^{\sigma_2} (\not{q} + \not{p} - \not{\ell}_2) \gamma^{\sigma_1} (\not{q} + \not{p}) \gamma^\nu]}{\left[(q+p)^2 - i\epsilon \right] \left[(q+p' - \ell_2)^2 - i\epsilon \right] \left[(q+p - \ell_2)^2 + i\epsilon \right] \left[(q+p)^2 + i\epsilon \right]} d_{\sigma_4 \sigma_1}^{(\ell_2)} d_{\sigma_3 \sigma_2}^{(p_2)},
\end{aligned} \tag{47}$$

where the discontinuity in the final state photon and gluon propagators has been applied, namely

$$\begin{aligned}
\text{Disc} \left[\frac{1}{\ell_2^2 + i\epsilon} \right] &= 2\pi \delta(\ell_2^2), \\
\text{Disc} \left[\frac{1}{p_2^2 + i\epsilon} \right] &= 2\pi \delta(p_2^2).
\end{aligned} \tag{48}$$

Equation 47 exhibits a singularity when the quark propagator for p_1 , ℓ , ℓ' and p'_1 becomes on-shell. There are two simple poles for p^+ and p'^+ , respectively. The contour integration for p^+ in the complex plane gives

$$\begin{aligned}
\tilde{C}_1 &= \oint \frac{dp^+}{(2\pi)} \frac{e^{ip^+(x^- - z_2^-)}}{\left[(q+p)^2 + i\epsilon \right] \left[(q+p - \ell_2)^2 + i\epsilon \right]} \\
&= \frac{(2\pi i)}{2\pi} \frac{\theta(x^- - z_2^-)}{4q^- (q^- - \ell_2^-)} e^{-iq^+(x^- - z_2^-)} \left[\frac{-1 + e^{i\mathcal{G}_0^{(\ell_2)}(x^- - z_2^-)}}{\mathcal{G}_0^{(\ell_2)}} \right],
\end{aligned} \tag{49}$$

where

$$\mathcal{G}_0^{(\ell_2)} = \ell_2^+ + \frac{\ell_{2\perp}^2}{2(q^- - \ell_2^-)} = \frac{\ell_{2\perp}^2}{2y(1-y)q^-}. \tag{50}$$

On the other hand, the contour integration over p'^+ yields

$$\begin{aligned}
\tilde{C}_2 &= \oint \frac{dp'^+}{(2\pi)} \frac{e^{-ip'^+(y^- - z_3^-)}}{\left[(q+p')^2 - i\epsilon \right] \left[(q+p' - \ell_2)^2 - i\epsilon \right]} \\
&= \frac{(-2\pi i)}{2\pi} \frac{\theta(y^- - z_3^-)}{4q^- (q^- - \ell_2^-)} e^{iq^+(y^- - z_3^-)} \left[\frac{-1 + e^{-i\mathcal{G}_0^{(\ell_2)}(y^- - z_3^-)}}{\mathcal{G}_0^{(\ell_2)}} \right].
\end{aligned} \tag{51}$$

To perform the remaining integrals for p and p' , the same procedure as in Eq. 26 was followed yielding $(2\pi)^3 \delta(x^+ - z_2^+) \delta^2(\mathbf{x}_\perp - \mathbf{z}_{2\perp}) (2\pi)^3 \delta(-y^+ + z_3^+) \delta^2(-\mathbf{y}_\perp + \mathbf{z}_{3\perp})$. Using these δ -functions allows to performing the integral over spacetime variables (x^+, \mathbf{x}_\perp) and (y^+, \mathbf{y}_\perp) to give

$$\begin{aligned}
W_{2,c}^{\mu\nu} &= e^2 e_q^2 g_s^2 [C_f N_c] \int dx^- dy^- d^4 z_2 d^4 z_3 \int \frac{d^4 \ell_2}{(2\pi)^4} \frac{d^4 p_2}{(2\pi)^4} \left\langle P \left| \bar{\psi}(z_3^+, y^-, \mathbf{z}_{3\perp}) \frac{\gamma^+}{4} \psi(z_2^+, x^-, \mathbf{z}_{2\perp}) \right| P \right\rangle \\
&\times \frac{\theta(x^- - z_2^-) \theta(y^- - z_3^-)}{(2q^-)^2 [2(q^- - \ell_2^-)]^2} \left[\mathcal{G}_0^{(\ell_2)} \right]^{-2} e^{iq^+(y^- - x^- - z_3^- + z_2^-)} \left[-1 + e^{i\mathcal{G}_0^{(\ell_2)}(x^- - z_2^-)} \right] \left[-1 + e^{-i\mathcal{G}_0^{(\ell_2)}(y^- - z_3^-)} \right] \\
&\times e^{iz_3(q - p_2 - \ell_2)} e^{iz_2(\ell_2 + p_2 - q)} \left\langle P_{A-1} \left| \bar{\psi}(z_2) \frac{\gamma^+}{4} \psi(z_3) \right| P_{A-1} \right\rangle (2\pi) \delta(\ell_2^2) (2\pi) \delta(p_2^2) d_{\sigma_1 \sigma_4}^{(\ell_2)} d_{\sigma_3 \sigma_2}^{(p_2)} \\
&\times \text{Tr} [\gamma^- \gamma^\mu (\not{q} + \not{p}') \gamma^{\sigma_4} (\not{q} + \not{p}' - \not{\ell}_2) \gamma^{\sigma_3} \gamma^- \gamma^{\sigma_2} (\not{q} + \not{p} - \not{\ell}_2) \gamma^{\sigma_1} (\not{q} + \not{p}) \gamma^\nu].
\end{aligned} \tag{52}$$

Applying a similar algebraic manipulation to those presented in Eqs. 30 through 36, along with the momentum

fraction y as $\ell_2^- = yq^-$, allows to reduce the hadronic tensor $W_{2,c}^{\mu\nu}$ to

$$\begin{aligned}
W_{2,c}^{\mu\nu} &= e^2 e_q^2 g_s^2 [C_f N_c] \int dx^- dy^- d^4 z_2 d^4 z_3 \int \frac{dy d^2 \ell_{2\perp}}{(2\pi)^3} \frac{d^2 p_{2\perp}}{(2\pi)^2} \delta(z_2^+ - z_3^+) \left\langle P \left| \bar{\psi}(z_3^+, y^-, \mathbf{z}_{3\perp}) \frac{\gamma^+}{4} \psi(z_2^+, x^-, \mathbf{z}_{2\perp}) \right| P \right\rangle \\
&\times \frac{\theta(x^- - z_2^-) \theta(y^- - z_3^-)}{(2q^-)^2 [2(q^- - \ell_2^-)]^2} \left[\mathcal{G}_0^{(\ell_2)} \right]^{-2} e^{iq^+(y^- - x^-)} \left[-1 + e^{i\mathcal{G}_0^{(\ell_2)}(x^- - z_2^-)} \right] \left[-1 + e^{-i\mathcal{G}_0^{(\ell_2)}(y^- - z_3^-)} \right] \\
&\times e^{i(z_2^- - z_3^-) \mathcal{H}_0^{(\ell_2, p_2)}} e^{-i(\mathbf{p}_{2\perp} + \boldsymbol{\ell}_{2\perp}) \cdot (\mathbf{z}_{2\perp} - \mathbf{z}_{3\perp})} e^{-ik^-(z_3^+ - z_2^+)} \langle P_{A-1} | \bar{\psi}(z_2) \frac{\gamma^+}{4} \psi(z_3) | P_{A-1} \rangle \frac{1}{2y} \frac{1}{2(1-y+\eta y)q^-} \\
&\times \text{Tr} \left[\gamma^- \gamma^\mu (\not{q} + \not{p}') \gamma^{\sigma_4} (\not{q} + \not{p}' - \not{\ell}_2) \gamma^{\sigma_3} \gamma^- \gamma^{\sigma_2} (\not{q} + \not{p} - \not{\ell}_2) \gamma^{\sigma_1} (\not{q} + \not{p}) \gamma^\nu \right] d_{\sigma_1 \sigma_4}^{(\ell_2)} d_{\sigma_3 \sigma_2}^{(p_2)},
\end{aligned} \tag{53}$$

where $k^- = \eta \ell_2^- = \eta y q^-$ and

$$\mathcal{G}_0^{(\ell_2)} = \frac{\boldsymbol{\ell}_{2\perp}^2}{2y(1-y)q^-}, \tag{54}$$

$$\mathcal{H}_0^{(\ell_2, p_2)} = \ell_2^+ + p_2^+ = \frac{\boldsymbol{\ell}_{2\perp}^2}{2yq^-} + \frac{\mathbf{p}_{2\perp}^2}{2q^-(1-y+\eta y)}. \tag{55}$$

In Eq. 53, all phases that depend on the relative distances $y^- - x^-$ — i.e. $e^{iq^+(y^- - x^-)}$ herein — are absorbed in the definition of the quark parton distribution function (PDF), while all phases that depend on $z_3^- - z_2^-$ — specifically $e^{-i(z_3^- - z_2^-) \mathcal{H}_0^{(\ell_2, p_2)}}$ and $e^{i\mathbf{k}_\perp \cdot (\mathbf{z}_{3\perp} - \mathbf{z}_{2\perp})}$ — are part of the in-medium distribution function. Since the process (Fig. 7) in the amplitude and the complex conjugate are identical, the associated $W^{\mu\nu}$ or the amplitude square should be a real number, therefore, the remaining phase factors $\left[-1 + e^{i\mathcal{G}_0^{(\ell_2)}(x^- - z_2^-)} \right] \left[-1 + e^{-i\mathcal{G}_0^{(\ell_2)}(y^- - z_3^-)} \right]$ must be real-valued. Thus, using the same arguments as in Eq. 38 yields

$$\mathcal{R} = \left[2 - 2 \cos \left\{ \mathcal{G}_0^{(\ell_2)} (y^- - z_3^-) \right\} \right] = \left[2 - 2 \cos \left\{ \mathcal{G}_0^{(\ell_2)} (x^- - z_2^-) \right\} \right]. \tag{56}$$

Of course, as in Eq. 38, $\zeta^- = y^- - z_3^- = x^- - z_2^-$, given that $x^- - z_2^-$ represents the distance between the primary and secondary scattering vertex in the amplitude, while $y^- - z_3^-$ is that same distance in the complex conjugate. Furthermore, using the same variables change in Eq. 36 and 39, as well as $\mathbf{p}_{2\perp} + \boldsymbol{\ell}_{2\perp} = \mathbf{k}_\perp$, allows to express the hadronic tensor as

$$\begin{aligned}
W_{2,c}^{\mu\nu} &= e^2 e_q^2 g_s^2 [C_f N_c] \int d(\Delta X^-) d\zeta^- d(\Delta z^-) d^2 \Delta z_\perp \int \frac{dy d^2 \ell_{2\perp}}{2\pi} \frac{d^2 k_\perp}{(2\pi)^2} \frac{d^2 p_{2\perp}}{(2\pi)^2} e^{iq^+ \Delta X^-} \left\langle P \left| \bar{\psi}(\Delta X^-) \frac{\gamma^+}{4} \psi(0) \right| P \right\rangle \\
&\times \frac{\theta(\zeta^-)}{(2q^-)^2 [2(q^- - \ell_2^-)]^2} \left[\mathcal{G}_0^{(\ell_2)} \right]^{-2} \left[2 - 2 \cos \left\{ \mathcal{G}_0^{(\ell_2)} \zeta^- \right\} \right] \frac{1}{2y} \frac{1}{2(1-y+\eta y)q^-} \\
&\times e^{-i\Delta z^- \mathcal{H}_0^{(\ell_2, p_2)}} e^{i\mathbf{k}_\perp \cdot \Delta \mathbf{z}_\perp} \left\langle P_{A-1} \left| \bar{\psi}(\zeta^-, 0) \frac{\gamma^+}{4} \psi(\zeta^-, \Delta z^-, \Delta \mathbf{z}_\perp) \right| P_{A-1} \right\rangle \\
&\times \text{Tr} \left[\gamma^- \gamma^\mu (\not{q} + \not{p}') \gamma^{\sigma_4} (\not{q} + \not{p}' - \not{\ell}_2) \gamma^{\sigma_3} \gamma^- \gamma^{\sigma_2} (\not{q} + \not{p} - \not{\ell}_2) \gamma^{\sigma_1} (\not{q} + \not{p}) \gamma^\nu \right] d_{\sigma_1 \sigma_4}^{(\ell_2)} d_{\sigma_3 \sigma_2}^{(p_2)}.
\end{aligned} \tag{57}$$

The trace in the equation above (Eq. 57) is now evaluated, giving

$$\begin{aligned}
&\text{Tr} \left[\gamma^- \gamma^\mu (\not{q} + \not{p}') \gamma^{\sigma_4} (\not{q} + \not{p}' - \not{\ell}_2) \gamma^{\sigma_3} \gamma^- \gamma^{\sigma_2} (\not{q} + \not{p} - \not{\ell}_2) \gamma^{\sigma_1} (\not{q} + \not{p}) \gamma^\nu \right] d_{\sigma_4 \sigma_1}^{(\ell_2)} d_{\sigma_3 \sigma_2}^{(p_2)} \\
&= (q^-)^2 [-g_{\perp\perp}^{\mu\nu}] \text{Tr} \left[\gamma^- \gamma^+ \gamma^{\sigma_4} (\not{q} + \not{p}' - \not{\ell}_2) \gamma^{\sigma_3} \gamma^- \gamma^{\sigma_2} (\not{q} + \not{p} - \not{\ell}_2) \gamma^{\sigma_1} \gamma^+ \right] d_{\sigma_4 \sigma_1}^{(\ell_2)} d_{\sigma_3 \sigma_2}^{(p_2)}.
\end{aligned} \tag{58}$$

The first non-vanishing term in $d_{\sigma_4 \sigma_1}^{(\ell_2)} d_{\sigma_3 \sigma_2}^{(p_2)}$ comes from $g_{\sigma_4 \sigma_1} g_{\sigma_3 \sigma_2}$, giving

$$\begin{aligned}
&(q^-)^2 [-g_{\perp\perp}^{\mu\nu}] \text{Tr} \left[\gamma^- \gamma^+ \gamma^{\sigma_4} (\not{q} + \not{p}' - \not{\ell}_2) \gamma^{\sigma_3} \gamma^- \gamma^{\sigma_2} (\not{q} + \not{p} - \not{\ell}_2) \gamma^{\sigma_1} \gamma^+ \right] g_{\sigma_4 \sigma_1} g_{\sigma_3 \sigma_2} \\
&= 32 [-g_{\perp\perp}^{\mu\nu}] (q^-)^2 \boldsymbol{\ell}_{2\perp}^2,
\end{aligned} \tag{59}$$

while the second stems from $\frac{n_{\sigma_4} \ell_{2\sigma_1}}{\ell_2^-} g_{\sigma_3\sigma_2}$ yielding ⁹

$$\begin{aligned}
& (q^-)^2 [-g_{\perp\perp}^{\mu\nu}] \text{Tr} [\gamma^- \gamma^+ \gamma^{\sigma_4} (\not{q} + \not{p}' - \not{\ell}_2) \gamma^{\sigma_3} \gamma^- \gamma^{\sigma_2} (\not{q} + \not{p} - \not{\ell}_2) \gamma^{\sigma_1} \gamma^+] \frac{(n_{\sigma_4} \ell_{2\sigma_1} + n_{\sigma_1} \ell_{2\sigma_4})}{n^+ \ell_2^-} (-g_{\sigma_3\sigma_2}) \\
& = 2 (q^-)^2 [-g_{\perp\perp}^{\mu\nu}] \text{Tr} [\gamma^- \gamma^+ \gamma^{\sigma_4} (\not{q} + \not{p}' - \not{\ell}_2) \gamma^{\sigma_3} \gamma^- \gamma^{\sigma_2} (\not{q} + \not{p} - \not{\ell}_2) \gamma^{\sigma_1} \gamma^+] \frac{n_{\sigma_4} \ell_{2\sigma_1}}{\ell_2^-} (-g_{\sigma_3\sigma_2}) \\
& = 64 [-g_{\perp\perp}^{\mu\nu}] (q^-)^2 \boldsymbol{\ell}_{2\perp}^2 \left[\frac{(1-y)^2}{y^2} + \frac{1-y}{y} \right].
\end{aligned} \tag{60}$$

Combining terms together, the trace is expressed as

$$\begin{aligned}
& \text{Tr} [\gamma^- \gamma^\mu (\not{q} + \not{p}') \gamma^{\sigma_4} (\not{q} + \not{p}' - \not{\ell}_2) \gamma^{\sigma_3} \gamma^- \gamma^{\sigma_2} (\not{q} + \not{p} - \not{\ell}_2) \gamma^{\sigma_1} (\not{q} + \not{p}) \gamma^\nu] d_{\sigma_4\sigma_1}^{(\ell_2)} d_{\sigma_3\sigma_2}^{(p_2)} \\
& = 32 [-g_{\perp\perp}^{\mu\nu}] (q^-)^2 \boldsymbol{\ell}_{2\perp}^2 \left[\frac{1 + (1-y)^2}{y^2} \right].
\end{aligned} \tag{61}$$

The final expression for the hadronic tensor (see Fig. 7) as

$$\begin{aligned}
W_{2,c}^{\mu\nu} & = 2e^2 e_q^2 g_s^2 C_f N_c [-g_{\perp\perp}^{\mu\nu}] \int d(\Delta X^-) e^{iq^+(\Delta X^-)} \left\langle P \left| \bar{\psi}(\Delta X^-) \frac{\gamma^+}{4} \psi(0) \right| P \right\rangle \\
& \times \int d(\Delta z^-) d^2(\Delta z_\perp) \frac{dy d^2\ell_{2\perp} d^2k_\perp}{2\pi (2\pi)^2 (2\pi)^2} \left[\frac{1 + (1-y)^2}{y} \right] e^{-i\Delta z^- \mathcal{H}_0^{(\ell_2, p_2)}} e^{i\mathbf{k}_\perp \cdot \Delta \mathbf{z}_\perp} \\
& \times \int d\zeta^- \frac{\theta(\zeta^-)}{(1-y+\eta y)q^-} \frac{1}{\boldsymbol{\ell}_{2\perp}^2} \left[2 - 2 \cos \left\{ \mathcal{G}_0^{(\ell_2)} \zeta^- \right\} \right] \left\langle P_{A-1} \left| \bar{\psi}(\zeta^-, 0) \frac{\gamma^+}{4} \psi(\zeta^-, \Delta z^-, \Delta \mathbf{z}_\perp) \right| P_{A-1} \right\rangle,
\end{aligned} \tag{62}$$

where

$$\mathcal{H}_0^{(\ell_2, p_2)} = \ell_2^+ + p_2^+ = \frac{\boldsymbol{\ell}_{2\perp}^2}{2yq^-} + \frac{(\boldsymbol{\ell}_{2\perp} - \mathbf{k}_\perp)^2}{2q^-(1-y+\eta y)}. \tag{63}$$

The above expression of the hadronic tensor (Eq. 62) when compared to the diagram in kernel-1, differs through the appearance of a two-point fermionic correlator $\langle \bar{\psi}(\zeta^-, 0) \frac{\gamma^+}{4} \psi(\zeta^-, \Delta z^-, \Delta \mathbf{z}_\perp) \rangle$, along with the factor of $(1-y+\eta y)q^-$ in the denominator. This indicates that the quark-to-gluon conversion processes are suppressed by the incoming energy of the quark, i.e., $(1-y+\eta y)q^-$. The five other diagrams contributing to kernel-2 are presented in Appendix B.

V. SINGLE-SCATTERING INDUCED EMISSION: WITH VIRTUAL PHOTON CORRECTIONS WITH A QUARK AND ANTIQUARK IN THE FINAL STATE

The possible diagrams at $\mathcal{O}(\alpha_s \alpha_{\text{EM}})$ involving a virtual photon with a quark and antiquark in the final state are given in Fig. 8, all of which contribute to kernel-3. There are 8 central-cut diagrams in this kernel. In this section, the main focus is given to the first diagram depicted in Fig. 9, where the radiated virtual photon absorbs an antiquark from the medium and turns into an antiquark. As the algebraic manipulation are identical to the ones illustrated in sections III and IV, a summary of the pole structure, phase/coherence factors, and traces evaluation is presented in this section.

⁹ Any term in $d_{\sigma_4\sigma_1}^{(\ell_2)} d_{\sigma_3\sigma_2}^{(p_2)}$ that is proportional to $n_{\sigma_3} \ell_{2\sigma_2}$ will contract with the $\gamma^{\sigma_3} \gamma^- \gamma^{\sigma_2}$ term in Eq. 59 to give $(n \cdot \gamma) \gamma^- (\ell_2 \cdot \gamma) = n_+ (\gamma^-)^2 (\ell_2 \cdot \gamma) \equiv 0$.

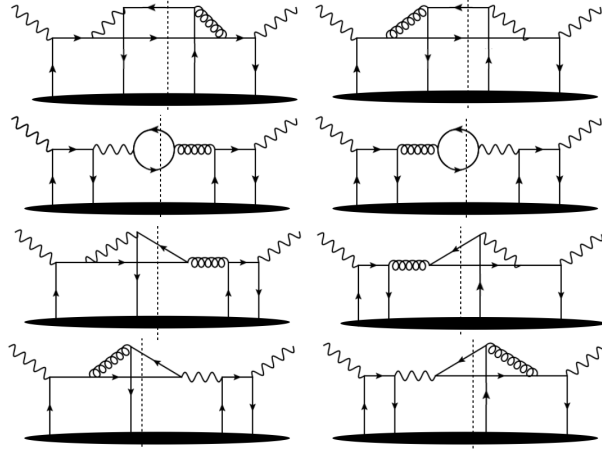


FIG. 8: Diagrams for single emission and single scattering kernel (kernel-3) giving quark and antiquark final states through a virtual photon.

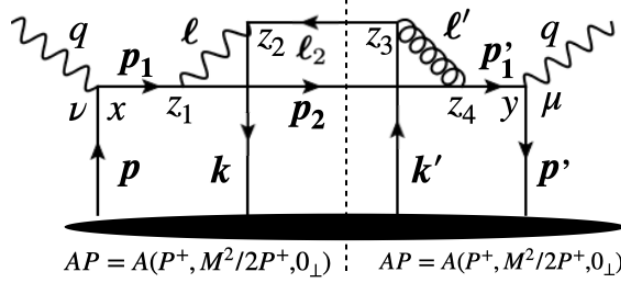


FIG. 9: The prototype diagram giving quark-antiquark final states involving a virtual photon.

The forward scattering amplitude $T_{3,c}^{\mu\nu}$ is shown in Fig. 9, whose mathematical expression reads

$$\begin{aligned}
T_{3,c}^{\mu\nu} &= e^2 e_q^2 g_s^2 N_f \int d^4 y d^4 x d^4 z_1 d^4 z_2 d^4 z_3 d^4 z_4 e^{iq(y-x)} \\
&\times \langle AP | \bar{\psi}(y) \gamma^\mu \int \frac{d^4 p'_1}{(2\pi)^4} \frac{i(\not{p}'_1 + M)}{p_1'^2 - M^2 + i\epsilon} e^{-ip'_1(y-z_4)} \gamma^{\sigma_4} \\
&\times \int \frac{d^4 p_2}{(2\pi)^4} \frac{i(\not{p}_2 + M)}{(p_2^2 - M^2 + i\epsilon)} e^{-ip_2(z_4-z_1)} \gamma^{\sigma_1} \int \frac{d^4 p_1}{(2\pi)^4} \frac{i(\not{p}_1 + M)}{(p_1^2 - M^2 + i\epsilon)} e^{-ip_1(z_1-x)} \gamma^\nu \psi(x) \\
&\times \bar{\psi}(z_2) \gamma^{\sigma_2} \int \frac{d^4 \ell_2}{(2\pi)^4} \frac{i\not{\ell}_2}{\ell_2^2 + i\epsilon} e^{-i\ell_2(z_3-z_2)} \gamma^{\sigma_3} \psi(z_3) |AP\rangle \\
&\times \int \frac{d^4 \ell}{(2\pi)^4} \frac{id_{\sigma_1 \sigma_2}^{(\ell)}}{\ell^2 + i\epsilon} \delta^{ab} \text{Tr} [t^a t^b] e^{-i\ell(z_2-z_1)} \int \frac{d^4 \ell'}{(2\pi)^4} \frac{id_{\sigma_3 \sigma_4}^{(\ell')}}{\ell'^2 + i\epsilon} e^{-i\ell'(z_4-z_3)},
\end{aligned} \tag{64}$$

where the factor N_f represents flavor degrees of freedom that can be exchanged with the QGP via scattering interactions. Equation 64 contains a product of two independent traces associated with two independent fermion

lines. Thus,

$$\begin{aligned}
T_{3,c}^{\mu\nu} &= e^2 e_q^2 g_s^2 N_f \int d^4x d^4y d^4z_1 d^4z_2 d^4z_3 d^4z_4 \int \frac{d^4p_1}{(2\pi)^4} \frac{d^4p'_1}{(2\pi)^4} \frac{d^4\ell}{(2\pi)^4} \frac{d^4\ell'}{(2\pi)^4} \frac{d^4\ell_2}{(2\pi)^4} \frac{d^4p_2}{(2\pi)^4} \\
&\times e^{i(q-p'_1)y} e^{-i(q-p_1)x} e^{i(\ell'-\ell_2)z_3} e^{i(-\ell+\ell_2)z_2} e^{i(p_2+\ell-p_1)z_1} e^{i(p'_1-\ell'-p_2)z_4} \\
&\times \left\langle P \left| \text{Tr} \left[\psi(x) \bar{\psi}(y) \gamma^\mu \frac{(\not{p}'_1 + M)}{[p_1'^2 - M^2 + i\epsilon]} \gamma^{\sigma_4} \frac{(\not{p}_2 + M)}{[p_2^2 - M^2 + i\epsilon]} \gamma^{\sigma_1} \frac{(\not{p}_1 + M)}{[p_1^2 - M^2 + i\epsilon]} \gamma^\nu \right] \right| P \right\rangle \\
&\times \left\langle P_{A-1} \left| \text{Tr} \left[\psi(z_3) \bar{\psi}(z_2) \gamma^{\sigma_2} \frac{\not{\ell}_2}{\ell_2^2 + i\epsilon} \gamma^{\sigma_3} \right] \right| P_{A-1} \right\rangle \frac{d_{\sigma_4 \sigma_3}^{(\ell')}}{\ell'^2 + i\epsilon} \frac{d_{\sigma_2 \sigma_1}^{(\ell)}}{\ell^2 + i\epsilon} \delta^{ab} \text{Tr} [t^a t^b].
\end{aligned} \tag{65}$$

Isolating the leading non-perturbative component in $\psi(x)\bar{\psi}(y)$ employs the prescription presented near Eq. 14 giving $\psi(x)\bar{\psi}(y) = \gamma^- \text{Tr} [\bar{\psi}(y) \frac{\gamma^+}{4} \psi(x)]$. Performing the d^4z_1 and d^4z_4 integration, yields

$$(2\pi)^4 \delta^4(q+p-\ell-p_2) (2\pi)^4 \delta^4(q+p'-\ell'-p_2). \tag{66}$$

These δ -functions allow integration over $d^4\ell$ and $d^4\ell'$, which, following the same procedure as that explained between Eqs. 15-18, gives

$$\begin{aligned}
W_{3,c}^{\mu\nu} &= e^2 e_q^2 g_s^2 N_f C_f N_c \int d^4x d^4y d^4z_2 d^4z_3 \int \frac{d^4p}{(2\pi)^4} \frac{d^4p'}{(2\pi)^4} \frac{d^4\ell_2}{(2\pi)^4} \frac{d^4p_2}{(2\pi)^4} e^{-ip'y} e^{ipx} \left\langle P \left| \bar{\psi}(y) \frac{\gamma^+}{4} \psi(x) \right| P \right\rangle \\
&\times e^{i(q+p'-p_2-\ell_2)z_3} e^{i(\ell_2+p_2-q-p)z_2} \frac{\text{Tr} \left[\gamma^- \gamma^\mu (\not{q} + \not{p}' + M) \gamma^{\sigma_4} (\not{p}_2 + M) \gamma^{\sigma_1} (\not{q} + \not{p} + M) \gamma^\nu \right]}{[(q+p')^2 - M^2 - i\epsilon] [(q+p)^2 - M^2 + i\epsilon]} \\
&\times \langle P_{A-1} | \text{Tr} [\psi(z_3) \bar{\psi}(z_2) \gamma^{\sigma_2} \not{\ell}_2 \gamma^{\sigma_3}] | P_{A-1} \rangle \frac{d_{\sigma_4 \sigma_3}^{(q+p'-p_2)}}{[(q+p'-p_2)^2 - i\epsilon]} \frac{d_{\sigma_2 \sigma_1}^{(q+p-p_2)}}{[(q+p-p_2)^2 + i\epsilon]} (2\pi) \delta(\ell_2^2) (2\pi) \delta(p_2^2 - M^2),
\end{aligned} \tag{67}$$

where color algebra gives the same result as in Eq. 46. Computing the complex contour integrals over propagator momenta gives

$$\begin{aligned}
\hat{C}_1 &= \oint \frac{dp^+}{(2\pi)} \frac{e^{ip^+(x^- - z_2^-)}}{[(q+p)^2 - M^2 + i\epsilon] [(q+p-p_2)^2 + i\epsilon]} \\
&= \frac{(2\pi i)}{2\pi} \frac{\theta(x^- - z_2^-)}{4q^-(q^- - p_2^-)} e^{i(-q^+ + \frac{M^2}{2q^-})(x^- - z_2^-)} \left[\frac{-1 + e^{i\mathcal{G}_M^{(p_2)}(x^- - z_2^-)}}{\mathcal{G}_M^{(p_2)}} \right],
\end{aligned} \tag{68}$$

where

$$\mathcal{G}_M^{(p_2)} = p_2^+ + \frac{\mathbf{p}_{2\perp}^2}{2(q^- - p_2^-)} - \frac{M^2}{2q^-}. \tag{69}$$

The contour integration for p'^+ gives

$$\begin{aligned}
\hat{C}_2 &= \oint \frac{dp'^+}{(2\pi)} \frac{e^{-ip'^+(y^- - z_3^-)}}{[(q+p')^2 - M^2 - i\epsilon] [(q+p'-p_2)^2 - i\epsilon]} \\
&= \frac{(-2\pi i)}{2\pi} \frac{\theta(y^- - z_3^-)}{4q^-(q^- - p_2^-)} e^{-i(-q^+ + \frac{M^2}{2q^-})(y^- - z_3^-)} \left[\frac{-1 + e^{-i\mathcal{G}_M^{(p_2)}(y^- - z_3^-)}}{\mathcal{G}_M^{(p_2)}} \right].
\end{aligned} \tag{70}$$

Using the following relationships for kinematic variables in the light-cone coordinates (c.f. Sec. III)

$$\begin{aligned}
p_2^+ &= \frac{M^2 + \mathbf{p}_{2\perp}^2}{2p_2^-}, \quad \ell_2^+ = \frac{\ell_{2\perp}^2}{2\ell_2^-}, \quad \eta = \frac{k^-}{yq^-}, \quad \ell_2^- = yq^-, \\
\mathbf{p}_{2\perp} &= -\ell_{2\perp} + \mathbf{k}_\perp, \quad p_2^- = q^- + k^- - \ell_2^- = q^-(1 - y + \eta y),
\end{aligned} \tag{71}$$

allows to rewrite the denominator in the square bracket of Eq. 68, as well as Eq. 70, as

$$\mathcal{G}_M^{(p_2)} = \frac{(\boldsymbol{\ell}_{2\perp} - \mathbf{k}_\perp)^2 + y^2(1-\eta)^2 M^2}{2q^- y(1-y+\eta y)(1-\eta)}. \quad (72)$$

Thus, the hadronic tensor $W_{3,c}^{\mu\nu}$ becomes

$$\begin{aligned} W_{3,c}^{\mu\nu} &= e^2 e_q^2 g_s^2 N_f C_f N_c \int dx^- dy^- d^4 z_2 d^4 z_3 \int \frac{d^4 \ell_2}{(2\pi)^4} \frac{d^4 p_2}{(2\pi)^4} e^{i(-q^+ + \frac{M^2}{2q^-})(x^- - y^- + z_3^- - z_2^-)} \left\langle P \left| \bar{\psi}(y) \frac{\gamma^+}{4} \psi(x) \right| P \right\rangle \\ &\times \left[-1 + e^{i\mathcal{G}_M^{(p_2)}(x^- - z_2^-)} \right] \left[-1 + e^{-i\mathcal{G}_M^{(p_2)}(y^- - z_3^-)} \right] e^{i(q^+ - p_2^+ - \ell_2^+)(z_3^- - z_2^-)} e^{i(q^- - p_2^- - \ell_2^-)(z_3^+ - z_2^+)} e^{i(\mathbf{p}_{2\perp} + \boldsymbol{\ell}_{2\perp}) \cdot (\mathbf{z}_{3\perp} - \mathbf{z}_{2\perp})} \\ &\times \frac{\theta(x^- - z_2^-) \theta(y^- - z_3^-)}{(2q^-)^2 [2yq^- (1-\eta)]^2} \left[\mathcal{G}_M^{(p_2)} \right]^{-2} \text{Tr} \left[\gamma^- \gamma^\mu (\not{q} + \not{p}' + M) \gamma^{\sigma_4} (\not{p}_2 + M) \gamma^{\sigma_1} (\not{q} + \not{p} + M) \gamma^\nu \right] \\ &\times \langle P_{A-1} | \text{Tr} [\psi(z_3) \bar{\psi}(z_2) \gamma^{\sigma_2} \not{\ell}_2 \gamma^{\sigma_3}] | P_{A-1} \rangle d_{\sigma_4 \sigma_3}^{(q+p'-p_2)} d_{\sigma_2 \sigma_1}^{(q+p-p_2)} (2\pi) \delta(\ell_2^2) (2\pi) \delta(p_2^2 - M^2). \end{aligned} \quad (73)$$

In the above expression, the phases that involve $x^- - y^-$ would be absorbed in the definition of the PDF of the correlator $\langle \bar{\psi}(y) \frac{\gamma^+}{4} \psi(x) \rangle$ and the phases that involve $z_3^- - z_2^-$ would be absorbed in the definition of the correlator $\langle \bar{\psi}(z_2) \frac{\gamma^+}{4} \psi(z_3) \rangle$. Since both of these distribution functions are real and finite, the remaining phase factor, i.e. $\left[-1 + e^{i\mathcal{G}_M^{(p_2)}(x^- - z_2^-)} \right] \left[-1 + e^{-i\mathcal{G}_M^{(p_2)}(y^- - z_3^-)} \right]$ must be a real-valued number, as in Eq. 38. Therefore,

$$\mathcal{R} = \left[2 - 2 \cos \left\{ \mathcal{G}_M^{(p_2)} (y^- - z_3^-) \right\} \right] = \left[2 - 2 \cos \left\{ \mathcal{G}_M^{(p_2)} (x^- - z_2^-) \right\} \right]. \quad (74)$$

The trace is now evaluated to give

$$\begin{aligned} &\text{Tr} \left[\gamma^- \gamma^\mu (\not{q} + \not{p} + M) \gamma^{\sigma_4} (\not{p}_2 + M) \gamma^{\sigma_1} (\not{q} + \not{p} + M) \gamma^\nu \right] \text{Tr} [\gamma^- \gamma^{\sigma_2} \not{\ell}_2 \gamma^{\sigma_3}] d_{\sigma_4 \sigma_3}^{(q+p'-p_2)} d_{\sigma_2 \sigma_1}^{(q+p-p_2)} \\ &= (q^-)^2 \text{Tr} \left[\gamma^- \gamma_\perp^\mu \left(\gamma^+ + \frac{M}{q^-} \right) \gamma^{\sigma_4} (\not{p}_2 + M) \gamma^{\sigma_1} \left(\gamma^+ + \frac{M}{q^-} \right) \gamma_\perp^\nu \right] \text{Tr} [\gamma^- \gamma^{\sigma_2} \not{\ell}_2 \gamma^{\sigma_3}] \\ &\times \left[-g_{\sigma_4 \sigma_3} + \frac{n_{\sigma_4} (q + p' - p_2)_{\sigma_3} + n_{\sigma_3} (q + p - p_2)_{\sigma_4}}{n \cdot (q + p' - p_2)} \right] \left[-g_{\sigma_2 \sigma_1} + \frac{n_{\sigma_2} (q + p - p_2)_{\sigma_1} + n_{\sigma_1} (q + p - p_2)_{\sigma_2}}{n \cdot (q + p - p_2)} \right], \end{aligned} \quad (75)$$

where the non-trivial contributions stem from

$$\begin{aligned} &(q^-)^2 \text{Tr} \left[\gamma^- \gamma_\perp^\mu \gamma^+ \gamma^{\sigma_4} (\not{p}_2 + M) \gamma^{\sigma_1} \gamma^+ \gamma_\perp^\nu \right] \text{Tr} [\gamma^- \gamma^{\sigma_2} \not{\ell}_2 \gamma^{\sigma_3}] [-g_{\sigma_4 \sigma_3}] [-g_{\sigma_2 \sigma_1}] \\ &= 64(q^-)^2 (-g_{\perp\perp}^{\mu\nu}) \left\{ \left(\frac{1-y+\eta y}{y} \right) \boldsymbol{\ell}_{2\perp}^2 + \frac{y}{1-y+\eta y} \left[\frac{M^2 + (\boldsymbol{\ell}_{2\perp} - \mathbf{k}_\perp)^2}{2} \right] + (\boldsymbol{\ell}_{2\perp} - \mathbf{k}_\perp)^2 \right\}, \end{aligned} \quad (76)$$

as well as

$$\begin{aligned} &(q^-)^2 \text{Tr} \left[\gamma^- \gamma_\perp^\mu \gamma^+ \gamma^{\sigma_4} (\not{p}_2 + M) \gamma^{\sigma_1} \gamma^+ \gamma_\perp^\nu \right] \text{Tr} [\gamma^- \gamma^{\sigma_2} \not{\ell}_2 \gamma^{\sigma_3}] \left[\frac{n_{\sigma_4} (q + p' - p_2)_{\sigma_3}}{n \cdot (q + p' - p_2)} \right] \left[\frac{n_{\sigma_1} (q + p - p_2)_{\sigma_2}}{n \cdot (q + p - p_2)} \right] \\ &= 64(q^-)^2 (-g_{\perp\perp}^{\mu\nu}) \left[\frac{1-y+\eta y}{y} \right] \left[-\boldsymbol{\ell}_{2\perp}^2 + (\boldsymbol{\ell}_{2\perp} - \mathbf{k}_\perp)^2 \right], \end{aligned} \quad (77)$$

where the same procedure as in Eqs. 58-61 was used to obtain this result. Adding contributions in Eq. 76 and Eq. 77 together gives

$$\begin{aligned} &\text{Tr} \left[\gamma^- \gamma^\mu (\not{q} + \not{p} + M) \gamma^{\sigma_4} (\not{p}_2 + M) \gamma^{\sigma_1} (\not{q} + \not{p} + M) \gamma^\nu \right] \text{Tr} [\gamma^- \gamma^{\sigma_2} \not{\ell}_2 \gamma^{\sigma_3}] d_{\sigma_4 \sigma_3}^{(q+p'-p_2)} d_{\sigma_2 \sigma_1}^{(q+p-p_2)} \\ &= 64(q^-)^2 (-g_{\perp\perp}^{\mu\nu}) \left[(\boldsymbol{\ell}_{2\perp} - \mathbf{k}_\perp)^2 \left\{ \frac{1+(1-y)^2}{2y(1-y+\eta y)} \right\} + \frac{M^2}{2} \left\{ \frac{y}{1-y+\eta y} \right\} \right] \\ &= 32(q^-)^2 (-g_{\perp\perp}^{\mu\nu}) \left\{ \frac{1+(1-y)^2}{y(1-y+\eta y)} \right\} \left[(\boldsymbol{\ell}_{2\perp} - \mathbf{k}_\perp)^2 + \kappa M^2 y^2 \right], \end{aligned} \quad (78)$$

where κ is given in Eq. 42. The final expression for the hadronic tensor is

$$\begin{aligned}
W_{3,c}^{\mu\nu} &= 2e^2 e_q^2 g_s^2 N_f C_f N_c [-g_{\perp\perp}^{\mu\nu}] \int d(\Delta X^-) e^{i\Delta X^- (q^+ - \frac{M^2}{2q^-})} \left\langle P \left| \bar{\psi}(\Delta X^-) \frac{\gamma^+}{4} \psi(0) \right| P \right\rangle \\
&\times \int d(\Delta z^-) d^2 \Delta \mathbf{z}_\perp \frac{dy}{2\pi} \frac{d^2 \ell_{2\perp}}{(2\pi)^2} \frac{d^2 k_\perp}{(2\pi)^2} \left[\frac{1 + (1-y)^2}{y} \right] e^{-i\Delta z^- \mathcal{H}_M^{(\ell_2, p_2)}} e^{i\mathbf{k}_\perp \cdot \Delta \mathbf{z}_\perp} \\
&\times \int d\zeta^- \frac{\theta(\zeta^-)}{yq^-} \frac{[(\ell_{2\perp} - \mathbf{k}_\perp)^2 + \kappa M^2 y^2]}{[(\ell_{2\perp} - \mathbf{k}_\perp)^2 + y^2 (1-\eta)^2 M^2]^2} \left[2 - 2 \cos \left\{ \mathcal{G}_M^{(p_2)} \zeta^- \right\} \right] \\
&\times \left\langle P_{A-1} \left| \text{Tr} \left[\bar{\psi}(\zeta^-, 0) \frac{\gamma^+}{4} \psi(\zeta^-, \Delta z^-, \Delta \mathbf{z}_\perp) \right] \right| P_{A-1} \right\rangle,
\end{aligned} \tag{79}$$

where $\mathcal{G}_M^{(p_2)}$ is defined in Eq. 72 and $\mathcal{H}_M^{(\ell_2, p_2)}$ is given as

$$\mathcal{H}_M^{(\ell_2, p_2)} = \ell_2^+ + p_2^+ - \frac{M^2}{2q^-} = \frac{\ell_{2\perp}^2}{2\ell_2^-} - \frac{M^2}{2q^-} + \frac{M^2 + \mathbf{p}_{2\perp}^2}{2p_2^-} = \frac{\ell_{2\perp}^2 - yM^2}{2yq^-} + \frac{(\ell_{2\perp} - \mathbf{k}_\perp)^2 + M^2}{2q^-(1-y+\eta y)}. \tag{80}$$

The third line of Eq. 79 contains the spacetime-dependent coherence factor, which in the limit $M = 0$ and $\eta = 0$, gives

$$\mathcal{I} = \int_0^{\tau_f} d\zeta^- \frac{2 - 2 \cos \left\{ \frac{(\ell_{2\perp} - \mathbf{k}_\perp)^2 \zeta^-}{2q^- y(1-y)} \right\}}{(\ell_{2\perp} - \mathbf{k}_\perp)^2}, \tag{81}$$

where $\tau_f = 2q^- y(1-y)/\ell_{2\perp}^2$ represents the formation time of the virtual radiated photon. In Eq. 81 the ζ^- dependence of the two-point fermionic correlator (see in the fourth line of Eq. 79) has been omitted. The integral \mathcal{I} encapsulates spacetime quantum interference between boson radiation vertex and subsequent in-medium splitting, i.e. when $\ell_{2\perp} \approx \mathbf{k}_\perp$ the value of this integral is dominant. Thus, in order for the in-medium quark to resolve the radiative splitting, the transverse size of the radiative splitting $\ell_{2\perp}$ should be of similar size to the in-medium quark's transverse momentum given by \mathbf{k}_\perp . Moreover, when comparing the hadronic tensor in Eq. 79 with Eq. 43 describing kernel-1, one notices an additional factor yq^- in the denominator. This indicates that diagrams involving a fermionic correlator are suppressed by the energy q^- of the hard quark. There are seven additional diagrams contributing to kernel-3 and thus to the $W_3^{\mu\nu}$ hadronic tensor; these are presented in Appendix C.

VI. SINGLE-SCATTERING INDUCED EMISSION: VIRTUAL PHOTON CORRECTIONS WITH TWO QUARKS IN THE FINAL STATE

This section briefly outlines the steps involved in deriving the hadronic tensor for kernel-4. The possible diagrams at $\mathcal{O}(\alpha_s \alpha_{EM})$ involving a virtual photon are given in Fig. 10 below. These consist of two quarks in the final state. There are a total of 4 possible diagrams leading to photon correction at $\mathcal{O}(\alpha_{em} \alpha_s)$. The diagrams contain one photon propagator and one gluon propagator on either side of the cut-line.

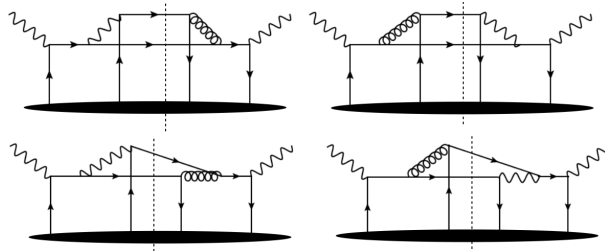


FIG. 10: All diagrams with quark-quark final states contributing to kernel-4.

As before, we present the calculation for one of the forward scattering diagrams shown in Fig 11. Since algebraic manipulations are similar to kernel-1, kernel-2 and kernel-3, we only present contour integration and involved traces

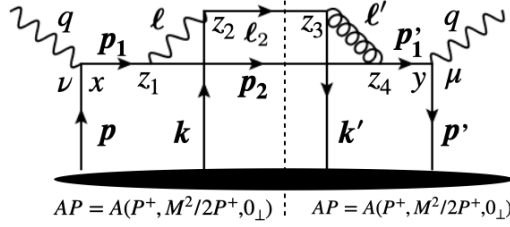


FIG. 11: The prototypical diagram contributing to kernel-4.

in the final calculation of the hadronic tensor. The hadronic tensor corresponding to the diagram (Fig. 11) is given as

$$\begin{aligned}
W_{4,c}^{\mu\nu} &= e^2 e_q^2 g_s^2 N_f \int d^4x d^4y d^4z_2 d^4z_3 \int \frac{d^4p}{(2\pi)^4} \frac{d^4p'}{(2\pi)^4} \frac{d^4\ell_2}{(2\pi)^4} \frac{d^4p_2}{(2\pi)^4} e^{-ip'y} e^{ipx} \left\langle P \left| \bar{\psi}(y) \frac{\gamma^+}{4} \psi(x) \right| P \right\rangle \delta^{cd} \text{Tr}[t^c t^d] \\
&\times e^{i(q+p'-p_2-\ell_2)z_3} e^{i(\ell_2+p_2-q-p)z_2} \left\langle P_{A-1} \left| \bar{\psi}(z_3) \frac{\gamma^+}{4} \psi(z_2) \right| P_{A-1} \right\rangle d_{\sigma_1\sigma_2}^{(q+p-p_2)} d_{\sigma_3\sigma_4}^{(q+p'-p_2)} (2\pi)\delta(\ell_2^2) (2\pi)\delta(p_2^2 - M^2) \\
&\times \frac{\text{Tr} \left[\gamma^- \gamma^\mu (\not{q} + \not{p}' + M) \gamma^{\sigma_4} (\not{p}_2 + M) \gamma^{\sigma_1} (\not{q} + \not{p} + M) \gamma^\nu \right] \text{Tr} [\gamma^- \gamma^{\sigma_3} \not{\ell}_2 \gamma^{\sigma_2}]}{\left[(q+p')^2 - M^2 - i\epsilon \right] \left[(q+p)^2 - M^2 + i\epsilon \right] \left[(q+p'-p_2)^2 - i\epsilon \right] \left[(q+p-p_2)^2 + i\epsilon \right]}.
\end{aligned} \tag{82}$$

Note, the diagram presented in the previous section (Fig. 9) is different than the current one. Previously, the internal parton line emerging from the nuclear medium was antiquark, whereas it is a quark line herein (Fig. 11). Therefore, the ordering of the quark fields is $\langle P_{A-1} | \bar{\psi}(z_3) \frac{\gamma^+}{4} \psi(z_2) | P_{A-1} \rangle$ instead of $\langle P_{A-1} | \bar{\psi}(z_2) \frac{\gamma^+}{4} \psi(z_3) | P_{A-1} \rangle$. The above expression (Eq. 82) of the hadronic tensor has singularity when the denominator of the propagator for p_1 , ℓ , ℓ' and p_1' becomes on-shell. It contains two simple poles for p^+ and p'^+ . The contour integration for p^+ gives

$$\begin{aligned}
\bar{C}_1 &= \oint \frac{dp^+}{(2\pi)} \frac{e^{ip^+(x^- - z_2^-)}}{\left[(q+p)^2 - M^2 + i\epsilon \right] \left[(q+p-p_2)^2 + i\epsilon \right]} \\
&= \oint \frac{dp^+}{(2\pi)} \frac{e^{ip^+(x^- - z_2^-)}}{2q^- \left[q^+ + p^+ - \frac{M^2}{2q^-} + i\epsilon \right] 2(q^- - p_2^-) \left[q^+ + p^+ - p_2^+ - \frac{\mathbf{p}_{2\perp}^2}{2(q^- - p_2^-)} + i\epsilon \right]} \\
&= \frac{(2\pi i)}{2\pi} \frac{\theta(x^- - z_2^-)}{4q^-(q^- - p_2^-)} e^{i(-q^+ + \frac{M^2}{2q^-})(x^- - z_2^-)} \left[\frac{-1 + e^{i\mathcal{G}_M^{(p_2)}(x^- - z_2^-)}}{\mathcal{G}_M^{(p_2)}} \right],
\end{aligned} \tag{83}$$

where

$$\mathcal{G}_M^{(p_2)} = p_2^+ + \frac{\mathbf{p}_{2\perp}^2}{2(q^- - p_2^-)} - \frac{M^2}{2q^-} = \frac{(\ell_{2\perp} - \mathbf{k}_\perp)^2 + y^2(1-\eta)^2 M^2}{2y(1-y+\eta y)(1-\eta)q^-}. \tag{84}$$

Similarly, the contour integration for p'^+ yields

$$\begin{aligned}
\bar{C}_2 &= \oint \frac{dp'^+}{(2\pi)} \frac{e^{-ip'^+(y^- - z_3^-)}}{\left[(q+p')^2 - M^2 - i\epsilon \right] \left[(q+p'-p_2)^2 - i\epsilon \right]} \\
&= \oint \frac{dp'^+}{(2\pi)} \frac{e^{-ip'^+(y^- - z_3^-)}}{2q^- \left[q^+ + p'^+ - \frac{M^2}{2q^-} - i\epsilon \right] 2(q^- - p_2^-) \left[q^+ + p'^+ - p_2^+ - \frac{\mathbf{p}_{2\perp}^2}{2(q^- - p_2^-)} - i\epsilon \right]} \\
&= \frac{(-2\pi i)}{2\pi} \frac{\theta(y^- - z_3^-)}{4q^-(q^- - p_2^-)} e^{i(q^+ - \frac{M^2}{2q^-})(y^- - z_3^-)} \left[\frac{-1 + e^{-i\mathcal{G}_M^{(p_2)}(y^- - z_3^-)}}{\mathcal{G}_M^{(p_2)}} \right].
\end{aligned} \tag{85}$$

The trace in the numerator of third line of Eq. 82 simplifies to

$$\begin{aligned}
&\text{Tr} \left[\gamma^- \gamma^\mu (\not{q} + \not{p}' + M) \gamma^{\sigma_4} (\not{p}_2 + M) \gamma^{\sigma_1} (\not{q} + \not{p} + M) \gamma^\nu \right] \text{Tr} [\gamma^- \gamma^{\sigma_3} \not{\ell}_2 \gamma^{\sigma_2}] \times d_{\sigma_1\sigma_2}^{(\ell)} d_{\sigma_3\sigma_4}^{(\ell')} \\
&= 32(q^-)^2 [-g_{\perp\perp}^{\mu\nu}] \left[\frac{1 + (1-y)^2}{y(1-y+\eta y)} \right] \left[(\ell_\perp - \mathbf{k}_\perp)^2 + \kappa y^2 M^2 \right],
\end{aligned} \tag{86}$$

with κ being defined in Eq. 42. Finally, the hadronic tensor [Fig. 11] reduces to the following form

$$\begin{aligned}
W_{4,c}^{\mu\nu} &= 2N_f[-g_{\perp\perp}^{\mu\nu}] \int d(\Delta X^-) e^{iq^+(\Delta X^-)} e^{-i[M^2/(2q^-)](\Delta X^-)} \left\langle P \left| \bar{\psi}(\Delta X^-) \frac{\gamma^+}{4} \psi(0) \right| P \right\rangle \\
&\times e^2 e_q^2 g_s^2 [C_f N_c] \int d(\Delta z^-) d^2 \Delta_{z\perp} \frac{dy}{2\pi} \frac{d^2 \ell_{2\perp}}{(2\pi)^2} \frac{d^2 k_{\perp}}{(2\pi)^2} \left[\frac{1 + (1-y)^2}{y} \right] e^{-i(\Delta z^-) \mathcal{H}_M^{(\ell_2, p_2)}} e^{i\mathbf{k}_{\perp} \cdot \Delta \mathbf{z}_{\perp}} \\
&\times \int d\zeta^- \theta(\zeta^-) \left[2 - 2 \cos \left\{ \mathcal{G}_M^{(p_2)} \zeta^- \right\} \right] \frac{\left[(\ell_{2\perp} - \mathbf{k}_{\perp})^2 + \kappa y^2 M^2 \right]}{\left[(\ell_{2\perp} - \mathbf{k}_{\perp})^2 + M^2 y^2 (1-\eta)^2 \right]^2} \\
&\times \frac{\left\langle P_{A-1} \left| \bar{\psi}(\zeta^-, \Delta z^-, \Delta \mathbf{z}_{\perp}) \frac{\gamma^+}{4} \psi(\zeta^-, 0) \right| P_{A-1} \right\rangle}{y q^-}, \tag{87}
\end{aligned}$$

where, $\mathcal{G}_M^{(p_2)}$ is defined in Eq. 84 and $\mathcal{H}_M^{(\ell_2, p_2)}$ is given as

$$\mathcal{H}_M^{(\ell_2, p_2)} = \ell_2^+ + p_2^+ - \frac{M^2}{2q^-} = \frac{\ell_{2\perp}^2 - y M^2}{2y q^-} + \frac{(\ell_{2\perp} - \mathbf{k}_{\perp})^2 + M^2}{2(1-y + \eta y) q^-}. \tag{88}$$

The third line of Eq. 87 contains the space-time coherence factor, which in limit $M = 0$ and $\eta = 0$, gives

$$\mathcal{I} = \int_0^{\tau_f} d\zeta^- \frac{2 - 2 \cos \left\{ \frac{(\ell_{2\perp} - \mathbf{k}_{\perp})^2 \zeta^-}{2q^- y (1-y)} \right\}}{(\ell_{2\perp} - \mathbf{k}_{\perp})^2}, \tag{89}$$

where $\tau_f = 2q^- y (1-y) / \ell_{2\perp}^2$ represents the formation time of the radiated virtual photon. In Eq. 89, the ζ^- dependence of the two-point fermionic correlator (see fourth line of Eq. 87) has been omitted. The integral represents coherence effects and the physical behaviour is analogous to that discussed below Eq. 81. There are three other diagrams contributing to kernel-4 which are presented in Appendix D.

VII. MEDIUM MODIFIED KV KERNELS FOR PHOTON PRODUCTION

In the preceding sections, we discussed in detail the steps involved in the derivation of the hadronic tensor for each kernel. In this section, we add contributions from all diagrams for each kernel and provide a full scattering kernel for each category.

A. Full KV scattering kernel without collinear expansion

In this section, a full algebraic form of the hadronic tensor is presented for each kernel. For kernel-1, total of 8 diagrams were identified including the left-cut and right-cut diagrams. These are presented in Appendix A. In order to add these diagrams, we institute $\Delta X^- = y^- - x^-$, $\Delta z^- = z_3^- - z_2^-$, and $\zeta^- = y^- - z_3 = x^- - z_2$. The exponentials that depend on ΔX^- are absorbed in the definition of the nucleon parton distribution function, whereas the exponentials that depend on the relative distance $\Delta z^- = z_3^- - z_2^-$ are absorbed in the definition of the gluon/quark distribution in the medium. Under these algebraic transformations, diagrams within each kernel can be summed. Including all diagrams for kernel type-1 (Fig. 4), the full hadronic tensor is given as

$$W_{1,\text{full}}^{\mu\nu} = 2[-g_{\perp\perp}^{\mu\nu}] e_q^2 \int d(\Delta X^-) e^{i\Delta X^- (q^+ - \frac{M^2}{2q^-})} \left\langle P \left| \bar{\psi}(\Delta X^-) \frac{\gamma^+}{4} \psi(0) \right| P \right\rangle \times \mathcal{K}_1^{\text{eff}}, \tag{90}$$

where we define $\mathcal{K}_1^{\text{eff}}$ as a effective medium-modified scattering kernel for type-1 process (Fig. 4) as

$$\begin{aligned}
\mathcal{K}_1^{\text{eff}} &= e^2 g_s^2 \int d(\Delta z^-) d^2 \Delta_{z\perp} \frac{dy}{2\pi} \frac{d^2 \ell_{2\perp}}{(2\pi)^2} \frac{d^2 k_{\perp}}{(2\pi)^2} e^{-i\Delta z^- \mathcal{H}_M^{(\ell_2, p_2)}} e^{i\mathbf{k}_{\perp} \cdot \Delta \mathbf{z}_{\perp}} \\
&\times \int d\zeta^- \theta(\zeta^-) \mathcal{S}_1^{\text{eff}} \langle P_{A-1} | A^+(\zeta^-, \Delta z^-, \Delta \mathbf{z}_{\perp}) A^+(\zeta^-, 0) | P_{A-1} \rangle, \tag{91}
\end{aligned}$$

where $\mathcal{S}_1^{\text{eff}}$ denotes the perturbative part in the integrand of the medium-modified kernel given as

$$\begin{aligned} \mathcal{S}_1^{\text{eff}} = & \left[\frac{1 + (1-y)^2}{y} \right] \left[\frac{\boldsymbol{\ell}_{2\perp}^2 + M^2 y^4 \kappa}{[\boldsymbol{\ell}_{2\perp}^2 + y^2 M^2]^2} \right] \left[1 - \cos \left\{ \mathcal{G}_M^{(\ell_2)} \zeta^- \right\} \right] \\ & + \left[\frac{(1+\eta y)^2 + (1-y+\eta y)^2}{y} \right] \left[\frac{\{(1+\eta y)\boldsymbol{\ell}_{2\perp} - y\mathbf{k}_\perp\}^2 + M^2 y^4 \kappa}{J_1^2} \right] \\ & - \left[\frac{1 + (1-y)^2 + \eta y(2-y)}{y} \right] \left[\frac{(1+\eta y)\boldsymbol{\ell}_{2\perp}^2 - y\mathbf{k}_\perp \cdot \boldsymbol{\ell}_{2\perp} + M^2 y^4 \kappa}{\{\boldsymbol{\ell}_{2\perp}^2 + M^2 y^2\} J_1} \right] \left[2 - 2 \cos \left\{ \mathcal{G}_M^{(\ell_2)} \zeta^- \right\} \right], \end{aligned} \quad (92)$$

where

$$J_1 = \{(1+\eta y)\boldsymbol{\ell}_{2\perp} - y\mathbf{k}_\perp\}^2 + y^2 M^2. \quad (93)$$

The quantity η is defined in Eq. 33 while κ is in Eq. 42. The functions $\mathcal{G}_M^{(\ell_2)}$ and $\mathcal{H}_M^{(\ell_2, p_2)}$ in Eq. 92 are provided in Eq. 44. We notice similarities between our calculation and those presented in Ref.[36]. The first line of Eq. 92 represents the contribution from central-cut (Fig. 5) and non-central-cut (Fig. 15) diagrams and contains identical formulae for the splitting function and the perturbative part of the scattering kernel when compared with the expression given in Eq. 26 of Ref. [36]. The first line in Eq. 92, which contains a $\boldsymbol{\ell}_{2\perp}$ -dependent phase factor, is not present in Ref. [36] as this term has been absorbed in the definition of the initial state PDF used by Ref. [36]. We decided to keep this $\boldsymbol{\ell}_{2\perp}$ -dependent phase factor within the scattering kernel herein as there is a ζ^- path length dependence between the first and second scattering. On the other hand, the modified splitting function and perturbative part in 2nd and 3rd line Eq. 92 are identical to Eq. 30 and Eq. 32, respectively, in Ref. [36].

Next, kernel-2 diagrams are considered, of which 6 are central-cut diagrams. The hadronic tensor associated with each diagram is presented in Appendix B. Adding all diagrams for kernel-2 depicted in Fig. 6, yields the full hadronic tensor

$$W_{2,\text{full}}^{\mu\nu} = 2[-g_{\perp\perp}^{\mu\nu}] e_q^2 \int d(\Delta X^-) e^{i\Delta X^- q^+} \left\langle P \left| \bar{\psi}(\Delta X^-) \frac{\gamma^+}{4} \psi(0) \right| P \right\rangle \times \mathcal{K}_2^{\text{eff}} \quad (94)$$

where we define $\mathcal{K}_2^{\text{eff}}$ as a effective medium-modified scattering kernel for type-2 processes via

$$\begin{aligned} \mathcal{K}_2^{\text{eff}} = & e^2 g_s^2 [C_f N_c] \int d(\Delta z^-) d^2 \Delta z_\perp \frac{dy}{2\pi} \frac{d^2 \ell_{2\perp}}{(2\pi)^2} \frac{d^2 k_\perp}{(2\pi)^2} e^{-i\Delta z^- \mathcal{H}_0^{(\ell_2, p_2)}} e^{i\mathbf{k}_\perp \cdot \Delta \mathbf{z}_\perp} \\ & \times \int d\zeta^- \theta(\zeta^-) \mathcal{S}_2^{\text{eff}} \left\langle P_{A-1} \left| \bar{\psi}(\zeta^-, 0) \frac{\gamma^+}{4} \psi(\zeta^-, \Delta z^-, \Delta \mathbf{z}_\perp) \right| P_{A-1} \right\rangle. \end{aligned} \quad (95)$$

$\mathcal{S}_2^{\text{eff}}$ denotes the perturbative part of the medium modified kernel given by

$$\begin{aligned} \mathcal{S}_2^{\text{eff}} = & \left[\frac{1 + (1-y)^2}{y} \right] \left[\frac{2 - 2 \cos \left\{ \mathcal{G}_0^{(\ell_2)} \zeta^- \right\}}{\boldsymbol{\ell}_{2\perp}^2 (1-y+\eta y) q^-} \right] \\ & + \left[\frac{1 + y^2 (1-\eta)^2}{1-y(1+\eta)} \right] \left[\frac{2 - 2 \cos \left\{ \mathcal{G}_0^{(p_2)} \zeta^- \right\}}{(\boldsymbol{\ell}_{2\perp} - \mathbf{k}_\perp)^2 y q^-} \right] \\ & - \left[\frac{1-y(1-2\eta)}{y} \right] \left[\frac{\boldsymbol{\ell}_{2\perp}^2 - \boldsymbol{\ell}_{2\perp} \cdot \mathbf{k}_\perp}{(\boldsymbol{\ell}_{2\perp} - \mathbf{k}_\perp)^2 \boldsymbol{\ell}_{2\perp}^2 (1-y+\eta y) q^-} \right] \left[2 - 2 \cos \left\{ \mathcal{G}_0^{(p_2)} \zeta^- \right\} - 2 \cos \left\{ \mathcal{G}_0^{(\ell_2)} \zeta^- \right\} + 2 \cos \left\{ \Delta \mathcal{G}_0 \zeta^- \right\} \right], \end{aligned} \quad (96)$$

where $\Delta \mathcal{G}_0 = \left(\mathcal{G}_0^{(p_2)} - \mathcal{G}_0^{(\ell_2)} \right)$, η is defined as in Eq. 33, while $\mathcal{G}_0^{(\ell_2)}$ and $\mathcal{H}_0^{(\ell_2, p_2)}$ are provided in Eq. 50 and 63, respectively. Also, $\mathcal{G}_0^{(p_2)}$ is given as

$$\mathcal{G}_0^{(p_2)} = p_2^+ + \frac{\mathbf{p}_{2\perp}^2}{2(q^- - p_2^-)} = \frac{(\boldsymbol{\ell}_{2\perp} - \mathbf{k}_\perp)^2}{2y(1-y+\eta y)(1-\eta)q^-}, \quad (97)$$

The first line in Eq. 96 represents the contribution from the diagram (Fig. 18(a)), the second corresponds to diagram (Fig. 18(b)), while the third line corresponds to diagrams (Fig. 19[a,b]). Each term in Eq. 96 carries a suppression

factor of $1/q^-$ compared to scattering processes in kernel-1. These terms indicate that the quark-to-gluon or quark-to-photon conversion induced in the nuclear medium is suppressed by the incoming energy of the quark, i.e. yq^- or $(1-y+\eta y)q^-$ in this case.

Diagrams contributing to kernel-3 are depicted in Fig. 8. This kernel has a total of 8 center-cut diagrams having a quark and antiquark in the final state. The hadronic tensor associated with each diagram is presented in Appendix C. Adding all diagrams for kernel-3, yields the full hadronic tensor

$$W_{3,\text{full}}^{\mu\nu} = 2[-g_{\perp\perp}^{\mu\nu}] e_q^2 \int d(\Delta X^-) e^{i\Delta X^- q^+} \left\langle P \left| \bar{\psi}(\Delta X^-) \frac{\gamma^+}{4} \psi(0) \right| P \right\rangle \times \mathcal{K}_3^{\text{eff}} \quad (98)$$

where we define $\mathcal{K}_3^{\text{eff}}$ as a effective medium-modified scattering kernel (Fig. 8) is

$$\begin{aligned} \mathcal{K}_3^{\text{eff}} &= e^2 g_s^2 [C_f N_c] \int d(\Delta z^-) d^2 \Delta_{z\perp} \frac{dy}{2\pi} \frac{d^2 \ell_{2\perp}}{(2\pi)^2} \frac{d^2 k_{\perp}}{(2\pi)^2} e^{-i\Delta z^- \mathcal{H}_0^{(\ell_2, p_2)}} e^{i\mathbf{k}_{\perp} \cdot \Delta \mathbf{z}_{\perp}} \\ &\times \int d\zeta^- \theta(\zeta^-) \mathcal{S}_3^{\text{eff}} \left\langle P_{A-1} \left| \bar{\psi}(\zeta^-, 0) \frac{\gamma^+}{4} \psi(\zeta^-, \Delta z^-, \Delta \mathbf{z}_{\perp}) \right| P_{A-1} \right\rangle. \end{aligned} \quad (99)$$

where $\mathcal{S}_3^{\text{eff}}$ denotes the perturbative part in the integrand of the medium-modified kernel given as

$$\begin{aligned} \mathcal{S}_3^{\text{eff}} &= 2N_f \left[\frac{1+(1-y)^2}{y} \right] \left[\frac{2-2\cos\left\{\mathcal{G}_0^{(p_2)}\zeta^-\right\}}{[\ell_{2\perp}-\mathbf{k}_{\perp}]^2 y q^-} \right] \\ &+ \frac{\left[y^2+(1-y+\eta y)^2\right]}{(1+\eta y)^2 q^-} \frac{2}{[(1+\eta y)\ell_{2\perp}-y\mathbf{k}_{\perp}]^2} \\ &- 2 \frac{1-y+\eta y}{(1+\eta y)(1-\eta)} \left[\frac{\left[2-2\cos\left\{\mathcal{G}_0^{(p_2)}\zeta^-\right\}\right] J_2}{[\ell_{2\perp}-\mathbf{k}_{\perp}]^2 [(1+\eta y)\ell_{2\perp}-y\mathbf{k}_{\perp}]^2 y q^-} \right]. \end{aligned} \quad (100)$$

In the above equation, η is defined as in Eq. 33, while $\mathcal{G}_0^{(p_2)}$ and $\mathcal{H}_0^{(\ell_2, p_2)}$ are provided in Eq. 72 and Eq. 80, respectively. Finally, J_2 is given by

$$J_2 = \ell_{2\perp}^2 \{-1+y-\eta y(1-y+\eta y)\} + y\mathbf{k}_{\perp}^2 \{-1+y-\eta y\} + \mathbf{k}_{\perp} \cdot \ell_{2\perp} \{1-y^2+2\eta y+\eta^2 y^2\}. \quad (101)$$

Each term in Eq. 100 also carries a suppression factor of $1/q^-$ compared to scattering processes in kernel-1, which indicates that the in-medium quark-to-gluon or quark-to-photon conversion is suppressed by the incoming quark energy q^- .

For the case of heavy quark (charm and bottom), the effective hadronic tensor for kernel-3 is given as

$$W_{3,\text{full}}^{\mu\nu, HQ} = 2[-g_{\perp\perp}^{\mu\nu}] e_q^2 \int d(\Delta X^-) e^{i\Delta X^- (q^+ - \frac{M^2}{2q^-})} \left\langle P \left| \bar{\psi}(\Delta X^-) \frac{\gamma^+}{4} \psi(0) \right| P \right\rangle \times \mathcal{K}_3^{\text{eff, HQ}}. \quad (102)$$

$\mathcal{K}_3^{\text{eff, HQ}}$ is the effective medium-modified scattering kernel for type-3 process and is given by

$$\begin{aligned} \mathcal{K}_3^{\text{eff, HQ}} &= e^2 g_s^2 [C_f N_c] \int d(\Delta z^-) d^2 \Delta_{z\perp} \frac{dy}{2\pi} \frac{d^2 \ell_{2\perp}}{(2\pi)^2} \frac{d^2 k_{\perp}}{(2\pi)^2} e^{-i\Delta z^- \mathcal{H}_M^{(\ell_2, p_2)}} e^{i\mathbf{k}_{\perp} \cdot \Delta \mathbf{z}_{\perp}} \\ &\times \int d\zeta^- \theta(\zeta^-) \mathcal{S}_3^{\text{eff, HQ}} \left\langle P_{A-1} \left| \bar{\psi}(\zeta^-, 0) \frac{\gamma^+}{4} \psi(\zeta^-, \Delta z^-, \Delta \mathbf{z}_{\perp}) \right| P_{A-1} \right\rangle, \end{aligned} \quad (103)$$

where $\mathcal{S}_3^{\text{eff, HQ}}$ denotes the perturbative part given as

$$\mathcal{S}_3^{\text{eff, HQ}} = 2N_f \left[\frac{1+(1-y)^2}{y} \right] \left[\frac{2-2\cos\left\{\mathcal{G}_M^{(p_2)}\zeta^-\right\}}{y q^-} \right] \left[\frac{(\ell_{2\perp}-\mathbf{k}_{\perp})^2 + \kappa y^2 M^2}{[(\ell_{2\perp}-\mathbf{k}_{\perp})^2 + y^2 M^2 (1-\eta)^2]^2} \right]. \quad (104)$$

The functions $\mathcal{G}_M^{(p_2)}$ and $\mathcal{H}_M^{(\ell_2, p_2)}$ are presented in Eqs. 72 and 80, respectively.

Kernel-4 is shown in Fig. 10 and contains 4 center-cut diagrams. The hadronic tensor associated with each diagram is presented in the Appendix D, which together give

$$W_{4,\text{full}}^{\mu\nu} = 2[-g_{\perp\perp}^{\mu\nu}] e_q^2 \int d(\Delta X^-) e^{i\Delta X^- q^+} \left\langle P \left| \bar{\psi}(\Delta X^-) \frac{\gamma^+}{4} \psi(0) \right| P \right\rangle \times \mathcal{K}_4^{\text{eff}}. \quad (105)$$

$\mathcal{K}_4^{\text{eff}}$ is the effective medium-modified scattering kernel for type-4 process and is given by

$$\begin{aligned} \mathcal{K}_4^{\text{eff}} &= e^2 g_s^2 [C_f N_c] \int d(\Delta z^-) d^2 \Delta_{z\perp} \frac{dy}{2\pi} \frac{d^2 \ell_{2\perp}}{(2\pi)^2} \frac{d^2 k_{\perp}}{(2\pi)^2} e^{-i\Delta z^- \mathcal{H}_0^{(\ell_2, p_2)}} e^{i\mathbf{k}_{\perp} \cdot \Delta \mathbf{z}_{\perp}} \\ &\times \int d\zeta^- \theta(\zeta^-) \mathcal{S}_4^{\text{eff}} \left\langle P_{A-1} \left| \bar{\psi}(\zeta^-, \Delta z^-, \Delta \mathbf{z}_{\perp}) \frac{\gamma^+}{4} \psi(\zeta^-, 0) \right| P_{A-1} \right\rangle, \end{aligned} \quad (106)$$

where $\mathcal{S}_4^{\text{eff}}$ denotes the perturbative part given as

$$\begin{aligned} \mathcal{S}_4^{\text{eff}} &= 2N_f \left[\frac{1 + (1-y)^2}{y} \right] \left[\frac{2 - 2 \cos \left\{ \mathcal{G}_0^{(p_2)} \zeta^- \right\}}{[\ell_{2\perp} - \mathbf{k}_{\perp}]^2 y q^-} \right] \\ &- \left[\frac{\ell_{2\perp}^2 - \ell_{2\perp} \cdot \mathbf{k}_{\perp}}{\ell_{2\perp}^2 (\ell_{2\perp} - \mathbf{k}_{\perp})^2} \right] \left[\frac{2 - 2 \cos \left\{ \mathcal{G}_0^{(\ell_2)} \zeta^- \right\} - 2 \cos \left\{ \mathcal{G}_0^{(p_2)} \zeta^- \right\} + 2 \cos \left\{ \left(\mathcal{G}_0^{(p_2)} - \mathcal{G}_0^{(\ell_2)} \right) \zeta^- \right\}}{(1-\eta)(1-y) y q^-} \right]. \end{aligned} \quad (107)$$

The functions $\mathcal{G}_0^{(\ell_2)}$, $\mathcal{G}_0^{(p_2)}$, and $\mathcal{H}_0^{(\ell_2, p_2)}$ are presented in Eqs. 54, 72, and 80, respectively.

For the case of heavy quark (charm and bottom), the effective hadronic tensor for kernel-4 is given as

$$W_{4,\text{full}}^{\mu\nu, HQ} = 2[-g_{\perp\perp}^{\mu\nu}] e_q^2 \int d(\Delta X^-) e^{i\Delta X^- (q^+ - \frac{M^2}{2q^-})} \left\langle P \left| \bar{\psi}(\Delta X^-) \frac{\gamma^+}{4} \psi(0) \right| P \right\rangle \times \mathcal{K}_4^{\text{eff}, HQ}. \quad (108)$$

$\mathcal{K}_4^{\text{eff}, HQ}$ is the effective medium-modified scattering kernel for type-4 process and is given by

$$\begin{aligned} \mathcal{K}_4^{\text{eff}, HQ} &= e^2 g_s^2 [C_f N_c] \int d(\Delta z^-) d^2 \Delta_{z\perp} \frac{dy}{2\pi} \frac{d^2 \ell_{2\perp}}{(2\pi)^2} \frac{d^2 k_{\perp}}{(2\pi)^2} e^{-i\Delta z^- \mathcal{H}_M^{(\ell_2, p_2)}} e^{i\mathbf{k}_{\perp} \cdot \Delta \mathbf{z}_{\perp}} \\ &\times \int d\zeta^- \theta(\zeta^-) \mathcal{S}_4^{\text{eff}, HQ} \left\langle P_{A-1} \left| \bar{\psi}(\zeta^-, \Delta z^-, \Delta \mathbf{z}_{\perp}) \frac{\gamma^+}{4} \psi(\zeta^-, 0) \right| P_{A-1} \right\rangle, \end{aligned} \quad (109)$$

where $\mathcal{S}_4^{\text{eff}, HQ}$ denotes the perturbative part given as

$$\mathcal{S}_4^{\text{eff}, HQ} = 2N_f \left[\frac{1 + (1-y)^2}{y} \right] \left[\frac{2 - 2 \cos \left\{ \mathcal{G}_M^{(p_2)} \zeta^- \right\}}{y q^-} \right] \left[\frac{(\ell_{2\perp} - \mathbf{k}_{\perp})^2 + \kappa y^2 M^2}{\left[(\ell_{2\perp} - \mathbf{k}_{\perp})^2 + y^2 M^2 (1-\eta)^2 \right]^2} \right]. \quad (110)$$

The functions $\mathcal{G}_M^{(p_2)}$ and $\mathcal{H}_M^{(\ell_2, p_2)}$ are presented in Eqs. 84 and 88, respectively.

B. Collinear expansion and jet transport coefficients at next-leading order (NLO) and next-to-leading twist (NLT)

In the previous section, we presented a full scattering kernel without invoking any collinear expansion for the soft in-medium gluon/quark. In this section, we carry out the momentum gradient expansion in \mathbf{k}_{\perp} and k^- of the perturbative function $\mathcal{S}_i^{\text{eff}}$ in the integrand of the scattering kernel. As in previous higher-twist calculations such as [36, 37], a Taylor expansion of $\mathcal{S}_i^{\text{eff}}$ in \mathbf{k}_{\perp} and k^- , around $\mathbf{k}_{\perp} = \mathbf{0}_{\perp}$ and $k^- = 0$, is performed

$$\begin{aligned} \mathcal{S}_i^{\text{eff}}(\mathbf{k}_{\perp}, k^-) &= \mathcal{S}_i^{\text{eff}}(\mathbf{k}_{\perp} = 0, k^- = 0) + \frac{\partial \mathcal{S}_i^{\text{eff}}}{\partial k_{\perp}^{\rho}} \Big|_{k=0} k_{\perp}^{\rho} + \frac{\partial^2 \mathcal{S}_i^{\text{eff}}}{\partial k_{\perp}^{\rho} \partial k_{\perp}^{\sigma}} \Big|_{k=0} k_{\perp}^{\rho} k_{\perp}^{\sigma} + \dots \\ &+ \frac{\partial \mathcal{S}_i^{\text{eff}}}{\partial k^-} \Big|_{k=0} k^- + \frac{\partial^2 \mathcal{S}_i^{\text{eff}}}{\partial k^{-2}} \Big|_{k=0} (k^-)^2 + \dots, \end{aligned} \quad (111)$$

where $|_{k=0}$ is shorthand notation for all components of k being evaluated to zero. In Eq. 111, the second term in the expansion will give a vanishing contribution to the scattering kernel (after integration over k_\perp is performed), if the nuclear medium is assumed to be homogenous and isotropic. This homogeneity and isotropy assumption also ensures that the third term in Eq. 111 is non-trivial solely when ρ and σ are identical.

Applying collinear expansion, the effective medium-modified scattering kernel ($\mathcal{K}_1^{\text{eff}}$) for type-1 processes can be written as

$$\mathcal{K}_1^{\text{eff}} = e^2 \int \frac{dy}{2\pi} \frac{d^2 \ell_{2\perp}}{(2\pi)^2} \left[\mathcal{R}_0^{(1)} \hat{\mathcal{A}}_0 + \left(\mathcal{R}_{T_2}^{(1)} \hat{\mathcal{A}}_{T_2} + \mathcal{R}_{T_4}^{(1)} \hat{\mathcal{A}}_{T_4} + \dots \right) + \left(\mathcal{R}_{L_1}^{(1)} \hat{\mathcal{A}}_{L_1} + \mathcal{R}_{L_2}^{(1)} \hat{\mathcal{A}}_{L_2} + \dots \right) \right] \quad (112)$$

where $\mathcal{R}_0^{(1)}$ is the zeroth order term in the Taylor expansion of $\mathcal{S}_1^{\text{eff}}$, $\mathcal{R}_{L,i}^{(1)}$ represents i^{th} order derivative of $\mathcal{S}_1^{\text{eff}}$ along k^- direction, and $\mathcal{R}_{T,i}^{(1)}$ denotes the i^{th} order derivative of $\mathcal{S}_1^{\text{eff}}$ along k_\perp direction. The operators $\hat{\mathcal{A}}_0$, $\hat{\mathcal{A}}_{T,i}$ and $\hat{\mathcal{A}}_{L,i}$ represent two-point gluonic jet-medium correlation functions (sometimes also called jet-medium transport coefficients), where the factors of k_\perp and k^- in the Taylor series expansion are converted into derivatives acting on A^+ -field and are thereby absorbed in the definition of jet-medium transport coefficients. The operator $\hat{\mathcal{A}}_{T,2}$ represents the gluonic contributions to the jet-medium transport coefficient known as \hat{q} characterizing the momentum broadening in the transverse direction. Note, $\mathcal{R}_i^{(1)}$'s are independent of the momentum k (and therefore independent of η), thus, only depend on the momentum fraction y , ζ^- , $\ell_{2\perp}^2$, and quark mass M . The function $\mathcal{R}_i^{(1)}$ for kernel-1 are given as

$$\mathcal{R}_0^{(1)} = \mathcal{S}_1^{\text{eff}}(k_\perp = 0, k^- = 0) = \frac{1}{\ell_{2\perp}^2} \left[\frac{1 + (1-y)^2}{y} \right] \left[\frac{1 + \chi y^2 \kappa}{[1 + \chi]^2} \right] \cos \left\{ \mathcal{G}_M^{(\ell_2)} \zeta^- \right\}, \quad (113)$$

$$\begin{aligned} \mathcal{R}_{T,2}^{(1)} &= \left. \frac{\partial^2 \mathcal{S}_1^{\text{eff}}}{\partial k_x^2} \right|_{k=0} + \left. \frac{\partial^2 \mathcal{S}_1^{\text{eff}}}{\partial k_y^2} \right|_{k=0} \\ &= \frac{4y^2}{\ell_{2\perp}^4 [1 + \chi]^4} \left[\frac{1 + (1-y)^2}{y} \right] \left[9 + 12\chi y^2 \kappa + \chi^2 - 2 \cos \left\{ \mathcal{G}_M^{(\ell_2)} \zeta^- \right\} (3 + \chi \{1 + 4y^2 \kappa\} + y^2 \chi^2 \kappa) \right] \end{aligned} \quad (114)$$

where $\chi = \frac{y^2 M^2}{\ell_1^2}$ and κ is defined in Eq. 42, while

$$\begin{aligned} \mathcal{R}_{L,1}^{(1)} = \left. \frac{\partial \mathcal{S}_1^{\text{eff}}}{\partial k^-} \right|_{k=0} &= \left[\frac{2-y}{y} \right] \left[\frac{1}{q^- \ell_{2\perp}^2} \right] \left[\frac{-2 + 2 \cos \left\{ \mathcal{G}_M^{(\ell_2)} \zeta^- \right\}}{1 + \chi} + 2 \left(\frac{1 + \chi y^2 \kappa}{(1 + \chi)^2} \right) \right] \\ &+ \left[\frac{1 + (1-y)^2}{y} \right] \left[\frac{-1 + \chi (1 - 2y^2 \kappa)}{q^- \ell_{2\perp}^2 (1 + \chi)^3} \right] \left[2 \cos \left\{ \mathcal{G}_M^{(\ell_2)} \zeta^- \right\} \right]. \end{aligned} \quad (115)$$

The jet transport coefficients for kernel-1 are also the moments in k momentum space of the in-medium gluon distribution, which, formally, are given by

$$\begin{aligned} \hat{\mathcal{A}}_0 &= g_s^2 \int d(\Delta z^-) d^2 \Delta z_\perp \frac{d^2 k_\perp}{(2\pi)^2} e^{-i\Delta z^- \mathcal{H}_M^{(\ell_2, p_2)}} e^{i\mathbf{k}_\perp \cdot \Delta \mathbf{z}_\perp} \\ &\times \theta(\zeta^-) \langle P_{A-1} | A^+(\zeta^-, \Delta z^-, \Delta z_\perp) A^+(\zeta^-, 0) | P_{A-1} \rangle, \end{aligned} \quad (116)$$

$$\begin{aligned} \hat{\mathcal{A}}_{L,1} &= g_s^2 \int d(\Delta z^-) d^2 \Delta z_\perp \frac{d^2 k_\perp}{(2\pi)^2} e^{-i\Delta z^- \mathcal{H}_M^{(\ell_2, p_2)}} e^{i\mathbf{k}_\perp \cdot \Delta \mathbf{z}_\perp} \\ &\times \theta(\zeta^-) \langle P_{A-1} | i\partial^- A^+(\zeta^-, \Delta z^-, \Delta z_\perp) A^+(\zeta^-, 0) | P_{A-1} \rangle, \end{aligned} \quad (117)$$

$$\begin{aligned} \hat{\mathcal{A}}_{T,2} &= g_s^2 \int d(\Delta z^-) d^2 \Delta z_\perp \frac{d^2 k_\perp}{(2\pi)^2} e^{-i\Delta z^- \mathcal{H}_M^{(\ell_2, p_2)}} e^{i\mathbf{k}_\perp \cdot \Delta \mathbf{z}_\perp} \\ &\times \theta(\zeta^-) \langle P_{A-1} | \partial_\perp A^+(\zeta^-, \Delta z^-, \Delta z_\perp) \partial_\perp A^+(\zeta^-, 0) | P_{A-1} \rangle. \end{aligned} \quad (118)$$

In the above equations, the function $\mathcal{H}_M^{(\ell_2, p_2)}$ is defined as Eq. 44, while $\hat{\mathcal{A}}_{T,2}$ is \hat{q} , $\hat{\mathcal{A}}_{L,1}$ is known as jet transport coefficient \hat{e} characterizing energy loss in a longitudinal direction, both of which are gluonic correlators. Note that $\hat{\mathcal{A}}_0$, $\hat{\mathcal{A}}_{L,1}$, and $\hat{\mathcal{A}}_{T,2}$ depend explicitly on $\ell_{2\perp}$ via the function $\mathcal{H}_M^{(\ell_2, p_2)}$, thus these are transverse-momentum-dependent gluon parton distribution functions (TMD-gPDFs).

Collinear expansion to kernel-2 is examined next. The effective medium-modified kernel for type-2 processes ($\mathcal{K}_2^{\text{eff}}$), is

$$\mathcal{K}_2^{\text{eff}} = e^2 [C_f N_c] \int \frac{dy}{2\pi} \frac{d^2 \ell_{2\perp}}{(2\pi)^2} \left[\mathcal{R}_0^{(2)} \hat{\mathcal{F}}_0 + \left(\mathcal{R}_{T,2}^{(2)} \hat{\mathcal{F}}_{T,2} + \mathcal{R}_{T,4}^{(2)} \hat{\mathcal{F}}_{T,4} + \dots \right) + \left(\mathcal{R}_{L,1}^{(2)} \hat{\mathcal{F}}_{L,1} + \mathcal{R}_{L,2}^{(2)} \hat{\mathcal{F}}_{L,2} + \dots \right) \right] \quad (119)$$

where $\mathcal{R}_0^{(2)}$ is the 0th order term in the Taylor expansion of $\mathcal{S}_2^{\text{eff}}$, $\mathcal{R}_{L,i}^{(2)}$ represents i^{th} order derivative of $\mathcal{S}_2^{\text{eff}}$ along k^- direction, and $\mathcal{R}_{T,i}^{(2)}$ denotes the i^{th} order derivative of $\mathcal{S}_2^{\text{eff}}$ along k_\perp direction, as before. The operators $\hat{\mathcal{F}}_0$, $\hat{\mathcal{F}}_{T,i}$ and $\hat{\mathcal{F}}_{L,i}$ represent two-point fermionic jet-medium correlation functions (or transport coefficients), where the factors of k_\perp and k^- in the Taylor series expansion are converted into derivatives acting on in-medium fermionic ψ fields and thereby, absorbed in the definition of the jet-medium transport coefficients. The operator $\hat{\mathcal{F}}_{T,2}$ represents the fermionic contributions to jet transport coefficient \hat{q} characterizing the momentum broadening in the transverse direction.¹⁰ As before, $\mathcal{R}_i^{(2)}$'s solely depend on the momentum fraction y , ζ^- , and $\ell_{2\perp}^2$.

The function $\mathcal{R}_i^{(2)}$ for kernel-2 are given as

$$\begin{aligned} \mathcal{R}_0^{(2)} = \mathcal{S}_2^{\text{eff}}(k_\perp, k^-)|_{k=0} &= \left[\frac{1 + (1-y)^2}{y} \right] \left[\frac{2 - 2 \cos \left\{ \mathcal{G}_0^{(\ell_2)} \zeta^- \right\}}{\ell_{2\perp}^2 (1-y) q^-} \right] + \left[\frac{1+y^2}{1-y} \right] \left[\frac{2 - 2 \cos \left\{ \mathcal{G}_0^{(\ell_2)} \zeta^- \right\}}{\ell_{2\perp}^2 y q^-} \right] \\ &- \left[\frac{1-y}{y} \right] \left[\frac{4 - 4 \cos \left\{ \mathcal{G}_0^{(\ell_2)} \zeta^- \right\}}{\ell_{2\perp}^2 (1-y) q^-} \right], \end{aligned} \quad (120)$$

$$\begin{aligned} \mathcal{R}_{T,2}^{(2)} &= \left. \frac{\partial^2 \mathcal{S}_2^{\text{eff}}}{\partial k_x^2} \right|_{k=0} + \left. \frac{\partial^2 \mathcal{S}_2^{\text{eff}}}{\partial k_y^2} \right|_{k=0} \\ &= \left[\frac{1+y^2}{1-y} \right] \left[\frac{1}{y q^-} \right] \left[\frac{8 - 8 \cos \left\{ \mathcal{G}_0^{(\ell_2)} \zeta^- \right\}}{\ell_{2\perp}^4} - \frac{8\beta \sin \left\{ \mathcal{G}_0^{(\ell_2)} \zeta^- \right\}}{\ell_{2\perp}^2} + 8\beta^2 \right], \end{aligned} \quad (121)$$

$$\mathcal{R}_{L,1}^{(2)} = \left. \frac{\partial \mathcal{S}_2^{\text{eff}}}{\partial k^-} \right|_{k=0} = \frac{[2 - 2 \cos \left\{ \mathcal{G}_0^{(\ell_2)} \zeta^- \right\}] (2y - 5)}{y (1-y)^2 \ell_{2\perp}^2 (q^-)^2} - \frac{\sin \left\{ \mathcal{G}_0^{(\ell_2)} \zeta^- \right\} \zeta^- (3+y)}{y (1-y)^3 (q^-)^3}, \quad (122)$$

where

$$\beta = \frac{\zeta^-}{2y(1-y)q^-}. \quad (123)$$

The jet-medium transport coefficients for kernel-2 at NLO and NLT are in-medium two-point fermionic field distributions given by

$$\begin{aligned} \hat{\mathcal{F}}_0 &= g_s^2 \int d(\Delta z^-) d^2 \Delta_{z\perp} \frac{d^2 k_\perp}{(2\pi)^2} e^{-i\Delta z^- \mathcal{H}_0^{(\ell_2, p_2)}} e^{i\mathbf{k}_\perp \cdot \Delta \mathbf{z}_\perp} \\ &\times \theta(\zeta^-) \left\langle P_{A-1} \left| \bar{\psi}(\zeta^-, 0) \frac{\gamma^+}{4} \psi(\zeta^-, \Delta z^-, \Delta \mathbf{z}_\perp) \right| P_{A-1} \right\rangle, \end{aligned} \quad (124)$$

$$\begin{aligned} \hat{\mathcal{F}}_{L,1} &= g_s^2 \int d(\Delta z^-) d^2 \Delta_{z\perp} \frac{d^2 k_\perp}{(2\pi)^2} e^{-i\Delta z^- \mathcal{H}_0^{(\ell_2, p_2)}} e^{i\mathbf{k}_\perp \cdot \Delta \mathbf{z}_\perp} \\ &\times \theta(\zeta^-) \left\langle P_{A-1} \left| i\partial^- \bar{\psi}(\zeta^-, 0) \frac{\gamma^+}{4} \psi(\zeta^-, \Delta z^-, \Delta \mathbf{z}_\perp) \right| P_{A-1} \right\rangle, \end{aligned} \quad (125)$$

$$\begin{aligned} \hat{\mathcal{F}}_{T,2} &= g_s^2 \int d(\Delta z^-) d^2 \Delta_{z\perp} \frac{d^2 k_\perp}{(2\pi)^2} e^{-i\Delta z^- \mathcal{H}_0^{(\ell_2, p_2)}} e^{i\mathbf{k}_\perp \cdot \Delta \mathbf{z}_\perp} \\ &\times \theta(\zeta^-) \left\langle P_{A-1} \left| \partial_\perp \bar{\psi}(\zeta^-, 0) \frac{\gamma^+}{4} \partial_\perp \psi(\zeta^-, \Delta z^-, \Delta \mathbf{z}_\perp) \right| P_{A-1} \right\rangle. \end{aligned} \quad (126)$$

¹⁰ The relative importance of the bosonic and fermionic contribution to \hat{q} depends on the composition of the plasma. At very early times, the plasma in heavy-ion collisions is gluon-dominated as the gluonic PDF is much larger than quark PDFs. As the plasma evolves, quark population densities will increase to reach near thermal equilibrium in the QGP. So, at hydrodynamization time, both quarks and gluons contribute to \hat{q} , while at early times, the gluonic contribution to \hat{q} is the only relevant one.

where $\mathcal{H}_0^{(\ell_2, p_2)}$ is given in Eq. 63. The $\hat{\mathcal{F}}_0, \hat{\mathcal{F}}_{L,1}$, and $\hat{\mathcal{F}}_{T,2}$ distribution functions depend explicitly on $\ell_{2\perp}$ via the function $\mathcal{H}_0^{(\ell_2, p_2)}$, as before, hence, these are transverse-momentum-dependent quark parton distribution functions (TMD-qPDFs).

The effective medium-modified kernel $\mathcal{K}_3^{\text{eff}}$, for type-3 processes, is expanded as

$$\mathcal{K}_3^{\text{eff}} = e^2 [C_f N_c] \int \frac{dy d^2 \ell_{2\perp}}{2\pi (2\pi)^2} \left[\mathcal{R}_0^{(3)} \hat{\mathcal{F}}_0 + \left(\mathcal{R}_{T_2}^{(3)} \hat{\mathcal{F}}_{T_2} + \mathcal{R}_{T_4}^{(3)} \hat{\mathcal{F}}_{T_4} + \dots \right) + \left(\mathcal{R}_{L_1}^{(3)} \hat{\mathcal{F}}_{L_1} + \mathcal{R}_{L_2}^{(3)} \hat{\mathcal{F}}_{L_2} + \dots \right) \right] \quad (127)$$

where $\mathcal{R}_0^{(3)}$ is the 0th order term in the Taylor expansion of $\mathcal{S}_3^{\text{eff}}$, with $\mathcal{R}_{L,i}^{(3)}$ and $\mathcal{R}_{T,i}^{(3)}$ denoting the same directional derivatives as before. The operators $\hat{\mathcal{F}}_0, \hat{\mathcal{F}}_{T,i}$ and $\hat{\mathcal{F}}_{L,i}$ represent two-point fermionic jet-medium correlation functions/transport coefficients and these are identical to the correlators for kernel-2 above.

The function $\mathcal{R}_i^{(3)}$ for kernel-3 are given as

$$\begin{aligned} \mathcal{R}_0^{(3)} = \mathcal{S}_3^{\text{eff}}(k_\perp, k^-)|_{k=0} &= 2N_f \left[\frac{1 + (1-y)^2}{y} \right] \left[\frac{2 - 2 \cos \left\{ \mathcal{G}_0^{(\ell_2)} \zeta^- \right\}}{\ell_{2\perp}^2 y q^-} \right] \\ &+ \frac{2 \left[y^2 + (1-y)^2 \right]}{\ell_{2\perp}^2 q^-} + \frac{2(1-y)^2 \left[2 - 2 \cos \left\{ \mathcal{G}_0^{(\ell_2)} \zeta^- \right\} \right]}{\ell_{2\perp}^2 y q^-}, \end{aligned} \quad (128)$$

$$\begin{aligned} \mathcal{R}_{T,2}^{(3)} = \frac{\partial^2 \mathcal{S}_3^{\text{eff}}}{\partial k_x^2} \Big|_{k=0} + \frac{\partial^2 \mathcal{S}_3^{\text{eff}}}{\partial k_y^2} \Big|_{k=0} &= \left[\frac{16 - 16 \cos \left\{ \mathcal{G}_0^{(\ell_2)} \zeta^- \right\}}{\ell_{2\perp}^4} \right] \left[\frac{N_f + N_f (1-y)^2 - y^2 (1-y) (y^2 + y - 2)}{y^2 q^-} \right] \\ &+ \left[16 \cos \left\{ \mathcal{G}_0^{(\ell_2)} \zeta^- \right\} \beta^2 \right] \left[\frac{N_f + N_f (1-y)^2 + y (1-y)^2}{y^2 q^-} \right] \\ &- \left[\frac{16 \sin \left\{ \mathcal{G}_0^{(\ell_2)} \zeta^- \right\} \beta}{\ell_{2\perp}^2} \right] \left[\frac{N_f + N_f (1-y)^2 + 2y^2 (1-y)^2}{y^2 q^-} \right] \\ &+ \frac{8y^2 \left[y^2 + (1-y)^2 \right]}{\ell_{2\perp}^2 q^-}, \end{aligned} \quad (129)$$

$$\begin{aligned} \mathcal{R}_{L,1}^{(3)} = \frac{\partial \mathcal{S}_3^{\text{eff}}}{\partial k^-} \Big|_{k=0} &= \frac{2(1-2y) \zeta^- \sin \left\{ \mathcal{G}_0^{(\ell_2)} \zeta^- \right\}}{(y q^-)^3} \left[1 + \frac{N_f \left\{ 1 + (1-y)^2 \right\}}{y (1-y)^2} \right] \\ &- \frac{2(2-3y+3y^2)}{\ell_{2\perp}^2 (q^-)^2} + \frac{2(1-y^2)}{(y q^-)^2 \ell_{2\perp}^2} \left[2 - 2 \cos \left\{ \mathcal{G}_0^{(\ell_2)} \zeta^- \right\} \right], \end{aligned} \quad (130)$$

where β is given in Eq. 123.

For heavy-quark channel, the relevant diagrams are the two diagrams in the first row of Fig 8. For heavy-quark

energy loss, the resulting functions $\mathcal{R}_i^{(3),\text{HQ}}$ for kernel-3 are

$$\mathcal{R}_0^{(3),\text{HQ}} = \mathcal{S}_3^{\text{eff,HQ}}(k_\perp, k^-)|_{k=0} = \frac{2N_f}{yq^-} \left[\frac{1+(1-y)^2}{y} \right] \left[\frac{2-2\cos\left\{\mathcal{G}_M^{(\ell_2)}\zeta^-\right\}}{\ell_{2\perp}^2} \right] \left[\frac{1+\kappa\chi}{(1+\chi)^2} \right], \quad (131)$$

$$\begin{aligned} \mathcal{R}_{T,2}^{(3),\text{HQ}} &= \left. \frac{\partial^2 \mathcal{S}_3^{\text{eff,HQ}}}{\partial k_x^2} \right|_{k=0} + \left. \frac{\partial^2 \mathcal{S}_3^{\text{eff,HQ}}}{\partial k_y^2} \right|_{k=0} \\ &= -\frac{32N_f}{yq^- \ell_{2\perp}^4 (1+\chi)^3} \left[\frac{1+(1-y)^2}{y} \right] \left[\left\{ \frac{3+\kappa\chi}{2} \right\} \left[2-2\cos\left\{\mathcal{G}_M^{(\ell_2)}\zeta^-\right\} \right] + 2\beta(1+\kappa\chi)\ell_{2\perp}^2 \sin\left\{\mathcal{G}_M^{(\ell_2)}\zeta^-\right\} \right] \\ &+ \frac{48N_f}{yq^- \ell_{2\perp}^4 (1+\chi)^4} \left[\frac{1+(1-y)^2}{y} \right] \left[2-2\cos\left\{\mathcal{G}_M^{(\ell_2)}\zeta^-\right\} \right] \\ &+ \frac{16N_f}{yq^- \ell_{2\perp}^4 (1+\chi)^2} \left[\frac{1+(1-y)^2}{y} \right] \left[2-2\cos\left\{\mathcal{G}_M^{(\ell_2)}\zeta^-\right\} + 2\beta\ell_{2\perp}^2(2+\kappa\chi)\sin\left\{\mathcal{G}_M^{(\ell_2)}\zeta^-\right\} \right. \\ &\quad \left. + 2\beta^2\ell_{2\perp}^4(1+\kappa\chi)\cos\left\{\mathcal{G}_M^{(\ell_2)}\zeta^-\right\} \right], \end{aligned} \quad (132)$$

$$\begin{aligned} \mathcal{R}_{L,1}^{(3),\text{HQ}} &= \left. \frac{\partial \mathcal{S}_3^{\text{eff,HQ}}}{\partial k^-} \right|_{k=0} \\ &= \frac{4N_f(1+\kappa\chi)}{(yq^-)^2(1+\chi)^2} \left[\frac{1+(1-y)^2}{y} \right] \left[\frac{4-4\cos\left\{\mathcal{G}_M^{(\ell_2)}\zeta^-\right\}}{\ell_{2\perp}^2} \frac{\chi}{1+\chi} + \frac{\beta(1-2y-\chi)}{1-y} \sin\left\{\mathcal{G}_M^{(\ell_2)}\zeta^-\right\} \right] \end{aligned} \quad (133)$$

The effective medium-modified kernel ($\mathcal{K}_4^{\text{eff}}$) for type-4 processes can be re-written as

$$\mathcal{K}_4^{\text{eff}} = e^2 [C_f N_c] \int \frac{dy}{2\pi} \frac{d^2\ell_{2\perp}}{(2\pi)^2} \left[\mathcal{R}_0^{(4)} \hat{\mathcal{F}}_0 + \left(\mathcal{R}_{T,2}^{(4)} \hat{\mathcal{F}}_{T,2} + \mathcal{R}_{T,4}^{(4)} \hat{\mathcal{F}}_{T,4} + \dots \right) + \left(\mathcal{R}_{L,1}^{(4)} \hat{\mathcal{F}}_{L,1} + \mathcal{R}_{L,2}^{(4)} \hat{\mathcal{F}}_{L,2} + \dots \right) \right] \quad (134)$$

where $\mathcal{R}_0^{(4)}$ is the 0th order term in the Taylor expansion of $\mathcal{S}_4^{\text{eff}}$, $\mathcal{R}_{L,i}^{(4)}$ represents i^{th} order derivative of $\mathcal{S}_4^{\text{eff}}$ along k^- direction, and $\mathcal{R}_{T,i}^{(4)}$ denotes the i^{th} order derivative of $\mathcal{S}_4^{\text{eff}}$ along k_\perp direction. The operators $\hat{\mathcal{F}}_0$, $\hat{\mathcal{F}}_{T,i}$ and $\hat{\mathcal{F}}_{L,i}$ represent two-point fermionic jet transport coefficients. Note, $\mathcal{R}_i^{(4)}$'s depend solely on y , ζ^- , and $\ell_{2\perp}^2$, while the momentum k dependence is incorporated in $\hat{\mathcal{F}}_0$, $\hat{\mathcal{F}}_{T,i}$ and $\hat{\mathcal{F}}_{L,i}$.

The functions $\mathcal{R}_i^{(4)}$ for kernel-4 are given as

$$\mathcal{R}_0^{(4)} = \mathcal{S}_4^{\text{eff}}(k_\perp, k^-)|_{k=0} = \left[\frac{4-4\cos\left\{\mathcal{G}_0^{(\ell_2)}\zeta^-\right\}}{yq^- \ell_{2\perp}^2} \right] \left[N_f \frac{1+(1-y)^2}{y} - \frac{1}{1-y} \right], \quad (135)$$

$$\begin{aligned} \mathcal{R}_{T,2}^{(4)} &= \left. \frac{\partial^2 \mathcal{S}_4^{\text{eff}}}{\partial k_x^2} \right|_{k=0} + \left. \frac{\partial^2 \mathcal{S}_4^{\text{eff}}}{\partial k_y^2} \right|_{k=0} \\ &= \left[\frac{2N_f}{yq^-} \right] \left[\frac{1+(1-y)^2}{y} \right] \left[\frac{8-8\cos\left\{\mathcal{G}_0^{(\ell_2)}\zeta^-\right\}}{\ell_{2\perp}^4} - \frac{8\beta\sin\left\{\mathcal{G}_0^{(\ell_2)}\zeta^-\right\}}{\ell_{2\perp}^2} + 8\beta^2\cos\left\{\mathcal{G}_0^{(\ell_2)}\zeta^-\right\} \right] \\ &+ \left[\frac{1}{(1-y)yq^-} \right] \left[\beta^2 \left(8-8\cos\left\{\mathcal{G}_0^{(\ell_2)}\zeta^-\right\} \right) - \frac{16\beta\sin\left\{\mathcal{G}_0^{(\ell_2)}\zeta^-\right\}}{\ell_{2\perp}^2} \right], \end{aligned} \quad (136)$$

$$\begin{aligned} \mathcal{R}_{L,1}^{(4)} &= \left. \frac{\partial \mathcal{S}_4^{\text{eff}}}{\partial k^-} \right|_{k=0} = \left[2N_f \left(\frac{1+(1-y)^2}{y} \right) - \frac{1}{1-y} \right] \frac{(1-2y)\zeta^- \sin\left\{\mathcal{G}_0^{(\ell_2)}\zeta^-\right\}}{(yq^-)^3(1-y)^2} \\ &- \left[\frac{4-4\cos\left\{\mathcal{G}_0^{(\ell_2)}\zeta^-\right\}}{(1-y)(yq^-)^2\ell_{2\perp}^2} \right], \end{aligned} \quad (137)$$

where, again, β is in Eq. 123.

For heavy-quark channels in the kernel-4, the contributing diagrams are the two diagrams in the first row of Fig .10. The corresponding functions $\mathcal{R}_i^{(4),\text{HQ}}$ are

$$\mathcal{R}_0^{(4),\text{HQ}} = \mathcal{S}_4^{\text{eff,HQ}}(k_\perp, k^-) \Big|_{k=0} = \frac{2N_f}{yq^-} \left[\frac{1+(1-y)^2}{y} \right] \left[\frac{2-2\cos\left\{\mathcal{G}_M^{(\ell_2)}\zeta^-\right\}}{\ell_{2\perp}^2} \right] \left[\frac{1+\kappa\chi}{(1+\chi)^2} \right], \quad (138)$$

$$\begin{aligned} \mathcal{R}_{T,2}^{(4),\text{HQ}} &= \frac{\partial^2 \mathcal{S}_4^{\text{eff,HQ}}}{\partial k_x^2} \Big|_{k=0} + \frac{\partial^2 \mathcal{S}_4^{\text{eff,HQ}}}{\partial k_y^2} \Big|_{k=0} \\ &= -\frac{32N_f}{yq^-\ell_{2\perp}^4(1+\chi)^3} \left[\frac{1+(1-y)^2}{y} \right] \left[\left\{ \frac{3+\kappa\chi}{2} \right\} \left[2-2\cos\left\{\mathcal{G}_M^{(\ell_2)}\zeta^-\right\} \right] + 2\beta(1+\kappa\chi)\ell_{2\perp}^2 \sin\left\{\mathcal{G}_M^{(\ell_2)}\zeta^-\right\} \right] \\ &\quad + \frac{48N_f}{yq^-\ell_{2\perp}^4(1+\chi)^4} \left[\frac{1+(1-y)^2}{y} \right] \left[2-2\cos\left\{\mathcal{G}_M^{(\ell_2)}\zeta^-\right\} \right] \\ &\quad + \frac{16N_f}{yq^-\ell_{2\perp}^4(1+\chi)^2} \left[\frac{1+(1-y)^2}{y} \right] \left[2-2\cos\left\{\mathcal{G}_M^{(\ell_2)}\zeta^-\right\} + 2\beta\ell_{2\perp}^2(2+\kappa\chi)\sin\left\{\mathcal{G}_M^{(\ell_2)}\zeta^-\right\} \right] \\ &\quad + 2\beta^2\ell_{2\perp}^4(1+\kappa\chi)\cos\left\{\mathcal{G}_M^{(\ell_2)}\zeta^-\right\} \end{aligned} \quad (139)$$

$$\begin{aligned} \mathcal{R}_{L,1}^{(4),\text{HQ}} &= \frac{\partial \mathcal{S}_4^{\text{eff,HQ}}}{\partial k^-} \Big|_{k=0} \\ &= \frac{4N_f(1+\kappa\chi)}{(yq^-)^2(1+\chi)^2} \left[\frac{1+(1-y)^2}{y} \right] \left[\frac{4-4\cos\left\{\mathcal{G}_M^{(\ell_2)}\zeta^-\right\}}{\ell_{2\perp}^2} \frac{\chi}{1+\chi} + \frac{\beta(1-2y-\chi)}{1-y} \sin\left\{\mathcal{G}_M^{(\ell_2)}\zeta^-\right\} \right] \end{aligned} \quad (140)$$

C. Length dependence of energy loss

In this section, a numerical evaluation of the second-order derivative that arises in the Taylor expansion of the full scattering kernel is carried out for each kernel. The collinear expansion outlined in the preceding subsection, allowed us to decouple the k_\perp dependence and absorb it in the definition of the jet transport coefficients.

Firstly, we consider the function $\mathcal{R}_{T,2}^{(1)}$ in kernel-1. We note that the length integration variable ζ^- only appears in $2-2\cos\left\{\mathcal{G}_0^{(\ell_2)}\zeta^-\right\}$ term and the two-point correlator $\langle P_{A-1}|A^+(\zeta^-, \Delta z^-)A^+(\zeta^-, 0)|P_{A-1}\rangle$. Under the translational invariance around ζ^- , the two-point correlator does not depend on the mean location ζ^- . It allows one to decouple the $d\zeta^-$ and $d\Delta z^-$ integrations. Under this assumption, Fig. 12 depicts the length-integrated $\mathcal{R}_{T,2}^{(i)}$ for each kernel, evaluated at three different momentum fractions: $y = 0.25, 0.5$, and 0.75 . Figure 12(a) and 12(b) show kernels for real photon production processes, whereas Fig. 12(c) and Fig. 12(d) are for virtual photon corrections, encoded in kernel-3 and kernel-4. For each kernel, the quark mass is set to $M = 0$.

In Fig. 13, we present the quark mass dependence of second-order gradient $\mathcal{R}_{T,2}^{(1)}$ (length integrated) for kernel-1. Each sub-figure represents a different momentum fraction, while containing three different quark masses. In the $\overline{\text{MS}}$ scheme [42], heavy-quark masses are set to: $M = 1.27$ GeV (charm-quark) and $M = 4.18$ GeV (bottom-quark). The results indicate no noticeable differences for the charm quark when compared to light quarks, however, a significant effect can be seen for the bottom quark for $y > 0.25$.

For the case of kernel-2, there are a total of 6 central-cut diagrams, however none of them contribute to the heavy-quark energy loss. This is mainly because the jet-energy scale is assumed to be larger than the QGP scale, thus preventing heavy-quarks to be absorbed by the medium after fermion-to-boson conversion. Indeed, heavy quarks are solely produced from the primary hard scattering in the forward scattering approximation. Therefore, the contribution to heavy-quark energy loss from diagrams in kernel-2 vanishes.

Figure 14 shows the length-integrated $\mathcal{R}_{T,2}^{(3)HQ}$ for kernel-3. Although, there are a total of 8 diagrams in kernel-3, only 2 diagrams contribute to heavy quark energy loss, which are illustrated in the first row of Fig. 8. For the momentum fraction $y = 0.25$, Fig. 14 shows no appreciable difference between the heavy-quark masses and light-quark masses. However, as momentum fraction increases (i.e. $y = 0.5$ and $y = 0.75$), mass effects for bottom quarks are significant. Since heavy-quark energy loss diagrams are the same in kernel-3 and kernel-4, except the ordering of the two-point fermion-fermion correlator, the second-order gradient term is identical, i.e. $\mathcal{R}_{T,2}^{(3)HQ} = \mathcal{R}_{T,2}^{(4)HQ}$.

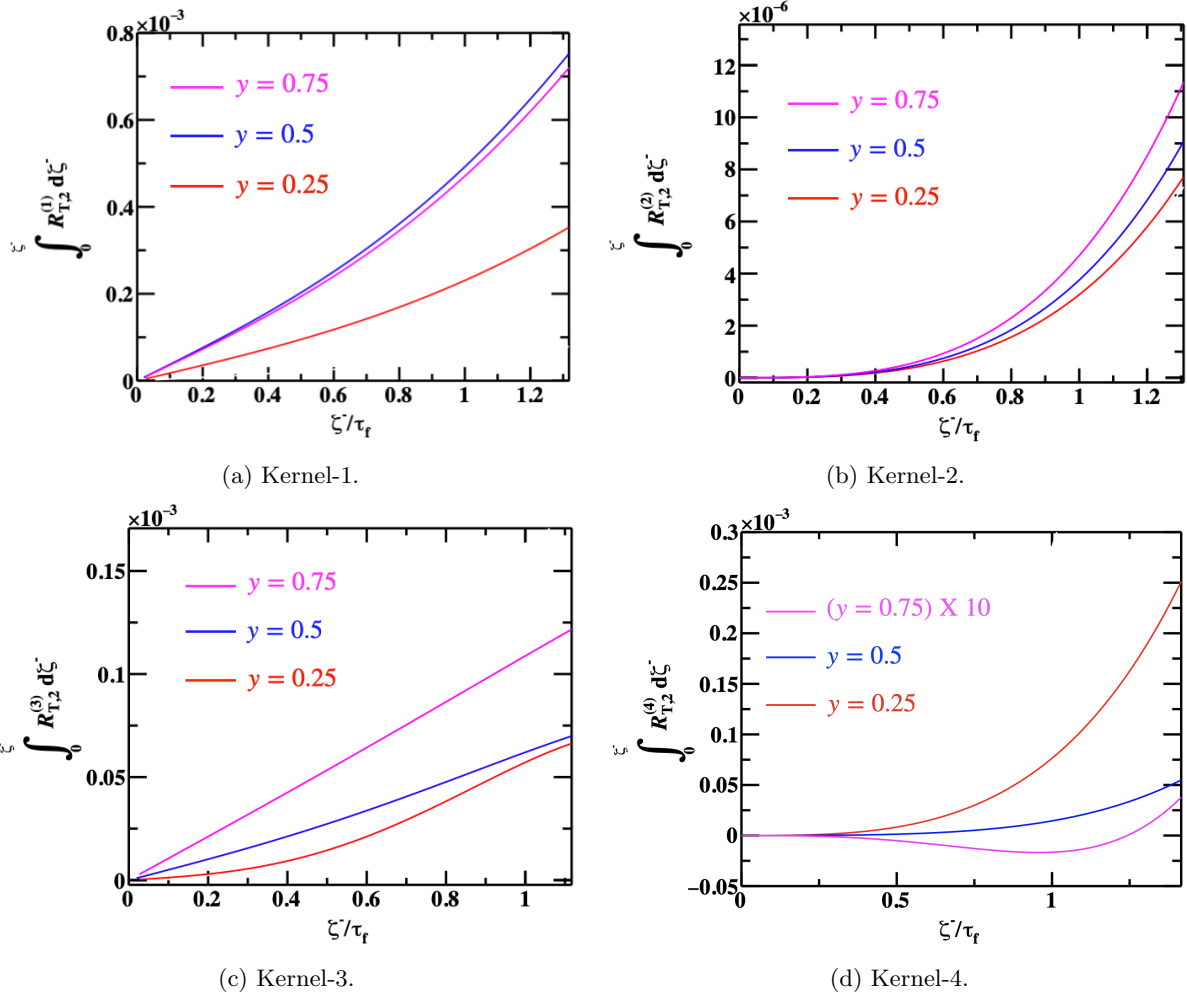


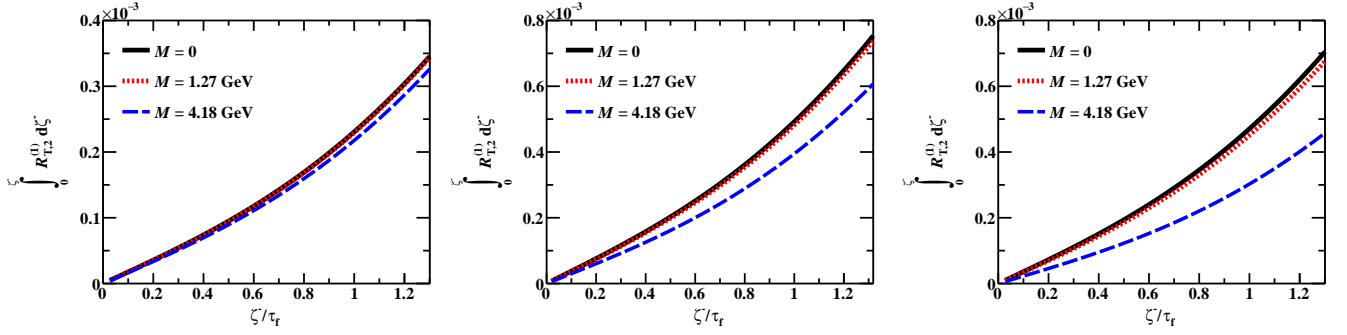
FIG. 12: Path length dependence of 2nd-order gradient term $\mathcal{R}_{T,2}^{(i)}$ (transverse direction) as a function of ζ^-/τ_f , where τ_f is a formation time given as $\tau_f = 2y(1-y)q^-/\ell_{2,1}^2$. Here, index i represents the type of kernel, and y is the momentum fraction carried away by the radiated photon. Other parameters are set to $q^- = 100$ GeV, $\ell_x = 10$ GeV, $\ell_y = 0$ GeV, $M = 0$ GeV.

Note that the calculations presented above are based on the collinear expansion approximation. However, a realistic numerical calculation of full scattering kernel requires estimates of the non-perturbative correlators and will be carried out in the future. Given the medium's contribution to all scattering kernels is encoded in the two-point correlation functions $\hat{\mathcal{A}}$ and $\hat{\mathcal{F}}$, our calculations are equally valid in cold nuclear matter or within hot QGP.

VIII. SUMMARY AND OUTLOOK

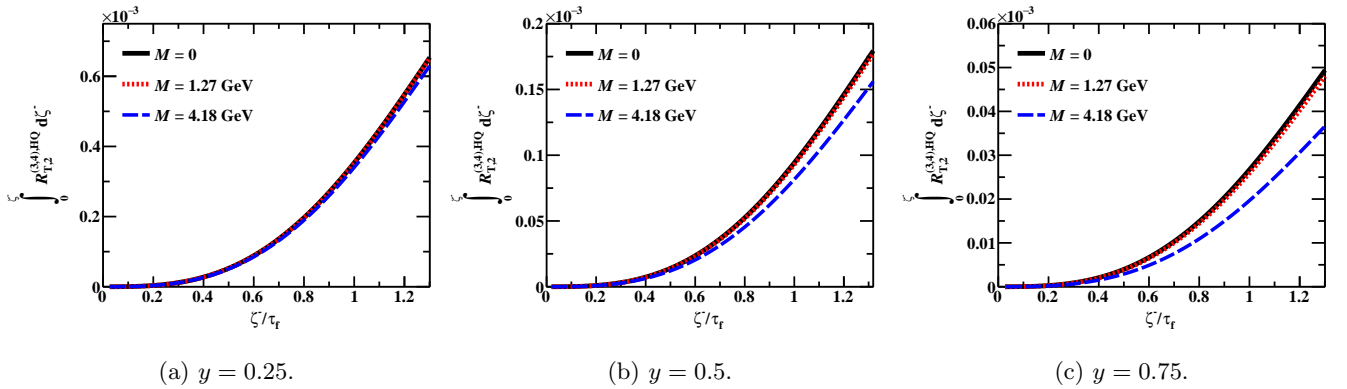
In this manuscript, a first calculation of Bremsstrahlung photon emission has been presented for a highly energetic and highly virtual quark traversing through a nuclear medium. At the perturbative scale $\mathcal{O}(\alpha_s \alpha_{em})$, four kernels have been identified. This classification is organized using the identity of particles in the final state. The first kernel and second kernel represent real photon emission off from an off-shell quark, whereas kernel-3 and kernel-4 are characterized by virtual photon corrections.

The calculation is carried out within the framework of perturbative QCD and by computing the hadronic tensor ($W^{\mu\nu}$) for the case of deep-inelastic scattering between the electron and the nucleus A . The calculation is performed in the Briet-frame with a light-cone gauge $A^- = 0$. The parton struck by the virtual photon coming off from the incoming electron is referred to as the primary hard parton and the associated scattering is the primary hard scattering. It is assumed that the subsequent scatterings of this hard parton traversing the remainder of the nucleus are uncorrelated with the scattering from the first-struck nucleon and therefore, these can be factorized from the initial



(a) Length integrated $\mathcal{R}_{T,2}^{(1)}$ for $y = 0.25$. (b) Length integrated $\mathcal{R}_{T,2}^{(1)}$ for $y = 0.5$. (c) Length integrated $\mathcal{R}_{T,2}^{(1)}$ for $y = 0.75$.

FIG. 13: Path length dependence of 2nd-order gradient term $\mathcal{R}_{T,2}^{(1)}$ (transverse direction) as a function of ζ^-/τ_f , where τ_f is a formation time given as $\tau_f = 2y(1-y)q^-/(\ell_{2\perp}^2 + y^2M^2)$. This is for kernel-1, and y is the momentum fraction carried away by the radiated photon. Other parameters are set to $q^- = 100$ GeV, $\ell_x = 10$ GeV, and $\ell_y = 0$ GeV.



(a) $y = 0.25$.

(b) $y = 0.5$.

(c) $y = 0.75$.

FIG. 14: Path length dependence of 2nd-order gradient term $\mathcal{R}_{T,2}^{(3,4)HQ}$ (transverse direction) as a function of ζ^-/τ_f , where τ_f is a formation time given as $\tau_f = 2y(1-y)q^-/(\ell_{2\perp}^2 + y^2M^2)$. For heavy-quark channels in kernel-3 and kernel-4, we have $\mathcal{R}_{T,2}^{(3)HQ} = \mathcal{R}_{T,2}^{(4)HQ}$. Here, y is the momentum fraction carried away by the radiated photon. Other parameters are set to $q^- = 100$ GeV, $\ell_x = 10$ GeV, and $\ell_y = 0$ GeV.

state nucleon parton distribution function. In the calculation of the hadronic tensor, the phase-space exponentials that contain relative distances ($\Delta x^- = y^- - x^-$) between the primary (hard) scattering in the amplitude (x^-) and its complex conjugate (y^-) are absorbed in the definition of the parton distribution function of the struck nucleon. Similarly, the phase-space exponentials that contain the relative distance ($\Delta z^- = z_3^- - z_2^-$) between the second scattering in the amplitude (z_2^-) and the complex-conjugate (z_3^-) are absorbed in the definition of non-perturbative jet-medium transport coefficients. It is argued that the remainder of the phase-space exponentials should be a real number. This led us to define the path length integration variable ζ^- representing the relative distance ($x^- - z_2^-$ and $y^- - z_3^-$) between the first scattering and second scattering in the amplitude (and also its complex conjugate). In this calculation, the phase factors $[2 - 2 \cos\{\mathcal{G}_0^{(\ell_2)} \zeta^-\}]$ and $e^{-i\mathcal{H}_0^{(\ell, p_2)} \Delta z^-}$ contain explicit $\ell_{2\perp}$ dependence and have been kept in the definition of the scattering kernel.

For all the calculations presented herein, it has been assumed that the second scattering occurs via an exchange of the Glauber gluon (or quark), which has a transverse momentum ($\mathbf{k}_\perp \gg k^-, k^+$) larger than its (plus and minus) light-cone components. The hadronic tensors for kernel-2, kernel-3, and kernel-4 involve an additional factor of yq^- or $(1-y+\eta y)q^-$ in the denominator when compared to kernel-1 diagram, indicating that the fermion-to-boson conversion processes are suppressed by the hard quark energy scale. For each kernel, a full scattering kernel was presented first before a systematic (Taylor) expansion was employed. These kernels are planned to be implemented within a comprehensive Monte-Carlo simulation. Such a simulation will enable more precise constraints on parton energy loss transport coefficients to be obtained.

Furthermore, the effects of quark masses have been studied for the first time at $\mathcal{O}(\alpha_{em}\alpha_s)$. We have shown the sensitivity of kernel-1, kernel-3, and kernel-4 to quark masses, and bottom quarks demonstrate a large effect on the second-order gradient terms ($\mathcal{R}_{T,2}^{(1,3,4)HQ}$). Thus, heavy-quark mass scale plays an important role in the parton energy loss at high virtuality.

One of the striking outcomes of this study has been the derivation of the non-perturbative (NP) function at NLO (and NLT), along with the appearance of the universal function $\mathcal{H}_0^{(\ell,p_2)}$ in phase space as $e^{-i\mathcal{H}_0^{(\ell,p_2)}\Delta z^-}$. We show that these NP correlators ($\hat{\mathcal{A}}_0, \hat{\mathcal{A}}_{T,2}, \dots, \hat{\mathcal{F}}_0, \hat{\mathcal{F}}_{T,2}, \dots$ and so on) depend on the semi-hard scale $\ell_{2\perp} \gg \Lambda_{\text{QCD}}$ momentum, i.e. on the transverse momentum generated in the radiative splitting. We have also linked the NLO jet-medium transport coefficients to transverse-momentum-dependent PDFs (TMD-PDFs). In future, it would be interesting to study the transverse momentum dependence and the temperature dependence of these correlators using the finite temperature field theory and lattice gauge theory.

ACKNOWLEDGMENTS

The authors would like to thank Abhijit Majumder and Chathuranga Sirimanna for invaluable discussions. This work was supported by the Canada Research Chair under grant number CRC-2022-00146 and the Natural Sciences and Engineering Research Council (NSERC) of Canada under grant number SAPIN-2023-00029. This work was also supported in part by the National Science Foundation (NSF) within the framework of the JETSCAPE collaboration, under grant number OAC- 2004571 (CSSI:X-SCAPE).

Appendix A: THE KERNEL FOR SINGLE-SCATTERING INDUCED EMISSION: ONE PHOTON AND ONE QUARK IN THE FINAL STATE

In this section, we summarize the calculation of all possible diagrams at next-leading-order (NLO) and next-leading-twist(NLT) contributing to kernel-1 with a photon and a quark in the final state. We discuss singularity structure, contour integrations and involved Traces in the final calculation of the hadronic tensor.

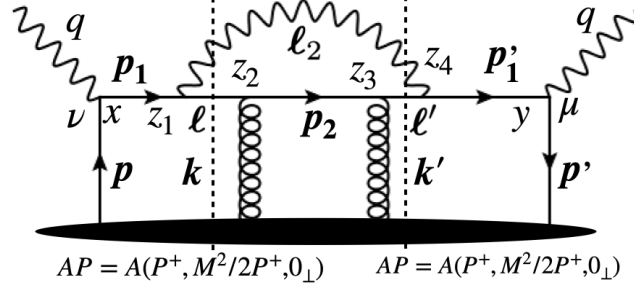


FIG. 15: A forward scattering diagram contributing to kernel-1 at NLO. The left-cut line corresponds to an interference between the single emission no scattering process and the single emission double scattering process. The right-cut line generates a process that is the complex conjugate of the process generated by the left-cut.

The Fig. 15 represents a forward scattering diagram contributing to the type-1 kernel at NLO and NLT. The left-cut gives rise to an interference between the single-photon emission with no scattering process and single photon pre-emission with double in-medium gluon scattering. The hadronic tensor for the left-cut diagram (Fig. 15) is given as

$$\begin{aligned}
W_{1,\ell}^{\mu\nu} &= e^2 e_q^2 g_s^2 \int d^4x d^4y d^4z_2 d^4z_3 \int \frac{d^4\ell}{(2\pi)^4} \frac{d^4p'}{(2\pi)^4} \frac{d^4\ell_2}{(2\pi)^4} \frac{d^4p_2}{(2\pi)^4} e^{-ip'y} e^{i(-q+\ell+\ell_2)x} \left\langle P \left| \bar{\psi}(y) \frac{\gamma^+}{4} \psi(x) \right| P \right\rangle \\
&\times e^{i(q+p'-p_2-\ell_2)z_3} e^{i(p_2-\ell)z_2} (P_{A-1} | A^+(z_3) A^+(z_2) | P_{A-1}) d_{\sigma_1 \sigma_4}^{(\ell_2)} (2\pi) \delta(\ell_2^2) (2\pi) \delta(\ell^2 - M^2) \\
&\times \frac{\text{Tr} \left[\gamma^- \gamma^\mu (\not{q} + \not{p}' + M) \gamma^{\sigma_4} (\not{q} + \not{p}' - \not{\ell}_2 + M) \gamma^- (\not{p}_2 + M) \gamma^\nu (\not{\ell} + M) \gamma^{\sigma_1} (\not{\ell}_2 + \not{\ell} + M) \gamma^\nu \right]}{\left[(q+p')^2 - M^2 - i\epsilon \right] \left[(q+p'-\ell_2)^2 - M^2 - i\epsilon \right] \left[p_2^2 - M^2 - i\epsilon \right] \left[(\ell_2 + \ell)^2 - M^2 + i\epsilon \right]}.
\end{aligned} \tag{141}$$

The above expression admits singularities owing to the presence of two simple poles for momentum variable p'^+ and one simple pole for p_2^+ . The contour integration for momentum p_2^+ gives

$$C_1 = \oint \frac{dp_2^+}{(2\pi)} \frac{e^{-ip_2^+(z_3^- - z_2^-)}}{[p_2^2 - M^2 - i\epsilon]} = \oint \frac{dp_2^+}{(2\pi)} \frac{e^{-ip_2^+(z_3^- - z_2^-)}}{2p_2^- \left[p_2^+ - \frac{p_{2\perp}^2 + M^2}{2p_2^-} - i\epsilon \right]} = \frac{(-2\pi i)}{2\pi} \frac{\theta(z_3^- - z_2^-)}{2p_2^-} e^{-i\left(\frac{p_{2\perp}^2 + M^2}{2p_2^-}\right)(z_3^- - z_2^-)}. \tag{142}$$

Similarly, the contour integration for p'^+ can be done

$$\begin{aligned}
C_2 &= \oint \frac{dp'^+}{(2\pi)} \frac{e^{-ip'^+(y^- - z_3^-)}}{\left[(q+p')^2 - M^2 - i\epsilon \right] \left[(q+p'-\ell_2)^2 - M^2 - i\epsilon \right]} \\
&= \oint \frac{dp'^+}{(2\pi)} \frac{e^{-ip'^+(y^- - z_3^-)}}{2q^- \left[q^+ + p'^+ - \frac{M^2}{2q^-} - i\epsilon \right] 2(q^- - \ell_2^-) \left[q^+ + p'^+ - \ell_2^+ - \frac{\ell_{2\perp}^2 + M^2}{2(q^- - \ell_2^-)} - i\epsilon \right]} \\
&= \frac{(-2\pi i)}{2\pi} \frac{\theta(y^- - z_3^-)}{4q^-(q^- - \ell_2^-)} e^{i\left(q^+ - \frac{M^2}{2q^-}\right)(y^- - z_3^-)} \left[\frac{-1 + e^{-i\mathcal{G}_M^{(\ell_2)}(y^- - z_3^-)}}{\mathcal{G}_M^{(\ell_2)}} \right],
\end{aligned} \tag{143}$$

where

$$\mathcal{G}_M^{(\ell_2)} = \ell_2^+ + \frac{\ell_{2\perp}^2 + M^2}{2(q^- - \ell_2^-)} - \frac{M^2}{2q^-} = \frac{\ell_{2\perp}^2 + y^2 M^2}{2y(1-y)q^-}. \tag{144}$$

The trace in the numerator of the third line of Eq. 141 yields

$$\begin{aligned} & \text{Tr} \left[\gamma^- \gamma^\mu (\not{q} + \not{p}' + M) \gamma^{\sigma_4} (\not{q} + \not{p}' - \not{\ell}_2 + M) \gamma^- (\not{p}_2 + M) \gamma^- (\not{\ell} + M) \gamma^{\sigma_1} (\not{\ell}_2 + \not{\ell} + M) \gamma^\nu \right] d_{\sigma_1 \sigma_4}^{(\ell_2)} \\ &= 32(q^-)^3 [-g_{\perp\perp}^{\mu\nu}] \left[\frac{1-y+\eta y}{y} \right] \left[\frac{1+(1-y)^2}{y} \right] [\ell_{2\perp}^2 + M^2 y^4 \kappa], \end{aligned} \quad (145)$$

where

$$\kappa = \left[1 + (1-y)^2 \right]^{-1}. \quad (146)$$

The final expression of the hadronic tensor for the left-cut diagram (Fig. 15) is given by

$$\begin{aligned} W_{1,\ell}^{\mu\nu} &= 2[-g_{\perp\perp}^{\mu\nu}] \int d(\Delta x^-) e^{iq^+(\Delta x^-)} \left\langle P \left| \bar{\psi}(\Delta X^-) \frac{\gamma^+}{4} \psi(0) \right| P \right\rangle \\ &\times e^2 e_q^2 g_s^2 \int d\zeta^- d(\Delta z^-) d^2 \Delta z_\perp \frac{dy}{2\pi} \frac{d^2 \ell_{2\perp}}{(2\pi)^2} \frac{d^2 k_\perp}{(2\pi)^2} \left[1 - e^{-i\mathcal{G}_M^{(\ell_2)}(y^- - z_3^-)} \right] e^{-ip_2^+(\Delta z^-)} e^{i\mathbf{k}_\perp \cdot \Delta \mathbf{z}_\perp} \\ &\times \frac{\theta(z_3^- - z_2^-) \theta(y^- - z_3^-) [\ell_{2\perp}^2 + \kappa y^4 M^2]}{[\ell_{2\perp}^2 + M^2 y^2]^2} \langle P_{A-1} | A^+(\zeta^-, \Delta z^-, \Delta z_\perp) A^+(\zeta^-, 0) | P_{A-1} \rangle \\ &\times \left[\frac{1+(1-y)^2}{y} \right] e^{i(\ell_2^+ + \ell^+)x^-} e^{-i\ell_2^+ z_3^-} e^{-i\ell^+ z_2^-} e^{-i[M^2/(2q^-)](y^- - z_3^-)}, \end{aligned} \quad (147)$$

where $\mathcal{G}_M^{(\ell_2)}$ is defined in Eq. 144, and

$$\ell_2^+ = \frac{\ell_{2\perp}^2}{2yq^-}; \quad \ell^+ = \frac{\ell_{2\perp}^2 + M^2}{2(1-y)q^-}; \quad p_2^+ = \frac{[(\ell_{2\perp} - \mathbf{k}_\perp)^2 + M^2]}{2(1-y+\eta y)q^-}. \quad (148)$$

However, Eq. 147 can be recast into the form

$$\begin{aligned} W_{1,\ell}^{\mu\nu} &= 2[-g_{\perp\perp}^{\mu\nu}] \int d(\Delta x^-) e^{iq^+(\Delta x^-)} \left\langle P \left| \bar{\psi}(\Delta X^-) \frac{\gamma^+}{4} \psi(0) \right| P \right\rangle \\ &\times e^2 e_q^2 g_s^2 \int d\zeta^- d(\Delta z^-) d^2 \Delta z_\perp \frac{dy}{2\pi} \frac{d^2 \ell_{2\perp}}{(2\pi)^2} \frac{d^2 k_\perp}{(2\pi)^2} \left[1 - e^{-i\mathcal{G}_M^{(\ell_2)}(y^- - z_3^-)} \right] e^{-i(\ell_2^+ + p_2^+)(\Delta z^-)} e^{i\mathbf{k}_\perp \cdot \Delta \mathbf{z}_\perp} \\ &\times \frac{\theta(z_3^- - z_2^-) \theta(y^- - z_3^-) [\ell_{2\perp}^2 + \kappa y^4 M^2]}{[\ell_{2\perp}^2 + M^2 y^2]^2} \langle P_{A-1} | A^+(\zeta^-, \Delta z^-, \Delta z_\perp) A^+(\zeta^-, 0) | P_{A-1} \rangle \\ &\times \left[\frac{1+(1-y)^2}{y} \right] e^{i(\ell_2^+ + \ell^+)(x^- - z_2^-)} e^{-i[M^2/(2q^-)](y^- - z_3^-)}, \end{aligned} \quad (149)$$

by using the change of variables $\Delta z^- = z_3^- - z_2^-$.

The right-cut diagram shown in Fig. 15 is a complex-conjugate of the left-cut diagram. The final expression of the hadronic tensor for the right-cut diagram reduces to the following form

$$\begin{aligned} W_{1,r}^{\mu\nu} &= 2[-g_{\perp\perp}^{\mu\nu}] \int d(\Delta x^-) e^{iq^+(\Delta x^-)} \left\langle P \left| \bar{\psi}(\Delta X^-) \frac{\gamma^+}{4} \psi(0) \right| P \right\rangle \\ &\times e^2 e_q^2 g_s^2 \int d\zeta^- d(\Delta z^-) d^2 \Delta z_\perp \frac{dy}{2\pi} \frac{d^2 \ell_{2\perp}}{(2\pi)^2} \frac{d^2 k_\perp}{(2\pi)^2} \left[1 - e^{i\mathcal{G}_M^{(\ell_2)}(x^- - z_2^-)} \right] e^{-ip_2^+(\Delta z^-)} e^{i\mathbf{k}_\perp \cdot \Delta \mathbf{z}_\perp} \\ &\times \frac{\theta(-z_3^- + z_2^-) \theta(x^- - z_2^-) [\ell_{2\perp}^2 + \kappa y^4 M^2]}{[\ell_{2\perp}^2 + M^2 y^2]^2} \langle P_{A-1} | A^+(\zeta^-, \Delta z^-, \Delta z_\perp) A^+(\zeta^-, 0) | P_{A-1} \rangle \\ &\times \left[\frac{1+(1-y)^2}{y} \right] e^{-i(\ell_2^+ + \ell'^+)y^-} e^{i\ell'^+ z_3^-} e^{i\ell_2^+ z_2^-} e^{i[M^2/(2q^-)](x^- - z_2^-)}, \end{aligned} \quad (150)$$

where $\mathcal{G}_M^{(\ell_2)}$ is defined in Eq. 144, κ is in Eq. 146 and

$$\ell_2^+ = \frac{\ell_{2\perp}^2}{2yq^-}; \quad \ell'^+ = \frac{\ell_{2\perp}^2 + M^2}{2(1-y)q^-}; \quad p_2^+ = \frac{[(\ell_{2\perp} - \mathbf{k}_\perp)^2 + M^2]}{2(1-y + \eta y)q^-}. \quad (151)$$

The above expression can be recast by instituting $\Delta z^- = z_3^- - z_2^-$ into the following form

$$\begin{aligned} W_{1,r}^{\mu\nu} &= 2[-g_{\perp\perp}^{\mu\nu}] \int d(\Delta x^-) e^{iq^+(\Delta X^-)} \left\langle P \left| \bar{\psi}(\Delta X^-) \frac{\gamma^+}{4} \psi(0) \right| P \right\rangle \\ &\times e^2 e_q^2 g_s^2 \int d\zeta^- d(\Delta z^-) d^2 \Delta z_\perp \frac{dy d^2 \ell_{2\perp}}{2\pi} \frac{d^2 k_\perp}{(2\pi)^2} \frac{d^2 k_\perp}{(2\pi)^2} \left[1 - e^{i\mathcal{G}_M^{(\ell_2)}(x^- - z_2^-)} \right] e^{-i(\ell_2^+ + p_2^+)(\Delta z^-)} e^{i\mathbf{k}_\perp \cdot \Delta \mathbf{z}_\perp} \\ &\times \frac{\theta(-z_3^- + z_2^-) \theta(x^- - z_2^-) [\ell_{2\perp}^2 + \kappa y^4 M^2]}{[\ell_{2\perp}^2 + M^2 y^2]^2} \langle P_{A-1} | A^+(\zeta^-, \Delta z^-, \Delta z_\perp) A^+(\zeta^-, 0) | P_{A-1} \rangle \\ &\times \left[\frac{1 + (1-y)^2}{y} \right] e^{-i(\ell_2^+ + \ell'^+)(y^- - z_3^-)} e^{i[M^2/(2q^-)](x^- - z_2^-)}. \end{aligned} \quad (152)$$

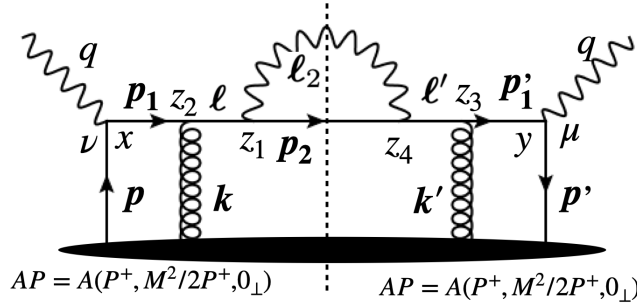


FIG. 16: A forward scattering diagram contributing to kernel-1.

Next, the hadronic tensor for the central-cut diagram shown in Fig. 16 can be written as

$$\begin{aligned} W_{1,c}^{\mu\nu} &= e^2 e_q^2 g_s^2 \int d^4 x d^4 y d^4 z_2 d^4 z_3 \int \frac{d^4 p}{(2\pi)^4} \frac{d^4 p'}{(2\pi)^4} \frac{d^4 \ell_2}{(2\pi)^4} \frac{d^4 p_2}{(2\pi)^4} e^{-ip'y} e^{ipx} \left\langle P \left| \bar{\psi}(y) \frac{\gamma^+}{4} \psi(x) \right| P \right\rangle \\ &\times e^{i(q+p'-p_2-\ell_2)z_3} e^{i(\ell_2+p_2-q-p)z_2} \langle P_{A-1} | A^+(z_3) A^+(z_2) | P_{A-1} \rangle d_{\sigma_1 \sigma_4}^{(\ell_2)} (2\pi) \delta(\ell_2^+) (2\pi) \delta(p_2^+ - M^2) \\ &\times \frac{\text{Tr} \left[\gamma^- \gamma^\mu (\not{q} + \not{p}' + M) \gamma^- (\not{\ell}_2 + \not{p}_2 + M) \gamma^{\sigma_4} (\not{p}_2 + M) \gamma^{\sigma_1} (\not{\ell}_2 + \not{p}_2 + M) \gamma^- (\not{q} + \not{p} + M) \gamma^\nu \right]}{\left[(q+p')^2 - M^2 - i\epsilon \right] \left[(\ell_2 + p_2)^2 - M^2 - i\epsilon \right] \left[(\ell_2 + p_2)^2 - M^2 + i\epsilon \right] \left[(q+p)^2 - M^2 + i\epsilon \right]}. \end{aligned} \quad (153)$$

Equation 153 has singularity arising from the denominator of the quark propagator with momentum p_1 and p'_1 . We identify one pole for each momentum variable p^+ and p'^+ . The contour integration for momentum p^+ in the complex plane is given by

$$C_1 = \oint \frac{dp^+}{(2\pi)} \frac{e^{ip^+(x^- - z_2^-)}}{[(q+p)^2 - M^2 + i\epsilon]} = \oint \frac{dp^+}{(2\pi)} \frac{e^{ip^+(x^- - z_2^-)}}{2q^- [q^+ + p^+ - [M^2/(2q^-)] + i\epsilon]} = \frac{(2\pi i)}{2\pi} \frac{\theta(x^- - z_2^-)}{2q^-} e^{i(-q^+ + \frac{M^2}{2q^-})(x^- - z_2^-)}. \quad (154)$$

Similarly, the contour integration for momentum p'^+ is carried out

$$C_2 = \oint \frac{dp'^+}{(2\pi)} \frac{e^{-ip'^+(y^- - z_3^-)}}{[(q+p')^2 - M^2 - i\epsilon]} = \oint \frac{dp'^+}{(2\pi)} \frac{e^{-ip'^+(y^- - z_3^-)}}{2q^- [q^+ + p'^+ - [M^2/(2q^-)] - i\epsilon]} = \frac{(-2\pi i)}{2\pi} \frac{\theta(y^- - z_3^-)}{2q^-} e^{i(q^+ - \frac{M^2}{2q^-})(y^- - z_3^-)}. \quad (155)$$

Including mass correction up to $\mathcal{O}(M^2)$, the trace yields

$$\begin{aligned} &\text{Tr} \left[\gamma^- \gamma^\mu (\not{q} + \not{p}' + M) \gamma^- (\not{\ell}_2 + \not{p}_2 + M) \gamma^{\sigma_4} (\not{p}_2 + M) \gamma^{\sigma_1} (\not{\ell}_2 + \not{p}_2 + M) \gamma^- (\not{q} + \not{p} + M) \gamma^\nu \right] d_{\sigma_1 \sigma_4}^{(\ell_2)} \\ &= \frac{32[-g_{\perp\perp}^{\mu\nu}](q^-)^3}{y(1-y+\eta y)} \left[\frac{(1+\eta y)^2 + (1-y+\eta y)^2}{y} \right] \left[\{ (1+\eta y) \ell_{2\perp} - y \mathbf{k}_\perp \}^2 + \kappa y^4 M^2 \right]. \end{aligned} \quad (156)$$

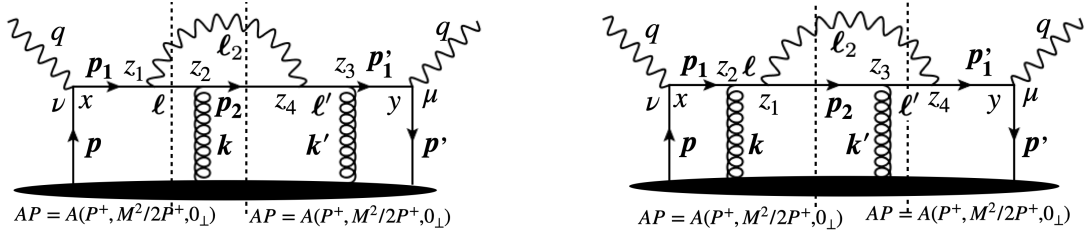
The final expression of the hadronic tensor for the central-cut (Fig. 16) is

$$\begin{aligned}
W_{1,c}^{\mu\nu} &= 2[-g_{\perp\perp}^{\mu\nu}] \int d(\Delta X^-) e^{iq^+(\Delta X^-)} e^{-i[M^2/(2q^-)](\Delta X^-)} \left\langle P \left| \bar{\psi}(\Delta X^-) \frac{\gamma^+}{4} \psi(0) \right| P \right\rangle \\
&\times e^2 e_q^2 g_s^2 \int d\zeta^- d(\Delta z^-) d^2 \Delta_{z\perp} \frac{dy}{2\pi} \frac{d^2 \ell_{2\perp}}{(2\pi)^2} \frac{d^2 k_{\perp}}{(2\pi)^2} e^{-i\mathcal{H}_M^{(\ell_2, p_2)}(\Delta z^-)} e^{i\mathbf{k}_{\perp} \cdot \Delta \mathbf{z}_{\perp}} \\
&\times \frac{\theta(x^- - z_2^-) \theta(y^- - z_3^-) \left[\{(1 + \eta y) \ell_{2\perp} - y \mathbf{k}_{\perp}\}^2 + \kappa y^4 M^2 \right]}{\left[(\ell_{2\perp} - y \mathbf{k}_{\perp})^2 + 2y\eta(\ell_{2\perp}^2 - y \ell_{2\perp} \cdot \mathbf{k}_{\perp}) + \eta^2 y^2 \ell_{2\perp}^2 + y^2 M^2 \right]^2} \langle P_{A-1} | A^+(\zeta^-, \Delta z^-, \Delta z_{\perp}) A^+(\zeta^-, 0) | P_{A-1} \rangle \\
&\times \left[\frac{(1 + \eta y)^2 + (1 - y + \eta y)^2}{y} \right],
\end{aligned} \tag{157}$$

where

$$\mathcal{H}_M^{(\ell_2, p_2)} = \ell_2^+ + p_2^+ - \frac{M^2}{2q^-} = \frac{\ell_{2\perp}^2 - y M^2}{2yq^-} + \frac{(\ell_{2\perp} - \mathbf{k}_{\perp})^2 + M^2}{2q^-(1 - y + \eta y)}, \tag{158}$$

and κ is defined in Eq. 146.



(a) Interference diagram. There are two possible cuts leading to a photon and a quark as final state. (b) Complex conjugate of the diagram on the left panel. There are two possible cuts leading to a photon and a quark as final state.

FIG. 17: A forward scattering diagram contributing to kernel-1.

The hadronic tensor for the right-cut diagram shown in Fig. 17(a) is

$$\begin{aligned}
W_{1,r}^{\mu\nu} &= e^2 e_q^2 g_s^2 \int d^4 x d^4 y d^4 z_2 d^4 z_3 \int \frac{d^4 p}{(2\pi)^4} \frac{d^4 p'}{(2\pi)^4} \frac{d^4 \ell_2}{(2\pi)^4} \frac{d^4 p_2}{(2\pi)^4} e^{-ip'y} e^{ipx} \left\langle P \left| \bar{\psi}(y) \frac{\gamma^+}{4} \psi(x) \right| P \right\rangle \\
&\times e^{i(q+p'-p_2-\ell_2)z_3} e^{i(\ell_2+p_2-q-p)z_2} \langle P_{A-1} | A^+(z_3) A^+(z_2) | P_{A-1} \rangle d_{\sigma_1 \sigma_4}^{(\ell_2)}(2\pi) \delta(\ell_2^2) (2\pi) \delta(p_2^2 - M^2) \\
&\times \frac{\text{Tr} \left[\gamma^- \gamma^\mu (\not{q} + \not{p}' + M) \gamma^- (\not{\ell}_2 + \not{p}_2 + M) \gamma^{\sigma_4} (\not{p}_2 + M) \gamma^- (\not{q} + \not{p} - \not{\ell}_2 + M) \gamma^{\sigma_1} (\not{q} + \not{p} + M) \gamma^\nu \right]}{\left[(q+p')^2 - M^2 - i\epsilon \right] \left[(\ell_2 + p_2)^2 - M^2 - i\epsilon \right] \left[(q+p-\ell_2)^2 - M^2 + i\epsilon \right] \left[(q+p)^2 - M^2 + i\epsilon \right]}.
\end{aligned} \tag{159}$$

The above expression (Eq. 159) has singularity arising from the denominator of the quark propagator with momentum p_1 , ℓ and p'_1 . It has two simple poles for the momentum variable p^+ and one simple pole for p'^+ . The contour integration for momentum p^+ in the complex plane gives

$$\begin{aligned}
C_1 &= \oint \frac{dp^+}{(2\pi)} \frac{e^{ip^+(x^- - z_2^-)}}{\left[(q+p)^2 - M^2 + i\epsilon \right] \left[(q+p-\ell_2)^2 - M^2 + i\epsilon \right]} \\
&= \oint \frac{dp^+}{(2\pi)} \frac{e^{ip^+(x^- - z_2^-)}}{2q^- \left[q^+ + p^+ - \frac{M^2}{2q^-} + i\epsilon \right] 2(q^- - \ell_2^-) \left[q^+ + p^+ - \ell_2^+ - \frac{\ell_{2\perp}^2 + M^2}{2(q^- - \ell_2^-)} + i\epsilon \right]} \\
&= \frac{(2\pi i)}{2\pi} \frac{\theta(x^- - z_2^-)}{4q^-(q^- - \ell_2^-)} e^{i(-q^+ + \frac{M^2}{2q^-})(x^- - z_2^-)} \left[\frac{-1 + e^{i\mathcal{G}_M^{(\ell_2)}(x^- - z_2^-)}}{\mathcal{G}_M^{(\ell_2)}} \right],
\end{aligned} \tag{160}$$

where $\mathcal{G}_M^{(\ell_2)}$ is defined in Eq. 144.

Similarly, the contour integration for momentum p'^+ is carried out as

$$C_2 = \oint \frac{dp'^+}{(2\pi)} \frac{e^{-ip'^+(y^- - z_3^-)}}{[(q+p')^2 - M^2 - i\epsilon]} = \frac{(-2\pi i)}{2\pi} \frac{\theta(y^- - z_3^-)}{2q^-} e^{i(q^+ - \frac{M^2}{2q^-})(y^- - z_3^-)}. \quad (161)$$

Including mass correction up to $\mathcal{O}(M^2)$, the trace yields

$$\begin{aligned} & \text{Tr} \left[\gamma^- \gamma^\mu (\not{q} + \not{p}' + M) \gamma^- (\not{\ell}_2 + \not{p}_2 + M) \gamma^{\sigma_4} (\not{p}_2 + M) \gamma^- (\not{q} + \not{p} - \not{\ell}_2 + M) \gamma^{\sigma_1} (\not{q} + \not{p} + M) \gamma^\nu \right] d_{\sigma_1 \sigma_4}^{(\ell_2)} \\ &= \frac{32[-g_{\perp\perp}^{\mu\nu}](q^-)^3}{y} \left[\frac{1 + (1-y)^2 + \eta y(2-y)}{y} \right] [(1 + \eta y) \ell_{2\perp}^2 - y \mathbf{k}_\perp \cdot \ell_{2\perp} + \kappa y^4 M^2], \end{aligned} \quad (162)$$

where κ is defined in Eq. 146. The final expression of the hadronic tensor for the right-cut [Fig. 17(a)] is given as

$$\begin{aligned} W_{1,r}^{\mu\nu} &= 2[-g_{\perp\perp}^{\mu\nu}] \int d(\Delta x^-) e^{iq^+(\Delta x^-)} e^{-i[M^2/(2q^-)](\Delta x^-)} \left\langle P \left| \bar{\psi}(\Delta x^-) \frac{\gamma^+}{4} \psi(0) \right| P \right\rangle \\ &\times e^2 e_q^2 g_s^2 \int d\zeta^- d(\Delta z^-) d^2 \Delta z_\perp \frac{dy}{2\pi} \frac{d^2 \ell_{2\perp}}{(2\pi)^2} \frac{d^2 k_\perp}{(2\pi)^2} \left[-1 + e^{i\mathcal{G}_M^{(\ell_2)}(x^- - z_2^-)} \right] e^{-i\mathcal{H}_M^{(\ell_2, p_2)}(\Delta z^-)} e^{i\mathbf{k}_\perp \cdot \Delta z_\perp} \\ &\times \frac{\theta(x^- - z_2^-) \theta(y^- - z_3^-) [(1 + \eta y) \ell_{2\perp}^2 - y \mathbf{k}_\perp \cdot \ell_{2\perp} + \kappa y^4 M^2]}{[\ell_{2\perp}^2 + M^2 y^2] J_1} \langle P_{A-1} | A^+(\zeta^-, \Delta z^-, \Delta z_\perp) A^+(\zeta^-, 0) | P_{A-1} \rangle \\ &\times \left[\frac{1 + (1-y)^2 + \eta y(2-y)}{y} \right], \end{aligned} \quad (163)$$

where $\mathcal{G}_M^{(\ell_2)}$ is defined in Eq. 144, $\mathcal{H}_M^{(\ell_2, p_2)}$ defined in Eq. 158, and

$$J_1 = [(1 + \eta y) \ell_{2\perp} - y \mathbf{k}_\perp]^2 + y^2 M^2. \quad (164)$$

Next, we consider the left-cut diagram shown in Fig. 17(a). Its hadronic tensor can be written as

$$\begin{aligned} W_{1,\ell}^{\mu\nu} &= e^2 e_q^2 g_s^2 \int d^4 x d^4 y d^4 z_2 d^4 z_3 \int \frac{d^4 \ell}{(2\pi)^4} \frac{d^4 p'}{(2\pi)^4} \frac{d^4 \ell_2}{(2\pi)^4} \frac{d^4 p_2}{(2\pi)^4} e^{-ip'y} e^{i(\ell_2 + \ell - q)x} \left\langle P \left| \bar{\psi}(y) \frac{\gamma^+}{4} \psi(x) \right| P \right\rangle \\ &\times e^{i(q+p'-p_2-\ell_2)z_3} e^{i(p_2-\ell)z_2} \langle P_{A-1} | A^+(z_3) A^+(z_2) | P_{A-1} \rangle d_{\sigma_1 \sigma_4}^{(\ell_2)} (2\pi) \delta(\ell_2^2) (2\pi) \delta(\ell^2 - M^2) \\ &\times \frac{\text{Tr} \left[\gamma^- \gamma^\mu (\not{q} + \not{p}' + M) \gamma^- (\not{\ell}_2 + \not{p}_2 + M) \gamma^{\sigma_4} (\not{p}_2 + M) \gamma^- (\not{\ell} + M) \gamma^{\sigma_1} (\not{\ell}_2 + \not{\ell} + M) \gamma^\nu \right]}{[(q+p')^2 - M^2 - i\epsilon] [(\ell_2 + p_2)^2 - M^2 - i\epsilon] [p_2^2 - M^2 - i\epsilon] [(\ell_2 + \ell)^2 - M^2 + i\epsilon]}. \end{aligned} \quad (165)$$

The above expression (Eq. 165) has singularity arising from the denominator of the quark propagator with momentum p'_1 , ℓ' and p_2 . We identify two simple poles for the momentum variable p_2^+ and one simple pole for p'^+ . We compute the integral in the complex plane of p_2^+ and p'^+ . The contour integration for momentum p'^+ is carried out as

$$C_1 = \oint \frac{dp'^+}{(2\pi)} \frac{e^{-ip'^+(y^- - z_3^-)}}{[(q+p')^2 - M^2 - i\epsilon]} = \frac{(-2\pi i)}{2\pi} \frac{\theta(y^- - z_3^-)}{2q^-} e^{i(q^+ - \frac{M^2}{2q^-})(y^- - z_3^-)}. \quad (166)$$

Similarly, the contour integration for momentum p_2^+ is carried out as

$$\begin{aligned} C_2 &= \oint \frac{dp_2^+}{(2\pi)} \frac{e^{-ip_2^+(z_3^- - z_2^-)}}{[p_2^2 - M^2 - i\epsilon][(\ell_2 + p_2)^2 - M^2 - i\epsilon]} \\ &= \oint \frac{dp_2^+}{(2\pi)} \frac{e^{-ip_2^+(z_3^- - z_2^-)}}{[2p_2^- p_2^+ - (\mathbf{p}_{2\perp}^2 + M^2) - i\epsilon][2(1 + \eta y)q^-(\ell_2^+ + p_2^+) - (\mathbf{k}_\perp^2 + M^2) - i\epsilon]} \\ &= \frac{(-2\pi i)}{2\pi} \frac{\theta(z_3^- - z_2^-)}{4p_2^-(1 + \eta y)q^-} e^{-i\left(\frac{(\ell_{2\perp} - \mathbf{k}_\perp)^2 + M^2}{2(1-y+\eta y)q^-}\right)(z_3^- - z_2^-)} \left[\frac{1 - e^{i\mathcal{G}_M^{(\ell_2, p_2, k)}(z_3^- - z_2^-)}}{\mathcal{G}_M^{(\ell_2, p_2, k)}} \right], \end{aligned} \quad (167)$$

where

$$\mathcal{G}_M^{(\ell_2, p_2, k)} = \ell_2^+ + \frac{\mathbf{p}_{2\perp}^2 + M^2}{2p_2^-} - \frac{\mathbf{k}_\perp^2 + M^2}{2(1 + \eta y)q^-} = \frac{J_1}{2(1 + \eta y)y(1 - y + \eta y)q^-}, \quad (168)$$

where J_1 is given in Eq. 164. The trace in the numerator of the third line of Eq. 165 is the same as the trace for the right-cut diagram given in Eq. 162. The final expression of the hadronic tensor for the left-cut diagram [Fig. 17(a)] is given by

$$\begin{aligned}
W_{1,\ell}^{\mu\nu} &= 2[-g_{\perp\perp}^{\mu\nu}] \int d(\Delta x^-) e^{iq^+(\Delta X^-)} \left\langle P \left| \bar{\psi}(\Delta X^-) \frac{\gamma^+}{4} \psi(0) \right| P \right\rangle \\
&\times e^2 e_q^2 g_s^2 \int d\zeta^- d(\Delta z^-) d^2 \Delta_{z\perp} \frac{dy}{2\pi} \frac{d^2 \ell_{2\perp}}{(2\pi)^2} \frac{d^2 k_{\perp}}{(2\pi)^2} \left[-1 + e^{i\mathcal{G}_M^{(\ell_2, p_2, k)}(z_3^- - z_2^-)} \right] e^{-ip_2^+(\Delta z^-)} e^{i\mathbf{k}_{\perp} \cdot \Delta \mathbf{z}_{\perp}} \\
&\times \frac{\theta(z_3^- - z_2^-) \theta(y^- - z_3^-) [(1 + \eta y) \ell_{2\perp}^2 - y \mathbf{k}_{\perp} \ell_{2\perp} + \kappa y^4 M^2]}{[\ell_{2\perp}^2 + M^2 y^2] J_1} \langle P_{A-1} | A^+(\zeta^-, \Delta z^-, \Delta z_{\perp}) A^+(\zeta^-, 0) | P_{A-1} \rangle \\
&\times \left[\frac{1 + (1-y)^2 + \eta y(2-y)}{y} \right] e^{i(\ell_2^+ + \ell^+)x^-} e^{-i\ell_2^+ z_3^-} e^{-i\ell^+ z_2^-} e^{-i[M^2/(2q^-)](y^- - z_3^-)},
\end{aligned} \tag{169}$$

where $\mathcal{G}_M^{(\ell_2, p_2, k)}$ is defined in Eq. 168, κ is in Eq. 146 and

$$\ell_2^+ = \frac{\ell_{2\perp}^2}{2yq^-}; \quad \ell^+ = \frac{\ell_{2\perp}^2 + M^2}{2(1-y)q^-}; \quad p_2^+ = \frac{[(\ell_{2\perp} - \mathbf{k}_{\perp})^2 + M^2]}{2(1-y + \eta y)q^-}. \tag{170}$$

The above expression (Eq. 169) of the hadronic tensor can be recast by instituting $\Delta z^- = z_3^- - z_2^-$ into the following form

$$\begin{aligned}
W_{1,\ell}^{\mu\nu} &= 2[-g_{\perp\perp}^{\mu\nu}] \int d(\Delta x^-) e^{iq^+(\Delta X^-)} \left\langle P \left| \bar{\psi}(\Delta X^-) \frac{\gamma^+}{4} \psi(0) \right| P \right\rangle \\
&\times e^2 e_q^2 g_s^2 \int d\zeta^- d(\Delta z^-) d^2 \Delta_{z\perp} \frac{dy}{2\pi} \frac{d^2 \ell_{2\perp}}{(2\pi)^2} \frac{d^2 k_{\perp}}{(2\pi)^2} \left[-1 + e^{i\mathcal{G}_M^{(\ell_2, p_2, k)}(z_3^- - z_2^-)} \right] e^{-i(\ell_2^+ + p_2^+) \Delta z^-} e^{i\mathbf{k}_{\perp} \cdot \Delta \mathbf{z}_{\perp}} \\
&\times \frac{\theta(z_3^- - z_2^-) \theta(y^- - z_3^-) [(1 + \eta y) \ell_{2\perp}^2 - y \mathbf{k}_{\perp} \ell_{2\perp} + \kappa y^4 M^2]}{[\ell_{2\perp}^2 + M^2 y^2] J_1} \langle P_{A-1} | A^+(\zeta^-, \Delta z^-, \Delta z_{\perp}) A^+(\zeta^-, 0) | P_{A-1} \rangle \\
&\times \left[\frac{1 + (1-y)^2 + \eta y(2-y)}{y} \right] e^{i(\ell_2^+ + \ell^+)(x^- - z_2^-)} e^{-i[M^2/(2q^-)](y^- - z_3^-)}.
\end{aligned} \tag{171}$$

Next, we consider the diagram shown in the right panel of Fig. 17(b). The topology of the diagram is the same as the diagram on the left panel. Moreover, they are complex conjugate of each other. The hadronic tensor for the left-cut diagram shown in Fig. 17(b) can be written as

$$\begin{aligned}
W_{1,\ell}^{\mu\nu} &= 2[-g_{\perp\perp}^{\mu\nu}] \int d(\Delta x^-) e^{iq^+(\Delta X^-)} e^{-i[M^2/(2q^-)](\Delta X^-)} \left\langle P \left| \bar{\psi}(\Delta X^-) \frac{\gamma^+}{4} \psi(0) \right| P \right\rangle \\
&\times e^2 e_q^2 g_s^2 \int d\zeta^- d(\Delta z^-) d^2 \Delta_{z\perp} \frac{dy}{2\pi} \frac{d^2 \ell_{2\perp}}{(2\pi)^2} \frac{d^2 k_{\perp}}{(2\pi)^2} \left[-1 + e^{-i\mathcal{G}_M^{(\ell_2)}(y^- - z_3^-)} \right] e^{-i\mathcal{H}_M^{(\ell_2, p_2)}(\Delta z^-)} e^{i\mathbf{k}_{\perp} \cdot \Delta \mathbf{z}_{\perp}} \\
&\times \frac{\theta(x^- - z_2^-) \theta(y^- - z_3^-) [(1 + \eta y) \ell_{2\perp}^2 - y \mathbf{k}_{\perp} \ell_{2\perp} + \kappa y^4 M^2]}{[\ell_{2\perp}^2 + M^2 y^2] J_1} \langle P_{A-1} | A^+(\zeta^-, \Delta z^-, \Delta z_{\perp}) A^+(\zeta^-, 0) | P_{A-1} \rangle \\
&\times \left[\frac{1 + (1-y)^2 + \eta y(2-y)}{y} \right],
\end{aligned} \tag{172}$$

where $\mathcal{G}_M^{(\ell_2)}$ is defined in Eq. 144, $\mathcal{H}_M^{(\ell_2, p_2)}$ is defined in Eq. 158, and J_1 is defined in Eq. 164. Similarly, the final expression of the hadronic tensor for the right-cut diagram [Fig. 17(b)] is given as

$$\begin{aligned}
W_{1,r}^{\mu\nu} &= 2[-g_{\perp\perp}^{\mu\nu}] \int d(\Delta x^-) e^{iq^+(\Delta X^-)} \left\langle P \left| \bar{\psi}(\Delta X^-) \frac{\gamma^+}{4} \psi(0) \right| P \right\rangle \\
&\times e^2 e_q^2 g_s^2 \int d\zeta^- d(\Delta z^-) d^2 \Delta_{z\perp} \frac{dy}{2\pi} \frac{d^2 \ell_{2\perp}}{(2\pi)^2} \frac{d^2 k_{\perp}}{(2\pi)^2} \left[-1 + e^{i\mathcal{G}_M^{(\ell_2, p_2, k)}(z_3^- - z_2^-)} \right] e^{-ip_2^+(\Delta z^-)} e^{i\mathbf{k}_{\perp} \cdot \Delta \mathbf{z}_{\perp}} \\
&\times \frac{\theta(-z_3^- + z_2^-) \theta(x^- - z_2^-) [(1 + \eta y) \ell_{2\perp}^2 - y \mathbf{k}_{\perp} \ell_{2\perp} + \kappa y^4 M^2]}{[\ell_{2\perp}^2 + M^2 y^2] J_1} \langle P_{A-1} | A^+(\zeta^-, \Delta z^-, \Delta z_{\perp}) A^+(\zeta^-, 0) | P_{A-1} \rangle \\
&\times \left[\frac{1 + (1-y)^2 + \eta y(2-y)}{y} \right] e^{-i(\ell_2^+ + \ell^+)y^-} e^{i\ell_2^+ z_2^-} e^{i\ell^+ z_3^-} e^{i[M^2/(2q^-)](x^- - z_2^-)},
\end{aligned} \tag{173}$$

where $\mathcal{G}_M^{(\ell_2, p_2, k)}$ is defined in Eq. 168, and

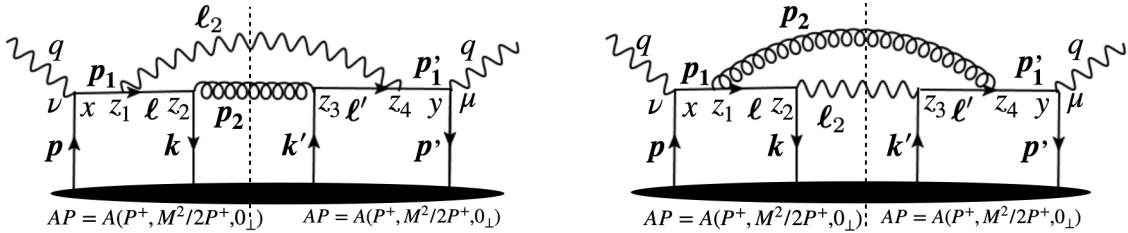
$$\ell_2^+ = \frac{\ell_{2\perp}^2}{2yq^-}; \quad \ell'^+ = \frac{\ell_{2\perp}^2 + M^2}{2(1-y)q^-}; \quad p_2^+ = \frac{[(\ell_{2\perp} - \mathbf{k}_\perp)^2 + M^2]}{2(1-y + \eta y)q^-}. \quad (174)$$

The above expression (Eq. 173) of the hadronic tensor can be recast by instituting $\Delta z^- = z_3^- - z_2^-$ into the following form

$$\begin{aligned} W_{1,r}^{\mu\nu} &= 2[-g_{\perp\perp}^{\mu\nu}] \int d(\Delta x^-) e^{iq^+(\Delta x^-)} \left\langle P \left| \bar{\psi}(\Delta X^-) \frac{\gamma^+}{4} \psi(0) \right| P \right\rangle \\ &\times e^2 e_q^2 g_s^2 \int d\zeta^- d(\Delta z^-) d^2 \Delta z_\perp \frac{dy}{2\pi} \frac{d^2 \ell_{2\perp}}{(2\pi)^2} \frac{d^2 k_\perp}{(2\pi)^2} \left[-1 + e^{i\mathcal{G}_M^{(\ell_2, p_2, k)}(z_3^- - z_2^-)} \right] e^{-i(\ell_2^+ + p_2^+)(\Delta z^-)} e^{i\mathbf{k}_\perp \cdot \Delta \mathbf{z}_\perp} \\ &\times \frac{\theta(-z_3^- + z_2^-) \theta(x^- - z_2^-) [(1 + \eta y) \ell_{2\perp}^2 - y \mathbf{k}_\perp \cdot \ell_{2\perp} + \kappa y^4 M^2]}{[\ell_{2\perp}^2 + M^2 y^2] J_1} \langle P_{A-1} | A^+(\zeta^-, \Delta z^-, \Delta z_\perp) A^+(\zeta^-, 0) | P_{A-1} \rangle \\ &\times \left[\frac{1 + (1-y)^2 + \eta y(2-y)}{y} \right] e^{-i(\ell_2^+ + \ell'^+)(y^- - z_3^-)} e^{i[M^2/(2q^-)](x^- - z_2^-)}. \end{aligned} \quad (175)$$

Appendix B: SINGLE-EMISSION SINGLE-SCATTERING KERNEL: ONE PHOTON AND ONE GLUON IN THE FINAL STATE

This section summarizes the calculation of all possible diagrams contributing to kernel-2. The final state consists of a photon and a gluon with an in-medium quark exchange from the medium.



(a) The final state contains a gluon generated from the conversion process and a bremsstrahlung photon. (b) The final state contains a photon generated from the conversion process and a bremsstrahlung gluon.

FIG. 18: A forward scattering diagram contributing to kernel-2.

The hadronic tensor for Fig. 18(a) has the following form

$$\begin{aligned} W_{2,c}^{\mu\nu} &= e^2 e_q^2 g_s^2 \int d^4 x d^4 y d^4 z_2 d^4 z_3 \int \frac{d^4 p}{(2\pi)^4} \frac{d^4 p'}{(2\pi)^4} \frac{d^4 \ell_2}{(2\pi)^4} \frac{d^4 p_2}{(2\pi)^4} e^{-ip'y} e^{ipx} \left\langle P \left| \bar{\psi}(y) \frac{\gamma^+}{4} \psi(x) \right| P \right\rangle \delta^{bc} \text{Tr}[t^b t^c] \\ &\times e^{i(q+p'-p_2-\ell_2)z_3} e^{i(\ell_2+p_2-q-p)z_2} \left\langle P_{A-1} \left| \bar{\psi}(z_2) \frac{\gamma^+}{4} \psi(z_3) \right| P_{A-1} \right\rangle d_{\sigma_1 \sigma_4}^{(\ell_2)} d_{\sigma_3 \sigma_2}^{(p_2)} (2\pi) \delta(\ell_2^2) (2\pi) \delta(p_2^2) \\ &\times \frac{\text{Tr}[\gamma^- \gamma^\mu (\not{q} + \not{p}') \gamma^{\sigma_4} (\not{q} + \not{p}' - \not{\ell}_2) \gamma^{\sigma_3} \gamma^- \gamma^{\sigma_2} (\not{q} + \not{p} - \not{\ell}_2) \gamma^{\sigma_1} (\not{q} + \not{p}) \gamma^\nu]}{[(q+p')^2 - i\epsilon] [(q+p)^2 + i\epsilon] [(q+p'-\ell_2)^2 - i\epsilon] [(q+p-\ell_2)^2 + i\epsilon]}. \end{aligned} \quad (176)$$

The above expression of the hadronic tensor has singularity when the denominator of the propagator for p_1 , ℓ , ℓ'

and p'_1 becomes on-shell. It contains two simple poles for p^+ and p'^+ . The contour integration for p^+ gives

$$\begin{aligned}
C_1 &= \oint \frac{dp^+}{(2\pi)} \frac{e^{ip^+(x^- - z_2^-)}}{\left[(q+p)^2 + i\epsilon\right] \left[(q+p - \ell_2)^2 + i\epsilon\right]} \\
&= \oint \frac{dp^+}{(2\pi)} \frac{e^{ip^+(x^- - z_2^-)}}{2q^- [q^+ + p^+ + i\epsilon] 2(q^- - \ell_2^-) \left[q^+ + p^+ - \ell_2^+ - \frac{\ell_{2\perp}^2}{2(q^- - \ell_2^-)} + i\epsilon\right]} \\
&= \frac{(2\pi i)}{2\pi} \frac{\theta(x^- - z_2^-)}{4q^-(q^- - \ell_2^-)} e^{-iq^+(x^- - z_2^-)} \left[\frac{-1 + e^{i\mathcal{G}_0^{(\ell_2)}(x^- - z_2^-)}}{\mathcal{G}_0^{(\ell_2)}} \right],
\end{aligned} \tag{177}$$

where

$$\mathcal{G}_0^{(\ell_2)} = \ell_2^+ + \frac{\ell_{2\perp}^2}{2(q^- - \ell_2^-)} = \frac{\ell_{2\perp}^2}{2y(1-y)q^-}. \tag{178}$$

Similarly, the contour integration for p'^+ gives

$$\begin{aligned}
C_2 &= \oint \frac{dp'^+}{(2\pi)} \frac{e^{-ip'^+(y^- - z_3^-)}}{\left[(q+p')^2 - i\epsilon\right] \left[(q+p' - \ell_2)^2 - i\epsilon\right]} \\
&= \oint \frac{dp'^+}{(2\pi)} \frac{e^{-ip'^+(y^- - z_3^-)}}{2q^- [q^+ + p'^+ - i\epsilon] 2(q^- - \ell_2^-) \left[q^+ + p'^+ - \ell_2^+ - \frac{\ell_{2\perp}^2}{2(q^- - \ell_2^-)} - i\epsilon\right]} \\
&= \frac{(-2\pi i)}{2\pi} \frac{\theta(y^- - z_3^-)}{4q^-(q^- - \ell_2^-)} e^{iq^+(y^- - z_3^-)} \left[\frac{-1 + e^{-i\mathcal{G}_0^{(\ell_2)}(y^- - z_3^-)}}{\mathcal{G}_0^{(\ell_2)}} \right].
\end{aligned} \tag{179}$$

The trace in the third line of Eq. 176 simplifies to

$$\begin{aligned}
&\text{Tr} \left[\gamma^- \gamma^\mu (\not{q} + \not{p}') \gamma^{\sigma_4} (\not{q} + \not{p}' - \not{\ell}_2) \gamma^{\sigma_3} \gamma^- \gamma^{\sigma_2} (\not{q} + \not{p} - \not{\ell}_2) \gamma^{\sigma_1} (\not{q} + \not{p}) \gamma^\nu \right] d_{\sigma_1 \sigma_4}^{(\ell_2)} d_{\sigma_3 \sigma_2}^{(p_2)} \\
&= 32[-g_{\perp\perp}^{\mu\nu}](q^-)^2 \left[\frac{1 + (1-y)^2}{y^2} \right] \ell_{2\perp}^2.
\end{aligned} \tag{180}$$

Finally, the hadronic tensor [Fig. 18(a)] reduces to the following form

$$\begin{aligned}
W_{2,c}^{\mu\nu} &= 2[-g_{\perp\perp}^{\mu\nu}] \int d(\Delta x^-) e^{iq^+(\Delta x^-)} \left\langle P \left| \bar{\psi}(\Delta x^-) \frac{\gamma^+}{4} \psi(0) \right| P \right\rangle \\
&\times e^2 e_q^2 g_s^2 \int d\zeta^- d(\Delta z^-) d^2 \Delta z_\perp \frac{dy}{2\pi} \frac{d^2 \ell_{2\perp}}{(2\pi)^2} \frac{d^2 k_\perp}{(2\pi)^2} \left[2 - 2 \cos \left\{ \mathcal{G}_0^{(\ell_2)} \zeta^- \right\} \right] e^{-i(\Delta z^-) \mathcal{H}_0^{(\ell_2, p_2)}} e^{i\mathbf{k}_\perp \cdot \Delta \mathbf{z}_\perp} \\
&\times \frac{\theta(x^- - z_2^-) \theta(y^- - z_3^-)}{\ell_{2\perp}^2} \frac{1}{(1-y + \eta y)q^-} \left\langle P_{A-1} \left| \bar{\psi}(\zeta^-, 0) \frac{\gamma^+}{4} \psi(\zeta^-, \Delta z^-, \Delta z_\perp) \right| P_{A-1} \right\rangle \\
&\times \left[\frac{1 + (1-y)^2}{y} \right] [C_f N_c],
\end{aligned} \tag{181}$$

where $\mathcal{G}_0^{(\ell_2)}$ is given in Eq. 178 and

$$\mathcal{H}_0^{(\ell_2, p_2)} = \ell_2^+ + p_2^+ = \frac{\ell_{2\perp}^2}{2yq^-} + \frac{(\ell_{2\perp} - \mathbf{k}_\perp)^2}{2(1-y + \eta y)q^-}. \tag{182}$$

Next, we consider a forward scattering diagram [Fig. 18(b)] where the final state contains a photon generated from the conversion process and a bremsstrahlung gluon. The associated hadronic tensor is given as

$$\begin{aligned}
W_{2,c}^{\mu\nu} &= e^2 e_q^2 g_s^2 \int d^4 x d^4 y d^4 z_2 d^4 z_3 \int \frac{d^4 p}{(2\pi)^4} \frac{d^4 p'}{(2\pi)^4} \frac{d^4 \ell_2}{(2\pi)^4} \frac{d^4 p_2}{(2\pi)^4} e^{-ip'y} e^{ipx} \left\langle P \left| \bar{\psi}(y) \frac{\gamma^+}{4} \psi(x) \right| P \right\rangle \delta^{ad} \text{Tr}[t^a t^d] \\
&\times e^{i(q+p'-p_2-\ell_2)z_3} e^{i(\ell_2+p_2-q-p)z_2} \left\langle P_{A-1} \left| \bar{\psi}(z_2) \frac{\gamma^+}{4} \psi(z_3) \right| P_{A-1} \right\rangle d_{\sigma_3 \sigma_2}^{(\ell_2)} d_{\sigma_4 \sigma_1}^{(p_2)} (2\pi) \delta(\ell_2^2) (2\pi) \delta(p_2^2) \\
&\times \frac{\text{Tr} \left[\gamma^- \gamma^\mu (\not{q} + \not{p}') \gamma^{\sigma_4} (\not{q} + \not{p}' - \not{p}_2) \gamma^{\sigma_3} \gamma^- \gamma^{\sigma_2} (\not{q} + \not{p} - \not{p}_2) \gamma^{\sigma_1} (\not{q} + \not{p}) \gamma^\nu \right]}{\left[(q+p')^2 - i\epsilon \right] \left[(q+p)^2 + i\epsilon \right] \left[(q+p-p_2)^2 - i\epsilon \right] \left[(q+p-p_2)^2 + i\epsilon \right]}.
\end{aligned} \tag{183}$$

The above expression of the hadronic tensor has singularity when the denominator of the propagator for p_1 , ℓ , ℓ' and p_1' becomes on-shell. It contains two simple poles for p^+ and p'^+ . The contour integration for p^+ gives

$$\begin{aligned}
C_1 &= \oint \frac{dp^+}{(2\pi)} \frac{e^{ip^+(x^- - z_2^-)}}{[(q+p)^2 + i\epsilon][(q+p-p_2)^2 + i\epsilon]} \\
&= \oint \frac{dp^+}{(2\pi)} \frac{e^{ip^+(x^- - z_2^-)}}{2q^- [q^+ + p^+ + i\epsilon] 2(q^- - p_2^-) \left[q^+ + p^+ - p_2^+ - \frac{\mathbf{p}_{2\perp}^2}{2(q^- - p_2^-)} + i\epsilon \right]} \\
&= \frac{(2\pi i)}{2\pi} \frac{\theta(x^- - z_2^-)}{4q^-(q^- - p_2^-)} e^{-iq^+(x^- - z_2^-)} \left[\frac{-1 + e^{i\mathcal{G}_0^{(p_2)}(x^- - z_2^-)}}{\mathcal{G}_0^{(p_2)}} \right],
\end{aligned} \tag{184}$$

where

$$\mathcal{G}_0^{(p_2)} = p_2^+ + \frac{\mathbf{p}_{2\perp}^2}{2(q^- - p_2^-)} = \frac{\mathbf{p}_{2\perp}^2}{2y(1-y+\eta y)(1-\eta)q^-}. \tag{185}$$

Similarly, the contour integration for p'^+ gives

$$\begin{aligned}
C_2 &= \oint \frac{dp'^+}{(2\pi)} \frac{e^{-ip'^+(y^- - z_3^-)}}{[(q+p')^2 - i\epsilon][(q+p'-p_2)^2 - i\epsilon]} \\
&= \oint \frac{dp'^+}{(2\pi)} \frac{e^{-ip'^+(y^- - z_3^-)}}{2q^- [q^+ + p'^+ - i\epsilon] 2(q^- - p_2^-) \left[q^+ + p'^+ - p_2^+ - \frac{\mathbf{p}_{2\perp}^2}{2(q^- - p_2^-)} - i\epsilon \right]} \\
&= \frac{(-2\pi i)}{2\pi} \frac{\theta(y^- - z_3^-)}{4q^-(q^- - p_2^-)} e^{iq^+(y^- - z_3^-)} \left[\frac{-1 + e^{-i\mathcal{G}_0^{(p_2)}(y^- - z_3^-)}}{\mathcal{G}_0^{(p_2)}} \right].
\end{aligned} \tag{186}$$

The trace in the third line of Eq. 183 simplifies to

$$\begin{aligned}
&\text{Tr} \left[\gamma^- \gamma^\mu (\not{q} + \not{p}') \gamma^{\sigma_4} (\not{q} + \not{p}' - \not{p}_2) \gamma^{\sigma_3} \gamma^- \gamma^{\sigma_2} (\not{q} + \not{p} - \not{p}_2) \gamma^{\sigma_1} (\not{q} + \not{p}) \gamma^\nu \right] d_{\sigma_1 \sigma_4}^{(p_2)} d_{\sigma_3 \sigma_2}^{(\ell_2)} \\
&= 32[-g_{\perp\perp}^{\mu\nu}] (q^-)^2 \left[\frac{1 + y^2 + \eta y^2 (\eta - 2)}{(1 - y + \eta y)^2} \right] \mathbf{p}_{2\perp}^2.
\end{aligned} \tag{187}$$

Finally, the hadronic tensor [Fig. 18(b)] reduces to the following form

$$\begin{aligned}
W_{2,c}^{\mu\nu} &= 2[-g_{\perp\perp}^{\mu\nu}] \int d(\Delta x^-) e^{iq^+(\Delta x^-)} \left\langle P \left| \bar{\psi}(\Delta x^-) \frac{\gamma^+}{4} \psi(0) \right| P \right\rangle \\
&\times e^2 e_q^2 g_s^2 \int d\zeta^- d(\Delta z^-) d^2 \Delta z_\perp \frac{dy}{2\pi} \frac{d^2 \ell_{2\perp}}{(2\pi)^2} \frac{d^2 k_\perp}{(2\pi)^2} \left[2 - 2 \cos \left\{ \mathcal{G}_0^{(p_2)} \zeta^- \right\} \right] e^{-i(\Delta z^-) \mathcal{H}_0^{(\ell_2, p_2)}} e^{i\mathbf{k}_\perp \cdot \Delta \mathbf{z}_\perp} \\
&\times \frac{\theta(x^- - z_2^-) \theta(y^- - z_3^-)}{(\ell_{2\perp} - \mathbf{k}_\perp)^2} \frac{1}{yq^-} \left\langle P_{A-1} \left| \bar{\psi}(\zeta^-, 0) \frac{\gamma^+}{4} \psi(\zeta^-, \Delta z^-, \Delta z_\perp) \right| P_{A-1} \right\rangle \\
&\times \left[\frac{1 + y^2 + \eta y^2 (\eta - 2)}{(1 - y + \eta y)} \right] [C_f N_c],
\end{aligned} \tag{188}$$

where $\mathcal{H}_0^{(\ell_2, p_2)}$ is defined in Eq. 182, and

$$\mathcal{G}_0^{(p_2)} = p_2^+ + \frac{\mathbf{p}_{2\perp}^2}{2(q^- - p_2^-)} = \frac{(\ell_{2\perp} - \mathbf{k}_\perp)^2}{2y(1-y+\eta y)(1-\eta)q^-}, \tag{189}$$

Next, we consider a forward scattering diagram as shown in Fig. 19. The hadronic tensor for Fig. 19 (a) is

$$\begin{aligned}
W_{2,c}^{\mu\nu} &= e^2 e_q^2 g_s^2 \int d^4 x d^4 y d^4 z_2 d^4 z_3 \int \frac{d^4 p}{(2\pi)^4} \frac{d^4 p'}{(2\pi)^4} \frac{d^4 \ell_2}{(2\pi)^4} \frac{d^4 p_2}{(2\pi)^4} e^{-ip'y} e^{ipx} \left\langle P \left| \bar{\psi}(y) \frac{\gamma^+}{4} \psi(x) \right| P \right\rangle \delta^{ac} \text{Tr}[t^a t^c] \\
&\times e^{i(q+p'-p_2-\ell_2)z_3} e^{i(\ell_2+p_2-q-p)z_2} \left\langle P_{A-1} \left| \bar{\psi}(z_2) \frac{\gamma^+}{4} \psi(z_3) \right| P_{A-1} \right\rangle d_{\sigma_2 \sigma_4}^{(\ell_2)} d_{\sigma_3 \sigma_1}^{(p_2)} (2\pi) \delta(\ell_2^2) (2\pi) \delta(p_2^2) \\
&\times \frac{\text{Tr} \left[\gamma^- \gamma^\mu (\not{q} + \not{p}') \gamma^{\sigma_4} (\not{q} + \not{p}' - \not{\ell}_2) \gamma^{\sigma_3} \gamma^- \gamma^{\sigma_2} (\not{q} + \not{p} - \not{p}_2) \gamma^{\sigma_1} (\not{q} + \not{p}) \gamma^\nu \right]}{\left[(q+p')^2 - i\epsilon \right] \left[(q+p)^2 + i\epsilon \right] \left[(q+p'-\ell_2)^2 - i\epsilon \right] \left[(q+p-p_2)^2 + i\epsilon \right]}.
\end{aligned} \tag{190}$$

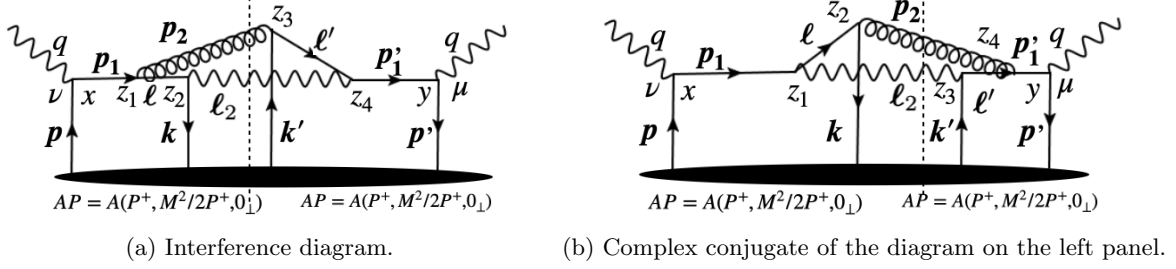


FIG. 19: A forward scattering diagram contributing to kernel-2.

The above expression has singularity when the denominator of the propagator for p_1 , ℓ , ℓ' and p'_1 becomes on-shell. It contains two simple poles for p^+ and p'^+ . The contour integration for p^+ gives

$$\begin{aligned}
C_1 &= \oint \frac{dp^+}{(2\pi)} \frac{e^{ip^+(x^- - z_2^-)}}{\left[(q+p)^2 + i\epsilon \right] \left[(q+p-p_2)^2 + i\epsilon \right]} \\
&= \oint \frac{dp^+}{(2\pi)} \frac{e^{ip^+(x^- - z_2^-)}}{2q^- [q^+ + p^+ + i\epsilon] 2(q^- - p_2^-) \left[q^+ + p^+ - p_2^+ - \frac{\mathbf{p}_{2\perp}^2}{2(q^- - p_2^-)} + i\epsilon \right]} \\
&= \frac{(2\pi i)}{2\pi} \frac{\theta(x^- - z_2^-)}{4q^-(q^- - p_2^-)} e^{-iq^+(x^- - z_2^-)} \left[\frac{-1 + e^{i\mathcal{G}_0^{(p_2)}(x^- - z_2^-)}}{\mathcal{G}_0^{(p_2)}} \right],
\end{aligned} \tag{191}$$

where $\mathcal{G}_0^{(p_2)}$ is defined in Eq. 189.

Similarly, the contour integration for p'^+ gives

$$\begin{aligned}
C_2 &= \oint \frac{dp'^+}{(2\pi)} \frac{e^{-ip'^+(y^- - z_3^-)}}{\left[(q+p')^2 - i\epsilon \right] \left[(q+p' - \ell_2)^2 - i\epsilon \right]} \\
&= \oint \frac{dp'^+}{(2\pi)} \frac{e^{-ip'^+(y^- - z_3^-)}}{2q^- [q^+ + p'^+ - i\epsilon] 2(q^- - \ell_2^-) \left[q^+ + p'^+ - \ell_2^+ - \frac{\ell_{2\perp}^2}{2(q^- - \ell_2^-)} - i\epsilon \right]} \\
&= \frac{(-2\pi i)}{2\pi} \frac{\theta(y^- - z_3^-)}{4q^-(q^- - \ell_2^-)} e^{iq^+(y^- - z_3^-)} \left[\frac{-1 + e^{-i\mathcal{G}_0^{(\ell_2)}(y^- - z_3^-)}}{\mathcal{G}_0^{(\ell_2)}} \right],
\end{aligned} \tag{192}$$

where $\mathcal{G}_0^{(\ell_2)}$ is defined in Eq. 178.

The trace in the third line of Eq. 190 simplifies to

$$\begin{aligned}
&\text{Tr} \left[\gamma^- \gamma^\mu (\not{q} + \not{p}') \gamma^{\sigma_4} (\not{q} + \not{p}' - \not{\ell}_2) \gamma^{\sigma_3} \gamma^- \gamma^{\sigma_2} (\not{q} + \not{p} - \not{p}_2) \gamma^{\sigma_1} (\not{q} + \not{p}) \gamma^\nu \right] d_{\sigma_2 \sigma_4}^{(\ell_2)} d_{\sigma_3 \sigma_1}^{(p_2)} \\
&= \frac{32 (q^-)^2 [-g_{\perp\perp}^{\mu\nu}] (1 - y + 2\eta y)}{(1 - y + \eta y)y} [-\ell_{2\perp}^2 + \ell_{2\perp} \cdot \mathbf{k}_\perp].
\end{aligned} \tag{193}$$

The final expression of the hadronic tensor for Fig. 19(a) is given by

$$\begin{aligned}
W_{2,c}^{\mu\nu} &= 2[-g_{\perp\perp}^{\mu\nu}] \int d(\Delta x^-) e^{iq^+(\Delta x^-)} \left\langle P \left| \bar{\psi}(\Delta X^-) \frac{\gamma^+}{4} \psi(0) \right| P \right\rangle \\
&\times e^2 e_q^2 g_s^2 \int d\zeta^- d(\Delta z^-) d^2 \Delta z_\perp \frac{dy d^2 \ell_{2\perp} d^2 k_\perp}{2\pi (2\pi)^2 (2\pi)^2} \left[-1 + e^{i\mathcal{G}_0^{(p_2)}(x^- - z_2^-)} \right] \left[-1 + e^{-i\mathcal{G}_0^{(\ell_2)}(y^- - z_3^-)} \right] e^{-i(\Delta z^-) \mathcal{H}_0^{(\ell_2, p_2)}} \\
&\times \frac{\theta(x^- - z_2^-) \theta(y^- - z_3^-)}{(1 - y + \eta y) q^-} \frac{[-\ell_{2\perp}^2 + \ell_{2\perp} \cdot \mathbf{k}_\perp]}{(\ell_{2\perp} - \mathbf{k}_{2\perp})^2 \ell_{2\perp}^2} e^{i\mathbf{k}_\perp \cdot \Delta \mathbf{z}_\perp} \left\langle P_{A-1} \left| \bar{\psi}(\zeta^-, 0) \frac{\gamma^+}{4} \psi(\zeta^-, \Delta z^-, \Delta z_\perp) \right| P_{A-1} \right\rangle \\
&\times \left[\frac{(1 - y + 2\eta y)}{y} \right] [C_f N_c],
\end{aligned} \tag{194}$$

where $\mathcal{G}_0^{(\ell_2)}$ is given in Eq. 178, $\mathcal{G}_0^{(p_2)}$ is given in Eq. 189, and $\mathcal{H}_0^{(\ell_2, p_2)}$ is defined in Eq. 182.

The forward scattering diagram shown in Fig. 19(b) is a complex conjugate of the diagram in Fig. 19 (a). The hadronic tensor of the diagram in Fig. 19(b) is given as

$$\begin{aligned}
W_{2,c}^{\mu\nu} &= e^2 e_q^2 g_s^2 \int d^4x d^4y d^4z_2 d^4z_3 \int \frac{d^4p}{(2\pi)^4} \frac{d^4p'}{(2\pi)^4} \frac{d^4\ell_2}{(2\pi)^4} \frac{d^4p_2}{(2\pi)^4} e^{-ip'y} e^{ipx} \left\langle P \left| \bar{\psi}(y) \frac{\gamma^+}{4} \psi(x) \right| P \right\rangle \delta^{ac} \text{Tr}[t^a t^c] \\
&\times e^{i(q+p'-p_2-\ell_2)z_3} e^{i(\ell_2+p_2-q-p)z_2} \left\langle P_{A-1} \left| \bar{\psi}(z_2) \frac{\gamma^+}{4} \psi(z_3) \right| P_{A-1} \right\rangle d_{\sigma_2\sigma_4}^{(p_2)} d_{\sigma_3\sigma_1}^{(\ell_2)} (2\pi)\delta(\ell_2^2) (2\pi)\delta(p_2^2) \\
&\times \frac{\text{Tr} \left[\gamma^- \gamma^\mu (\not{q} + \not{p}') \gamma^{\sigma_4} (\not{q} + \not{p}' - \not{p}_2) \gamma^{\sigma_3} \gamma^- \gamma^{\sigma_2} (\not{q} + \not{p} - \not{\ell}_2) \gamma^{\sigma_1} (\not{q} + \not{p}) \gamma^\nu \right]}{\left[(q+p)^2 - i\epsilon \right] \left[(q+p)^2 + i\epsilon \right] \left[(q+p-p_2)^2 - i\epsilon \right] \left[(q+p-\ell_2)^2 + i\epsilon \right]}.
\end{aligned} \tag{195}$$

The above expression of the hadronic tensor has singularity when the denominator of the propagator for p_1 , ℓ , ℓ' and p'_1 becomes on-shell. It contains two simple poles for p^+ and p'^+ . The contour integration for p^+ gives

$$\begin{aligned}
C_1 &= \oint \frac{dp^+}{(2\pi)} \frac{e^{ip^+(x^- - z_2^-)}}{\left[(q+p)^2 + i\epsilon \right] \left[(q+p-\ell_2)^2 + i\epsilon \right]} \\
&= \oint \frac{dp^+}{(2\pi)} \frac{e^{ip^+(x^- - z_2^-)}}{2q^- [q^+ + p^+ + i\epsilon] 2(q^- - \ell_2^-) \left[q^+ + p^+ - \ell_2^+ - \frac{\ell_{2\perp}^2}{2(q^- - \ell_2^-)} + i\epsilon \right]} \\
&= \frac{(2\pi i)}{2\pi} \frac{\theta(x^- - z_2^-)}{4q^-(q^- - \ell_2^-)} e^{-iq^+(x^- - z_2^-)} \left[\frac{-1 + e^{i\mathcal{G}_0^{(\ell_2)}(x^- - z_2^-)}}{\mathcal{G}_0^{(\ell_2)}} \right],
\end{aligned} \tag{196}$$

where $\mathcal{G}_0^{(\ell_2)}$ is given in Eq. 178.

Similarly, the contour integration for p'^+ gives

$$\begin{aligned}
C_2 &= \oint \frac{dp'^+}{(2\pi)} \frac{e^{-ip'^+(y^- - z_3^-)}}{\left[(q+p')^2 - i\epsilon \right] \left[(q+p'-p_2)^2 - i\epsilon \right]} \\
&= \oint \frac{dp'^+}{(2\pi)} \frac{e^{-ip'^+(y^- - z_3^-)}}{2q^- [q^+ + p'^+ - i\epsilon] 2(q^- - p_2^-) \left[q^+ + p'^+ - p_2^+ - \frac{p_{2\perp}^2}{2(q^- - p_2^-)} - i\epsilon \right]} \\
&= \frac{(-2\pi i)}{2\pi} \frac{\theta(y^- - z_3^-)}{4q^-(q^- - p_2^-)} e^{iq^+(y^- - z_3^-)} \left[\frac{-1 + e^{-i\mathcal{G}_0^{(p_2)}(y^- - z_3^-)}}{\mathcal{G}_0^{(p_2)}} \right],
\end{aligned} \tag{197}$$

where $\mathcal{G}_0^{(p_2)}$ is given in Eq. 189. The trace in 3rd line of Eq. 195 simplifies to

$$\begin{aligned}
&\text{Tr} \left[\gamma^- \gamma^\mu (\not{q} + \not{p}') \gamma^{\sigma_4} (\not{q} + \not{p}' - \not{p}_2) \gamma^{\sigma_3} \gamma^- \gamma^{\sigma_2} (\not{q} + \not{p} - \not{\ell}_2) \gamma^{\sigma_1} (\not{q} + \not{p}) \gamma^\nu \right] d_{\sigma_2\sigma_4}^{(p_2)} d_{\sigma_3\sigma_1}^{(\ell_2)} \\
&= \frac{32(q^-)^2 [-g_{\perp\perp}^{\mu\nu}] (1-y+2\eta y)}{(1-y+\eta y)y} [-\ell_{2\perp}^2 + \ell_{2\perp} \cdot \mathbf{k}_\perp].
\end{aligned} \tag{198}$$

The final expression of the hadronic tensor for Fig. 19(b) is given by

$$\begin{aligned}
W_{2,c}^{\mu\nu} &= 2[-g_{\perp\perp}^{\mu\nu}] \int d(\Delta x^-) e^{iq^+(\Delta x^-)} \left\langle P \left| \bar{\psi}(\Delta X^-) \frac{\gamma^+}{4} \psi(0) \right| P \right\rangle \\
&\times e^2 e_q^2 g_s^2 \int d\zeta^- d(\Delta z^-) d^2\Delta z_\perp \frac{dy}{2\pi} \frac{d^2\ell_{2\perp}}{(2\pi)^2} \frac{d^2k_\perp}{(2\pi)^2} \left[-1 + e^{i\mathcal{G}_0^{(\ell_2)}(x^- - z_2^-)} \right] \left[-1 + e^{-i\mathcal{G}_0^{(p_2)}(y^- - z_3^-)} \right] e^{-i(\Delta z^-) \mathcal{H}_0^{(\ell_2, p_2)}} \\
&\times \frac{\theta(x^- - z_2^-) \theta(y^- - z_3^-)}{(1-y+\eta y)q^-} \frac{[-\ell_{2\perp}^2 + \ell_{2\perp} \cdot \mathbf{k}_\perp]}{(\ell_{2\perp} - \mathbf{k}_{2\perp})^2 \ell_{2\perp}^2} e^{i\mathbf{k}_\perp \cdot \Delta z_\perp} \left\langle P_{A-1} \left| \bar{\psi}(\zeta^-, 0) \frac{\gamma^+}{4} \psi(\zeta^-, \Delta z^-, \Delta z_\perp) \right| P_{A-1} \right\rangle \\
&\times \left[\frac{(1-y+2\eta y)}{y} \right] [C_f N_c],
\end{aligned} \tag{199}$$

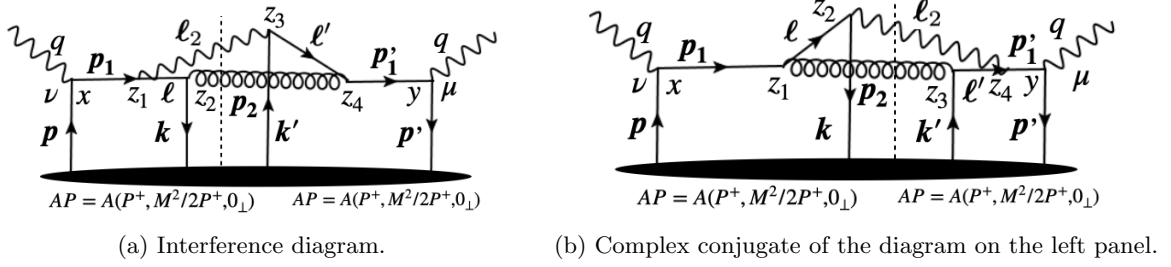


FIG. 20: A forward scattering diagram contributing to kernel-2.

where $\mathcal{G}_0^{(\ell_2)}$, $\mathcal{G}_0^{(p_2)}$, and $\mathcal{H}_0^{(\ell_2, p_2)}$ are given in Eq. 178, Eq. 189, Eq. 182, respectively.

The diagram presented in Fig. 20(a) is identical to the diagram shown in Fig 19(b); therefore, the hadronic tensors are identical. Similarly, The diagram presented in Fig. 20(b) is identical to the diagram shown in Fig 19(a); thus, the corresponding hadronic tensor is the same. We do not include the contributions to kernel-2 from Fig. 20(a) and Fig. 20(b), because doing so leads to double-counting.

Appendix C: SINGLE-EMISSION SINGLE-SCATTERING KERNEL: VIRTUAL PHOTON CORRECTIONS WITH A QUARK AND ANTI-QUARK IN FINAL STATE

This section summarizes the calculation of all possible diagrams contributing to kernel-3. The diagrams consist of a quark and anti-quark in the final state with an in-medium quark exchange with the medium. Each forward scattering diagram contains a photon propagator and a gluon propagator leading to correction $\mathcal{O}(\alpha_{em}\alpha_s)$.

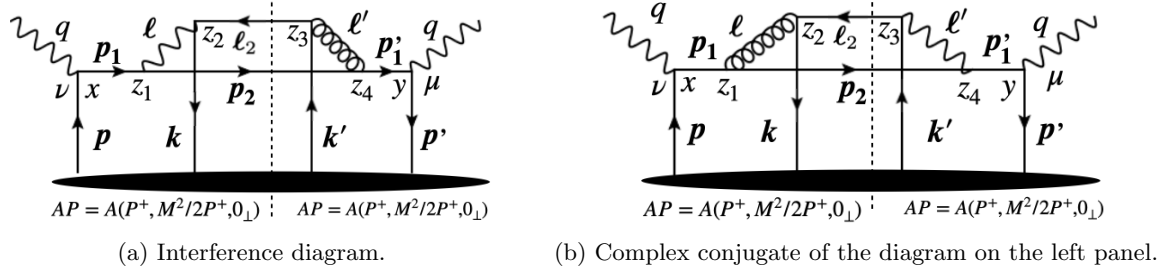


FIG. 21: A forward scattering diagram contributing to kernel-3.

The Fig. 21 represents a forward scattering diagram with virtual photon corrections that contribute to kernel type-3. The hadronic tensor for Fig. 21(a) has the following form

$$\begin{aligned}
W_{3,c}^{\mu\nu} &= e^2 e_q^2 g_s^2 \int d^4x d^4y d^4z_2 d^4z_3 \int \frac{d^4p}{(2\pi)^4} \frac{d^4p'}{(2\pi)^4} \frac{d^4\ell_2}{(2\pi)^4} \frac{d^4p_2}{(2\pi)^4} e^{-ip'y} e^{ipx} \left\langle P \left| \bar{\psi}(y) \frac{\gamma^+}{4} \psi(x) \right| P \right\rangle \delta^{cd} \text{Tr}[t^c t^d] \\
&\times e^{i(q+p'-p_2-\ell_2)z_3} e^{i(\ell_2+p_2-q-p)z_2} \left\langle P_{A-1} \left| \bar{\psi}(z_2) \frac{\gamma^+}{4} \psi(z_3) \right| P_{A-1} \right\rangle d_{\sigma_1\sigma_2}^{(q+p-p_2)} d_{\sigma_3\sigma_4}^{(q+p'-p_2)} (2\pi)\delta(\ell_2^2) (2\pi)\delta(p_2^2 - M^2) \\
&\times \frac{\text{Tr} \left[\gamma^- \gamma^\mu (\not{q} + \not{p}' + M) \gamma^{\sigma_4} (\not{p}_2 + M) \gamma^{\sigma_1} (\not{q} + \not{p} + M) \gamma^\nu \right] \text{Tr} \left[\gamma^- \gamma^{\sigma_2} \not{\ell}_2 \gamma^{\sigma_3} \right]}{\left[(q+p')^2 - M^2 - i\epsilon \right] \left[(q+p)^2 - M^2 + i\epsilon \right] \left[(q+p'-p_2)^2 - i\epsilon \right] \left[(q+p-p_2)^2 + i\epsilon \right]}.
\end{aligned} \tag{200}$$

The above expression of the hadonic tensor has singularity when the denominator of the propagator for p_1 , ℓ , ℓ' and

p'_1 becomes on-shell. It contains two simple poles for p^+ and p'^+ . The contour integration for p^+ gives

$$\begin{aligned}
C_1 &= \oint \frac{dp^+}{(2\pi)} \frac{e^{ip^+(x^- - z_2^-)}}{\left[(q+p)^2 - M^2 + i\epsilon\right] \left[(q+p-p_2)^2 + i\epsilon\right]} \\
&= \oint \frac{dp^+}{(2\pi)} \frac{e^{ip^+(x^- - z_2^-)}}{2q^- \left[q^+ + p^+ - \frac{M^2}{2q^-} + i\epsilon\right] 2(q^- - p_2^-) \left[q^+ + p^+ - p_2^+ - \frac{\mathbf{p}_{2\perp}^2}{2(q^- - p_2^-)} + i\epsilon\right]} \\
&= \frac{(2\pi i)}{2\pi} \frac{\theta(x^- - z_2^-)}{4q^-(q^- - p_2^-)} e^{i\left[-q^+ + \frac{M^2}{2q^-}\right](x^- - z_2^-)} \left[\frac{-1 + e^{i\mathcal{G}_M^{(p_2)}(x^- - z_2^-)}}{\mathcal{G}_M^{(p_2)}} \right],
\end{aligned} \tag{201}$$

where

$$\mathcal{G}_M^{(p_2)} = p_2^+ + \frac{\mathbf{p}_{2\perp}^2}{2(q^- - p_2^-)} - \frac{M^2}{2q^-} = \frac{(\ell_{2\perp} - \mathbf{k}_\perp)^2 + y^2(1-\eta)^2 M^2}{2y(1-y+\eta y)(1-\eta)q^-}. \tag{202}$$

Similarly, the contour integration for p'^+ can be done

$$\begin{aligned}
C_2 &= \oint \frac{dp'^+}{(2\pi)} \frac{e^{-ip'^+(y^- - z_3^-)}}{\left[(q+p')^2 - M^2 - i\epsilon\right] \left[(q+p'-p_2)^2 - i\epsilon\right]} \\
&= \oint \frac{dp'^+}{(2\pi)} \frac{e^{-ip'^+(y^- - z_3^-)}}{2q^- \left[q^+ + p'^+ - \frac{M^2}{2q^-} - i\epsilon\right] 2(q^- - p_2^-) \left[q^+ + p'^+ - p_2^+ - \frac{\mathbf{p}_{2\perp}^2}{2(q^- - p_2^-)} - i\epsilon\right]} \\
&= \frac{(-2\pi i)}{2\pi} \frac{\theta(y^- - z_3^-)}{4q^-(q^- - p_2^-)} e^{i\left(q^+ - \frac{M^2}{2q^-}\right)(y^- - z_3^-)} \left[\frac{-1 + e^{-i\mathcal{G}_M^{(p_2)}(y^- - z_3^-)}}{\mathcal{G}_M^{(p_2)}} \right].
\end{aligned} \tag{203}$$

The trace in the numerator of the third line of Eq. 200 gives

$$\begin{aligned}
&\text{Tr} \left[\gamma^- \gamma^\mu (\not{q} + \not{p}' + M) \gamma^{\sigma_4} (\not{p}_2 + M) \gamma^{\sigma_1} (\not{q} + \not{p} + M) \gamma^\nu \right] \text{Tr} \left[\gamma^- \gamma^{\sigma_2} \not{\ell}_2 \gamma^{\sigma_3} \right] d_{\sigma_1 \sigma_2}^{(q+p-p_2)} d_{\sigma_3 \sigma_4}^{(q+p'-p_2)} \\
&= 32[-g_{\perp\perp}^{\mu\nu}](q^-)^2 \left[\frac{1 + (1-y)^2}{y(1-y+\eta y)} \right] [(\ell_{2\perp} - \mathbf{k}_\perp)^2 + \kappa y^2 M^2],
\end{aligned} \tag{204}$$

where κ is defined in Eq. 146. Finally, the hadronic tensor [Fig. 21(a)] reduces to the following form

$$\begin{aligned}
W_{3,c}^{\mu\nu} &= 2[-g_{\perp\perp}^{\mu\nu}] \int d(\Delta x^-) e^{iq^+(\Delta x^-)} e^{-i[M^2/(2q^-)](\Delta x^-)} \left\langle P \left| \bar{\psi}(\Delta X^-) \frac{\gamma^+}{4} \psi(0) \right| P \right\rangle \\
&\times e^2 e_q^2 g_s^2 \int d\zeta^- d(\Delta z^-) d^2 \Delta z_\perp \frac{dy}{2\pi} \frac{d^2 \ell_{2\perp}}{(2\pi)^2} \frac{d^2 k_\perp}{(2\pi)^2} \left[2 - 2 \cos \left\{ \mathcal{G}_M^{(p_2)} \zeta^- \right\} \right] e^{-i(\Delta z^-) \mathcal{H}_M^{(\ell_2, p_2)}} e^{i\mathbf{k}_\perp \cdot \Delta \mathbf{z}_\perp} \\
&\times \frac{\theta(x^- - z_2^-) \theta(y^- - z_3^-) [(\ell_{2\perp} - \mathbf{k}_\perp)^2 + \kappa y^2 M^2]}{\left[(\ell_{2\perp} - \mathbf{k}_\perp)^2 + M^2 y^2 (1-\eta)^2 \right]^2} \frac{1}{yq^-} \left\langle P_{A-1} \left| \bar{\psi}(\zeta^-, 0) \frac{\gamma^+}{4} \psi(\zeta^-, \Delta z^-, \Delta z_\perp) \right| P_{A-1} \right\rangle \\
&\times \left[\frac{1 + (1-y)^2}{y} \right] [C_f N_c],
\end{aligned} \tag{205}$$

where $\mathcal{G}_M^{(p_2)}$ is given in Eq. 202 and $\mathcal{H}_M^{(\ell_2, p_2)}$ is defined in Eq. 158. Note, the hadronic tensor for the central-cut diagram in Fig 21(b) is identical to the diagram in Fig 21(a) and is given by Eq. 205.

Now, we consider a central-cut diagram shown in Fig. 22(a). The hadronic tensor has the following form

$$\begin{aligned}
W_{3,c}^{\mu\nu} &= e^2 e_q^2 g_s^2 \int d^4 x d^4 y d^4 z_2 d^4 z_3 \int \frac{d^4 p}{(2\pi)^4} \frac{d^4 p'}{(2\pi)^4} \frac{d^4 \ell_2}{(2\pi)^4} \frac{d^4 p_2}{(2\pi)^4} e^{-ip'y} e^{ipx} \left\langle P \left| \bar{\psi}(y) \frac{\gamma^+}{4} \psi(x) \right| P \right\rangle \delta^{ab} \text{Tr} [t^a t^b] \\
&\times e^{i(q+p'-p_2-\ell_2)z_3} e^{i(\ell_2+p_2-q-p)z_2} \left\langle P_{A-1} \left| \bar{\psi}(z_2) \frac{\gamma^+}{4} \psi(z_3) \right| P_{A-1} \right\rangle d_{\sigma_1 \sigma_2}^{(\ell_2+p_2)} d_{\sigma_3 \sigma_4}^{(\ell_2+p_2)} (2\pi) \delta(\ell_2^2 - M^2) (2\pi) \delta(p_2^2 - M^2) \\
&\times \frac{\text{Tr} \left[\gamma^- \gamma^\mu (\not{q} + \not{p}') \gamma^{\sigma_3} \gamma^- \gamma^{\sigma_2} (\not{q} + \not{p}) \gamma^\nu \right] \text{Tr} \left[(\not{\ell}_2 + M) \gamma^{\sigma_4} (\not{p}_2 + M) \gamma^{\sigma_1} \right]}{\left[(q+p')^2 - i\epsilon \right] \left[(\ell_2 + p_2)^2 - i\epsilon \right] \left[(\ell_2 + p_2)^2 + i\epsilon \right] \left[(q+p)^2 + i\epsilon \right]}.
\end{aligned} \tag{206}$$

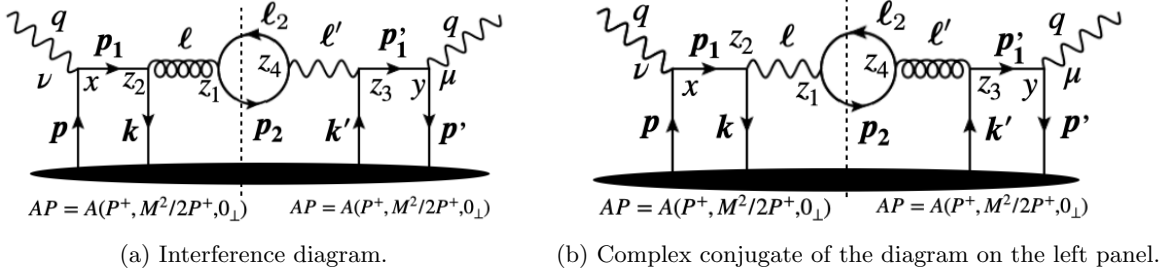


FIG. 22: A forward scattering diagram contributing to kernel-3.

The above expression (Eq. 206) has singularity arising from the denominator of the quark propagator with momentum p_1 and p'_1 . We identify one pole for each momentum variable p^+ and p'^+ . The contour integration for momentum p^+ is given as

$$C_1 = \oint \frac{dp^+}{(2\pi)} \frac{e^{ip^+(x^- - z_2^-)}}{[(q+p)^2 + i\epsilon]} = \frac{(2\pi i)}{2\pi} \frac{\theta(x^- - z_2^-)}{2q^-} e^{-iq^+(x^- - z_2^-)}. \quad (207)$$

Similarly, the contour integration for momentum p'^+ is carried out as

$$C_2 = \oint \frac{dp'^+}{(2\pi)} \frac{e^{-ip'^+(y^- - z_3^-)}}{[(q+p')^2 - i\epsilon]} = \frac{(-2\pi i)}{2\pi} \frac{\theta(y^- - z_3^-)}{2q^-} e^{iq^+(y^- - z_3^-)}. \quad (208)$$

Including mass correction up to $\mathcal{O}(M^2)$, the trace yields

$$\begin{aligned} & \text{Tr} [\gamma^- \gamma^\mu (\not{q} + \not{p}') \gamma^{\sigma_3} \gamma^- \gamma^{\sigma_2} (\not{q} + \not{p}) \gamma^\nu] \text{Tr} [(\not{\ell}_2 + M) \gamma^{\sigma_4} (\not{p}_2 + M) \gamma^{\sigma_1}] d_{\sigma_4 \sigma_3}^{(\ell_2 + p_2)} d_{\sigma_1 \sigma_2}^{(\ell_2 + p_2)} \\ &= 32 (q^-)^2 [-g_{\perp\perp}^{\mu\nu}] \left[\frac{\{(1 + \eta y) \ell_{2\perp} - y \mathbf{k}_\perp\}^2 + M^2 (1 + \eta y)^2}{y (1 - y + \eta y) (1 + \eta y)^2} \right] [y^2 + (1 - y + \eta y)^2]. \end{aligned} \quad (209)$$

The final expression of the hadronic tensor for the central-cut [Fig. 22(a)] is given as

$$\begin{aligned} W_{3,c}^{\mu\nu} &= 2 [-g_{\perp\perp}^{\mu\nu}] \int d(\Delta x^-) e^{iq^+(\Delta x^-)} \left\langle P \left| \bar{\psi}(\Delta X^-) \frac{\gamma^+}{4} \psi(0) \right| P \right\rangle \\ &\times e^2 e_q^2 g_s^2 \int d\zeta^- d(\Delta z^-) d^2 \Delta z_\perp \frac{dy}{2\pi} \frac{d^2 \ell_{2\perp}}{(2\pi)^2} \frac{d^2 k_\perp}{(2\pi)^2} e^{-i\mathcal{H}_1^{(\ell_2, p_2)}(\Delta z^-)} e^{-i\mathbf{k}_\perp \cdot \Delta \mathbf{z}_\perp} \\ &\times \frac{\theta(x^- - z^-) \theta(y^- - z_3^-)}{(1 + \eta y)^2 q^-} \frac{1}{[\{(1 + \eta y) \ell_{2\perp} - y \mathbf{k}_\perp\}^2 + M^2 (1 + \eta y)^2]} \left\langle P_{A-1} \left| \bar{\psi}(0) \frac{\gamma^+}{4} \psi(\zeta^-, \Delta z^-, \Delta \mathbf{z}_\perp) \right| P_{A-1} \right\rangle \\ &\times [y^2 + (1 - y + \eta y)^2] [C_f N_c], \end{aligned} \quad (210)$$

where,

$$\mathcal{H}_1^{(\ell_2, p_2)} = \ell_2^+ + p_2^+ = \frac{\ell_{2\perp}^2 + M^2}{2yq^-} + \frac{(\ell_{2\perp} - \mathbf{k}_\perp)^2 + M^2}{2(1 - y + \eta y)q^-}. \quad (211)$$

The diagram shown in Fig. 22(b) is identical to Fig. 22(a), except the photon propagator and gluon propagator are interchanged, and hence has an identical expression of the hadronic tensor.

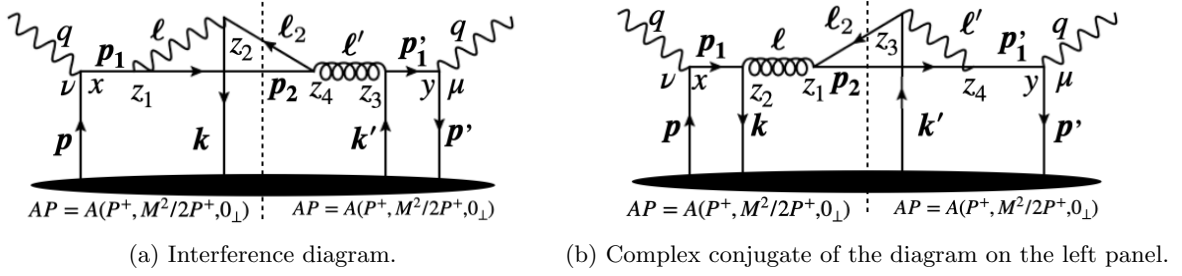


FIG. 23: A forward scattering diagram contributing to kernel-3.

Next, we consider an interference diagram shown in Fig 23(a). The hadronic tensor is given as

$$\begin{aligned}
W_{3,c}^{\mu\nu} &= e^2 e_q^2 g_s^2 \int d^4 x d^4 y \int d^4 z_2 d^4 z_3 \int \frac{d^4 p}{(2\pi)^4} \frac{d^4 p'}{(2\pi)^4} \frac{d^4 \ell_2}{(2\pi)^4} \frac{d^4 p_2}{(2\pi)^4} e^{-ip'y} e^{ipx} \langle P | \bar{\psi}(y) \frac{\gamma^+}{4} \psi(x) | P \rangle \\
&\times e^{iz_2(\ell_2 + p_2 - q - p)} e^{iz_3(-p_2 - \ell_2 + q + p')} \left\langle P_{A-1} \left| \bar{\psi}(z_2) \frac{\gamma^+}{4} \psi(z_3) \right| P_{A-1} \right\rangle \\
&\times \frac{\text{Tr} \left[\gamma^- \gamma^\mu (\not{q} + \not{p}') \gamma^{\sigma_3} \gamma^- \gamma^{\sigma_2} \not{\ell}_2 \gamma^{\sigma_4} \not{p}_2 \gamma^{\sigma_1} (\not{q} + \not{p}) \gamma^\nu \right]}{\left[(q+p)^2 - i\epsilon \right] \left[(q+p)^2 + i\epsilon \right]} \\
&\times \frac{d_{\sigma_4 \sigma_3}^{(\ell_2 + p_2)}}{\left[(\ell_2 + p_2)^2 - i\epsilon \right]} \frac{d_{\sigma_1 \sigma_2}^{(q+p-p_2)}}{\left[(q+p-p_2)^2 + i\epsilon \right]} \text{Tr} [t^c t^d] \delta^{cd} (2\pi) \delta(\ell_2^-) (2\pi) \delta(p_2^2).
\end{aligned} \tag{212}$$

The above expression has singularity when the denominator of the parton propagator for p_1 , ℓ and p'_1 becomes zero. We identify two poles for the momentum variable p and one pole for p' . We compute the integral in the complex plane of p^+ and p'^+ .

In this central-cut diagram, the momenta for the final state partons are $\ell_2^- = yq^-$ and $p_2^- = (1 - y + \eta y)q^-$. The contour integration for p^+ is given as

$$\begin{aligned}
C_1 &= \oint \frac{dp^+}{2\pi} \frac{e^{ip^+(x^- - z_2^-)}}{\left[(q+p)^2 + i\epsilon \right] \left[(q+p-p_2)^2 + i\epsilon \right]} \\
&= \left(\frac{2\pi i}{2\pi} \right) \frac{\theta(x^- - z_2^-)}{4q^-(1-\eta)yq^-} e^{-iq^+(x^- - z_2^-)} \left[\frac{-1 + e^{i\mathcal{G}(x^- - z_2^-)}}{\mathcal{G}_0^{(p_2)}} \right],
\end{aligned} \tag{213}$$

where $\mathcal{G}_0^{(p_2)}$ is given in Eq. 189.

Similarly, the contour integration for p'^+ is

$$C_2 = \oint \frac{dp'^+}{2\pi} \frac{e^{ip'^+(-y^- + z_3^-)}}{\left[(q+p')^2 - i\epsilon \right]} = \left(\frac{-2\pi i}{2\pi} \right) \frac{\theta(y^- - z_3^-)}{2q^-} e^{-iq^+(-y^- + z_3^-)}. \tag{214}$$

Simplifying the trace yields the following expression

$$\begin{aligned}
&\text{Tr} \left[\gamma^- \gamma^\mu (\not{q} + \not{p}') \gamma^{\sigma_3} \gamma^- \gamma^{\sigma_2} \not{\ell}_2 \gamma^{\sigma_4} \not{p}_2 \gamma^{\sigma_1} (\not{q} + \not{p}) \gamma^\nu \right] \times \left[-g_{\sigma_4 \sigma_3} + \frac{n_{\sigma_4} \ell'_{\sigma_3} + n_{\sigma_3} \ell'_{\sigma_4}}{\ell'^-} \right] \\
&\times \left[-g_{\sigma_1 \sigma_2} + \frac{n_{\sigma_1} \ell_{\sigma_2} + n_{\sigma_2} \ell_{\sigma_1}}{\ell^-} \right] \\
&= 32(q^-)^2 [-g_{\perp\perp}^{\mu\nu}] \left[\frac{1-y}{y} \right] \left[\frac{J_2}{y(1-\eta)(1+\eta y)} \right],
\end{aligned} \tag{215}$$

where

$$J_2 = \ell_{2\perp}^2 \{-1 + y - \eta y(1 - y + \eta y)\} + y \mathbf{k}_\perp^2 \{-1 + y - \eta y\} + \mathbf{k}_\perp \cdot \ell_{2\perp} \{1 - y^2 + 2\eta y + \eta^2 y^2\}. \tag{216}$$

The final expression for the hadronic tensor [Fig 23(a)] as

$$\begin{aligned}
W_{3,c}^{\mu\nu} &= 2[-g_{\perp\perp}^{\mu\nu}] \int d(\Delta x^-) e^{iq^+(\Delta x^-)} \left\langle P \left| \bar{\psi}(\Delta X^-) \frac{\gamma^+}{4} \psi(0) \right| P \right\rangle \\
&\times e^2 e_q^2 g_s^2 \int d\zeta^- d(\Delta z^-) d^2 \Delta z_\perp \frac{dy}{2\pi} \frac{d^2 \ell_{2\perp}}{(2\pi)^2} \frac{d^2 k_\perp}{(2\pi)^2} \left[-1 + e^{i\mathcal{G}_0^{(p_2)}(x^- - z_2^-)} \right] e^{-i\mathcal{H}_0^{(\ell_2, p_2)}(\Delta z^-)} e^{i\mathbf{k}_\perp \cdot \Delta \mathbf{z}_\perp} \\
&\times \frac{\theta(x^- - z_2^-) \theta(y^- - z_3^-)}{yq^-} \frac{J_2}{[\ell_{2\perp} - \mathbf{k}_\perp]^2 [(1 + \eta y) \ell_{2\perp} - y\mathbf{k}_\perp]^2} \left\langle P_{A-1} \left| \bar{\psi}(\zeta^-, 0) \frac{\gamma^+}{4} \psi(\zeta^-, \Delta z^-, \Delta \mathbf{z}_\perp) \right| P_{A-1} \right\rangle \\
&\times \left[\frac{1 - y + \eta y}{(1 + \eta y)(1 - \eta)} \right] [C_f N_c],
\end{aligned} \tag{217}$$

where $\mathcal{G}_0^{(p_2)}$ is given in Eq. 189 and $\mathcal{H}_0^{(\ell_2, p_2)}$ is given in Eq. 182.

Note that the diagram in Fig 23(b) and Fig 23(a) are complex-conjugate of each other. They differ only in contour integration over variable p^+ and p'^+ . The calculation of the hadronic tensor for Fig 23(b) involves the contour integration for p^+ and is given as

$$C_1 = \oint \frac{dp^+}{2\pi} \frac{e^{ip^+(x^- - z_2^-)}}{[(q+p)^2 + i\epsilon]} = \left(\frac{2\pi i}{2\pi} \right) \frac{\theta(x^- - z_2^-)}{2q^-} e^{-iq^+(x^- - z_2^-)}, \tag{218}$$

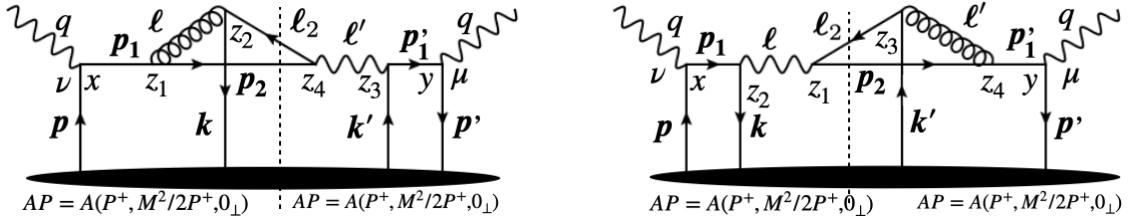
and, the contour integration for p'^+ is given as

$$\begin{aligned}
C_2 &= \oint \frac{dp'^+}{2\pi} \frac{e^{ip'^+(-y^- + z_3^-)}}{[(q+p')^2 - i\epsilon] [(q+p' - p_2)^2 - i\epsilon]} \\
&= \left(\frac{-2\pi i}{2\pi} \right) \frac{\theta(y^- - z_3^-)}{4q^-(q^- - p_2^-)} e^{iq^+(y^- - z_3^-)} \left[\frac{-1 + e^{-i\mathcal{G}_0^{(p_2)}(y^- - z_3^-)}}{\mathcal{G}_0^{(p_2)}} \right],
\end{aligned} \tag{219}$$

where $\mathcal{G}_0^{(p_2)}$ is given in Eq. 189. The final expression for the hadronic tensor [Fig 23(b)] yields

$$\begin{aligned}
W_{3,c}^{\mu\nu} &= 2[-g_{\perp\perp}^{\mu\nu}] \int d(\Delta x^-) e^{iq^+(\Delta x^-)} \left\langle P \left| \bar{\psi}(\Delta X^-) \frac{\gamma^+}{4} \psi(0) \right| P \right\rangle \\
&\times e^2 e_q^2 g_s^2 \int d\zeta^- d(\Delta z^-) d^2 \Delta z_\perp \frac{dy}{2\pi} \frac{d^2 \ell_{2\perp}}{(2\pi)^2} \frac{d^2 k_\perp}{(2\pi)^2} \left[-1 + e^{-i\mathcal{G}_0^{(p_2)}(y^- - z_3^-)} \right] e^{-i\mathcal{H}_0^{(\ell_2, p_2)}(\Delta z^-)} e^{i\mathbf{k}_\perp \cdot \Delta \mathbf{z}_\perp} \\
&\times \frac{\theta(x^- - z_2^-) \theta(y^- - z_3^-)}{yq^-} \frac{J_2}{[\ell_{2\perp} - \mathbf{k}_\perp]^2 [(1 + \eta y) \ell_{2\perp} - y\mathbf{k}_\perp]^2} \left\langle P_{A-1} \left| \bar{\psi}(\zeta^-, 0) \frac{\gamma^+}{4} \psi(\zeta^-, \Delta z^-, \Delta \mathbf{z}_\perp) \right| P_{A-1} \right\rangle \\
&\times \left[\frac{1 - y + \eta y}{(1 + \eta y)(1 - \eta)} \right] [C_f N_c],
\end{aligned} \tag{220}$$

where $\mathcal{G}_0^{(p_2)}$ is given in Eq. 189 and $\mathcal{H}_0^{(\ell_2, p_2)}$ is given in Eq. 182.



(a) Interference diagram.

(b) Complex conjugate of the diagram on the left panel.

FIG. 24: A forward scattering diagram contributing to kernel-3.

Next, we consider the interference diagram with virtual photon as shown in Fig. 24(a). Since the diagram is identical to Fig. 23(a), except that the photon propagator and the gluon propagator are interchanged between the amplitude side and the complex conjugate side, therefore, the hadronic tensor is the same as given in Eq. 217.

Similarly, the interference diagram shown in Fig. 24(b) is identical to Fig. 23(b), except that the photon propagator and the gluon propagator are interchanged between the amplitude side and the complex conjugate side, therefore, the hadronic tensor is the same as given in Eq. 220.

Appendix D: SINGLE-EMISSION SINGLE-SCATTERING KERNEL: VIRTUAL PHOTON CORRECTIONS WITH TWO QUARKS IN THE FINAL STATE

This section summarizes the calculation of all possible diagrams contributing to kernel-4. The diagrams consist of two quarks in the final state with an in-medium quark exchange with the medium. Each forward scattering diagram consists of a photon propagator and a gluon propagator leading to correction $\mathcal{O}(\alpha_{em}\alpha_s)$.

The hadronic tensor associated with the forward scattering diagram [Fig. 25(a)] is given as

$$\begin{aligned}
W_{4,c}^{\mu\nu} &= e^2 e_q^2 g_s^2 N_f \int d^4x d^4y d^4z_2 d^4z_3 \int \frac{d^4p}{(2\pi)^4} \frac{d^4p'}{(2\pi)^4} \frac{d^4\ell_2}{(2\pi)^4} \frac{d^4p_2}{(2\pi)^4} e^{-ip'y} e^{ipx} \left\langle P \left| \bar{\psi}(y) \frac{\gamma^+}{4} \psi(x) \right| P \right\rangle \delta^{cd} \text{Tr}[t^c t^d] \\
&\times e^{i(q+p'-p_2-\ell_2)z_3} e^{i(\ell_2+p_2-q-p)z_2} \left\langle P_{A-1} \left| \bar{\psi}(z_3) \frac{\gamma^+}{4} \psi(z_2) \right| P_{A-1} \right\rangle d_{\sigma_1\sigma_2}^{(q+p-p_2)} d_{\sigma_3\sigma_4}^{(q+p'-p_2)} (2\pi)\delta(\ell_2^2) (2\pi)\delta(p_2^2 - M^2) \\
&\times \frac{\text{Tr} \left[\gamma^- \gamma^\mu (\not{q} + \not{p}' + M) \gamma^{\sigma_4} (\not{p}_2 + M) \gamma^{\sigma_1} (\not{q} + \not{p} + M) \gamma^\nu \right] \text{Tr} \left[\gamma^- \gamma^{\sigma_3} \not{\ell}_2 \gamma^{\sigma_2} \right]}{\left[(q+p')^2 - M^2 - i\epsilon \right] \left[(q+p)^2 - M^2 + i\epsilon \right] \left[(q+p'-p_2)^2 - i\epsilon \right] \left[(q+p-p_2)^2 + i\epsilon \right]}.
\end{aligned} \tag{221}$$

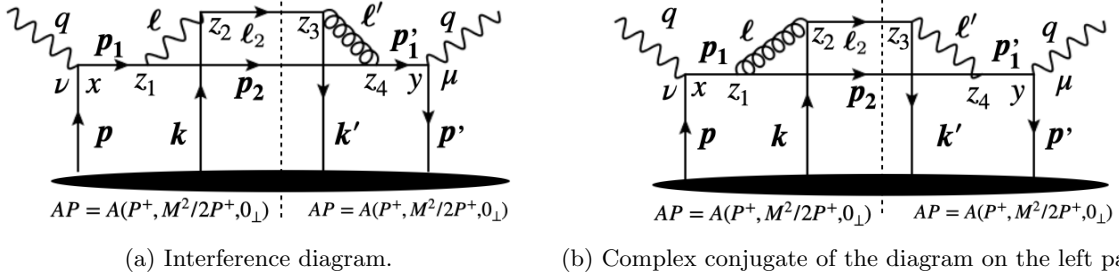


FIG. 25: A forward scattering diagram contributing to kernel-4.

The above expression of the hadronic tensor has singularity when the denominator of the propagator for p_1 , ℓ , ℓ' and p'_1 becomes on-shell. It contains two simple poles for p^+ and p'^+ . The contour integration for p^+ gives

$$\begin{aligned}
C_1 &= \oint \frac{dp^+}{(2\pi)} \frac{e^{ip^+(x^- - z_2^-)}}{\left[(q+p)^2 - M^2 + i\epsilon \right] \left[(q+p-p_2)^2 + i\epsilon \right]} \\
&= \oint \frac{dp^+}{(2\pi)} \frac{e^{ip^+(x^- - z_2^-)}}{2q^- \left[q^+ + p^+ - \frac{M^2}{2q^-} + i\epsilon \right] 2(q^- - p_2^-) \left[q^+ + p^+ - p_2^+ - \frac{p_{2\perp}^2}{2(q^- - p_2^-)} + i\epsilon \right]} \\
&= \frac{(2\pi i)}{2\pi} \frac{\theta(x^- - z_2^-)}{4q^-(q^- - p_2^-)} e^{i\left[-q^+ + \frac{M^2}{2q^-}\right](x^- - z_2^-)} \left[\frac{-1 + e^{i\mathcal{G}_M^{(p_2)}(x^- - z_2^-)}}{\mathcal{G}_M^{(p_2)}} \right],
\end{aligned} \tag{222}$$

where $\mathcal{G}_M^{(p_2)}$ is given in Eq. 202.

The contour integration for p'^+ can be done

$$\begin{aligned}
C_2 &= \oint \frac{dp'^+}{(2\pi)} \frac{e^{-ip'^+(y^- - z_3^-)}}{\left[(q+p')^2 - M^2 - i\epsilon\right] \left[(q+p' - p_2)^2 - i\epsilon\right]} \\
&= \oint \frac{dp'^+}{(2\pi)} \frac{e^{-ip'^+(y^- - z_3^-)}}{2q^- \left[q^+ + p'^+ - \frac{M^2}{2q^-} - i\epsilon\right] 2(q^- - p_2^-) \left[q^+ + p'^+ - p_2^+ - \frac{p_{2\perp}^2}{2(q^- - p_2^-)} - i\epsilon\right]} \\
&= \frac{(-2\pi i)}{2\pi} \frac{\theta(y^- - z_3^-)}{4q^-(q^- - p_2^-)} e^{i\left[q^+ - \frac{M^2}{2q^-}\right](y^- - z_3^-)} \left[\frac{-1 + e^{-i\mathcal{G}_M^{(p_2)}(y^- - z_3^-)}}{\mathcal{G}_M^{(p_2)}} \right].
\end{aligned} \tag{223}$$

The trace in the numerator of the third line of Eq. 221 gives

$$\begin{aligned}
&\text{Tr} \left[\gamma^- \gamma^\mu (\not{q} + \not{p}' + M) \gamma^{\sigma_4} (\not{p}_2 + M) \gamma^{\sigma_1} (\not{q} + \not{p} + M) \gamma^\nu \right] \text{Tr} \left[\gamma^- \gamma^{\sigma_3} \not{\ell}_2 \gamma^{\sigma_2} \right] d_{\sigma_1 \sigma_2}^{(\ell)} d_{\sigma_3 \sigma_4}^{(\ell')} \\
&= 32(q^-)^2 [-g_{\perp\perp}^{\mu\nu}] \left[\frac{1 + (1-y)^2}{y(1-y+\eta y)} \right] \left[(\boldsymbol{\ell}_\perp - \mathbf{k}_\perp)^2 + \kappa y^2 M^2 \right],
\end{aligned} \tag{224}$$

where κ is defined in Eq. 146. Finally, the hadronic tensor [Fig. 25(a)] reduces to

$$\begin{aligned}
W_{4,c}^{\mu\nu} &= 2[-g_{\perp\perp}^{\mu\nu}] N_f \int d(\Delta x^-) e^{iq^+(\Delta X^-)} e^{-i[M^2/(2q^-)](\Delta X^-)} \left\langle P \left| \bar{\psi}(\Delta X^-) \frac{\gamma^+}{4} \psi(0) \right| P \right\rangle \\
&\times e^2 e_q^2 g_s^2 \int d\zeta^- d(\Delta z^-) d^2 \Delta_{z\perp} \frac{dy}{2\pi} \frac{d^2 \ell_{2\perp}}{(2\pi)^2} \frac{d^2 k_\perp}{(2\pi)^2} \left[2 - 2 \cos \left\{ \mathcal{G}_M^{(p_2)} \zeta^- \right\} \right] e^{-i(\Delta z^-) \mathcal{H}_M^{(\ell_2, p_2)}} e^{i\mathbf{k}_\perp \cdot \Delta z_\perp} \\
&\times \frac{\theta(x^- - z_2^-) \theta(y^- - z_3^-) \left[(\boldsymbol{\ell}_{2\perp} - \mathbf{k}_\perp)^2 + \kappa y^2 M^2 \right]}{\left[(\boldsymbol{\ell}_{2\perp} - \mathbf{k}_\perp)^2 + M^2 y^2 (1-\eta)^2 \right]^2} \frac{1}{yq^-} \left\langle P_{A-1} \left| \bar{\psi}(\zeta^-, \Delta z^-, \Delta z_\perp) \frac{\gamma^+}{4} \psi(\zeta^-, 0) \right| P_{A-1} \right\rangle \\
&\times \left[\frac{1 + (1-y)^2}{y} \right] [C_f N_c],
\end{aligned} \tag{225}$$

where $\mathcal{G}_M^{(p_2)}$ is defined in Eq. 202 and $\mathcal{H}_M^{(\ell_2, p_2)}$ is defined in Eq. 158.

Note, the diagram shown in Fig. 25(a) is identical to Fig. 25(b) except the photon propagator and gluon propagator are interchanged between the amplitude side and complex-conjugate side. Hence, the corresponding hadronic tensors are identical.

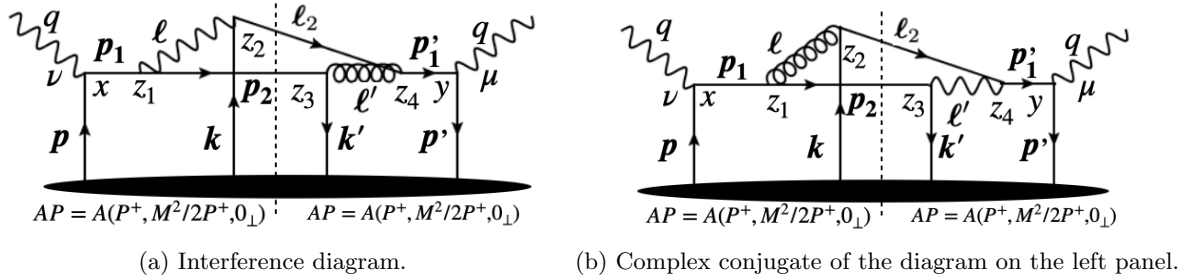


FIG. 26: A forward scattering diagram contributing to kernel-4.

Next, we consider a forward scattering diagram shown in Fig. 26. The hadronic tensor for Fig. 26(a) is given as

$$\begin{aligned}
W_{4,c}^{\mu\nu} &= e^2 e_q^2 g_s^2 \int d^4 x d^4 y d^4 z_2 d^4 z_3 \int \frac{d^4 p}{(2\pi)^4} \frac{d^4 p'}{(2\pi)^4} \frac{d^4 \ell_2}{(2\pi)^4} \frac{d^4 p_2}{(2\pi)^4} e^{-ip'y} e^{ipx} \left\langle P \left| \bar{\psi}(y) \frac{\gamma^+}{4} \psi(x) \right| P \right\rangle \delta^{cd} \text{Tr}[t^c t^d] \\
&\times e^{i(q+p'-p_2-\ell_2)z_3} e^{i(\ell_2+p_2-q-p)z_2} \left\langle P_{A-1} \left| \bar{\psi}(z_3) \frac{\gamma^+}{4} \psi(z_2) \right| P_{A-1} \right\rangle d_{\sigma_1 \sigma_2}^{(q+p-p_2)} d_{\sigma_3 \sigma_4}^{(q+p'-\ell_2)} (2\pi) \delta(\ell_2^2) (2\pi) \delta(p_2^2) \\
&\times \frac{\text{Tr} \left[\gamma^- \gamma^\mu (\not{q} + \not{p}') \gamma^{\sigma_4} \not{\ell}_2 \gamma^{\sigma_2} \gamma^- \gamma^{\sigma_3} \not{p}_2 \gamma^{\sigma_1} (\not{q} + \not{p}) \gamma^\nu \right]}{\left[(q+p')^2 - i\epsilon \right] \left[(q+p)^2 + i\epsilon \right] \left[(q+p' - \ell_2)^2 - i\epsilon \right] \left[(q+p - p_2)^2 + i\epsilon \right]}.
\end{aligned} \tag{226}$$

The above expression of the hadronic tensor has singularity when the denominator of the propagator for p_1 , ℓ , ℓ' and p'_1 becomes on-shell. It contains two simple poles for p^+ and p'^+ . The contour integration for p^+ gives

$$\begin{aligned}
C_1 &= \oint \frac{dp^+}{(2\pi)} \frac{e^{ip^+(x^- - z_2^-)}}{\left[(q+p)^2 + i\epsilon\right] \left[(q+p-p_2)^2 + i\epsilon\right]} \\
&= \oint \frac{dp^+}{(2\pi)} \frac{e^{ip^+(x^- - z_2^-)}}{2q^- [q^+ + p^+ + i\epsilon] 2(q^- - p_2^-) \left[q^+ + p^+ - p_2^+ - \frac{\mathbf{p}_{2\perp}^2}{2(q^- - p_2^-)} + i\epsilon\right]} \\
&= \frac{(2\pi i)}{2\pi} \frac{\theta(x^- - z_2^-)}{4q^-(q^- - p_2^-)} e^{-iq^+(x^- - z_2^-)} \left[\frac{-1 + e^{i\mathcal{G}_0^{(p_2)}(x^- - z_2^-)}}{\mathcal{G}_0^{(p_2)}} \right],
\end{aligned} \tag{227}$$

where $\mathcal{G}_0^{(p_2)}$ is defined in Eq. 189.

Similarly, the contour integration for p'^+ gives

$$\begin{aligned}
C_2 &= \oint \frac{dp'^+}{(2\pi)} \frac{e^{-ip'^+(y^- - z_3^-)}}{\left[(q+p')^2 - i\epsilon\right] \left[(q+p' - \ell_2)^2 - i\epsilon\right]} \\
&= \oint \frac{dp'^+}{(2\pi)} \frac{e^{-ip'^+(y^- - z_3^-)}}{2q^- [q^+ + p'^+ - i\epsilon] 2(q^- - \ell_2^-) \left[q^+ + p'^+ - \ell_2^+ - \frac{\ell_{2\perp}^2}{2(q^- - \ell_2^-)} - i\epsilon\right]} \\
&= \frac{(-2\pi i)}{2\pi} \frac{\theta(y^- - z_3^-)}{4q^-(q^- - \ell_2^-)} e^{iq^+(y^- - z_3^-)} \left[\frac{-1 + e^{-i\mathcal{G}_0^{(\ell_2)}(y^- - z_3^-)}}{\mathcal{G}_0^{(\ell_2)}} \right],
\end{aligned} \tag{228}$$

where $\mathcal{G}_0^{(\ell_2)}$ is defined in Eq. 178.

The trace in the third line of Eq. 226 simplifies as

$$\begin{aligned}
&\text{Tr} \left[\gamma^- \gamma^\mu (\not{q} + \not{p}') \gamma^{\sigma_4} \not{\ell}_2 \gamma^{\sigma_2} \gamma^- \gamma^{\sigma_3} \not{p}_2 \gamma^{\sigma_1} (\not{q} + \not{p}) \gamma^\nu \right] d_{\sigma_2 \sigma_1}^{(q+p-p_2)} d_{\sigma_4 \sigma_3}^{(q+p'-\ell_2)} \\
&= \frac{32(q^-)^2 [-g_{\perp\perp}^{\mu\nu}]}{(1-\eta)y(1-y)q^-} [-\ell_{2\perp}^2 + \ell_{2\perp} \cdot \mathbf{k}_\perp].
\end{aligned} \tag{229}$$

The final expression of the hadronic tensor for Fig. 26(a) is given by

$$\begin{aligned}
W_{4,c}^{\mu\nu} &= 2[-g_{\perp\perp}^{\mu\nu}] \int d(\Delta x^-) e^{iq^+(\Delta x^-)} \left\langle P \left| \bar{\psi}(\Delta X^-) \frac{\gamma^+}{4} \psi(0) \right| P \right\rangle \\
&\times e^2 e_q^2 g_s^2 \int d\zeta^- d(\Delta z^-) d^2 \Delta z_\perp \frac{dy}{2\pi} \frac{d^2 \ell_{2\perp}}{(2\pi)^2} \frac{d^2 k_\perp}{(2\pi)^2} \left[-1 + e^{i\mathcal{G}_0^{(p_2)}(x^- - z_2^-)} \right] \left[-1 + e^{-i\mathcal{G}_0^{(\ell_2)}(y^- - z_3^-)} \right] \\
&\times \frac{\theta(x^- - z_2^-) \theta(y^- - z_3^-)}{(1-\eta)(1-y)qq^-} \frac{[-\ell_{2\perp}^2 + \ell_{2\perp} \cdot \mathbf{k}_\perp]}{(\ell_{2\perp} - \mathbf{k}_{2\perp})^2 \ell_{2\perp}^2} e^{-i(\Delta z^-) \mathcal{H}_0^{(\ell_2, p_2)}} e^{i\mathbf{k}_\perp \cdot \Delta \mathbf{z}_\perp} \left\langle P_{A-1} \left| \bar{\psi}(\zeta^-, \Delta z^-, \Delta z_\perp) \frac{\gamma^+}{4} \psi(\zeta^-, 0) \right| P_{A-1} \right\rangle \\
&\times [C_f N_c],
\end{aligned} \tag{230}$$

where $\mathcal{G}_0^{(\ell_2)}$ is defined in Eq. 178, $\mathcal{G}_0^{(p_2)}$ is given in Eq. 189, and $\mathcal{H}_0^{(\ell_2, p_2)}$ is given in Eq. 182.

Note, the diagram shown in Fig. 26(a) is identical to Fig. 26(b) except the photon propagator and gluon propagator are interchanged between the amplitude side and complex-conjugate side. Hence, the corresponding hadronic tensors are identical.

-
- [1] K. Adcox *et al.* (PHENIX), “Suppression of hadrons with large transverse momentum in central Au+Au collisions at $\sqrt{s_{NN}} = 130$ -GeV,” *Phys. Rev. Lett.* **88**, 022301 (2002), [arXiv:nucl-ex/0109003](#).
- [2] S. S. Adler *et al.* (PHENIX), “High p_T charged hadron suppression in Au + Au collisions at $\sqrt{s_{NN}} = 200$ GeV,” *Phys. Rev. C* **69**, 034910 (2004), [arXiv:nucl-ex/0308006](#).
- [3] S. S. Adler *et al.* (PHENIX), “Suppressed π^0 production at large transverse momentum in central Au+ Au collisions at $\sqrt{s_{NN}} = 200$ GeV,” *Phys. Rev. Lett.* **91**, 072301 (2003), [arXiv:nucl-ex/0304022](#).
- [4] C. Adler *et al.* (STAR), “Centrality dependence of high p_T hadron suppression in Au+Au collisions at $\sqrt{s_{NN}} = 130$ -GeV,” *Phys. Rev. Lett.* **89**, 202301 (2002), [arXiv:nucl-ex/0206011](#).
- [5] J. Adams *et al.* (STAR), “Transverse momentum and collision energy dependence of high p(T) hadron suppression in Au+Au collisions at ultrarelativistic energies,” *Phys. Rev. Lett.* **91**, 172302 (2003), [arXiv:nucl-ex/0305015](#).
- [6] Morad Aaboud *et al.* (ATLAS), “Measurement of the nuclear modification factor for inclusive jets in Pb+Pb collisions at $\sqrt{s_{NN}} = 5.02$ TeV with the ATLAS detector,” *Phys. Lett. B* **790**, 108–128 (2019), [arXiv:1805.05635 \[nucl-ex\]](#).
- [7] Shreyasi Acharya *et al.* (ALICE), “Measurements of inclusive jet spectra in pp and central Pb-Pb collisions at $\sqrt{s_{NN}} = 5.02$ TeV,” *Phys. Rev. C* **101**, 034911 (2020), [arXiv:1909.09718 \[nucl-ex\]](#).
- [8] Vardan Khachatryan *et al.* (CMS), “Measurement of inclusive jet cross sections in pp and PbPb collisions at $\sqrt{s_{NN}} = 2.76$ TeV,” *Phys. Rev. C* **96**, 015202 (2017), [arXiv:1609.05383 \[nucl-ex\]](#).
- [9] Albert M Sirunyan *et al.* (CMS), “First measurement of large area jet transverse momentum spectra in heavy-ion collisions,” *JHEP* **05**, 284 (2021), [arXiv:2102.13080 \[hep-ex\]](#).
- [10] Morad Aaboud *et al.* (ATLAS), “Measurement of photon-jet transverse momentum correlations in 5.02 TeV Pb + Pb and pp collisions with ATLAS,” *Phys. Lett. B* **789**, 167–190 (2019), [arXiv:1809.07280 \[nucl-ex\]](#).
- [11] Georges Aad *et al.* (ATLAS), “Comparison of inclusive and photon-tagged jet suppression in 5.02 TeV Pb+Pb collisions with ATLAS,” *Phys. Lett. B* **846**, 138154 (2023), [arXiv:2303.10090 \[nucl-ex\]](#).
- [12] Albert M Sirunyan *et al.* (CMS), “Study of jet quenching with isolated-photon+jet correlations in PbPb and pp collisions at $\sqrt{s_{NN}} = 5.02$ TeV,” *Phys. Lett. B* **785**, 14–39 (2018), [arXiv:1711.09738 \[nucl-ex\]](#).
- [13] L. Adamczyk *et al.* (STAR), “Jet-like Correlations with Direct-Photon and Neutral-Pion Triggers at $\sqrt{s_{NN}} = 200$ GeV,” *Phys. Lett. B* **760**, 689–696 (2016), [arXiv:1604.01117 \[nucl-ex\]](#).
- [14] U. Acharya *et al.* (PHENIX), “Measurement of jet-medium interactions via direct photon-hadron correlations in Au+Au and $d + Au$ collisions at $\sqrt{s_{NN}} = 200$ GeV,” *Phys. Rev. C* **102**, 054910 (2020), [arXiv:2005.14270 \[hep-ex\]](#).
- [15] A. M. Sirunyan *et al.* (CMS), “Azimuthal anisotropy of charged particles with transverse momentum up to 100 GeV/ c in PbPb collisions at $\sqrt{s_{NN}} = 5.02$ TeV,” *Phys. Lett. B* **776**, 195–216 (2018), [arXiv:1702.00630 \[hep-ex\]](#).
- [16] Serguei Chatrchyan *et al.* (CMS), “Azimuthal Anisotropy of Charged Particles at High Transverse Momenta in PbPb Collisions at $\sqrt{s_{NN}} = 2.76$ TeV,” *Phys. Rev. Lett.* **109**, 022301 (2012), [arXiv:1204.1850 \[nucl-ex\]](#).
- [17] Morad Aaboud *et al.* (ATLAS), “Measurement of the azimuthal anisotropy of charged particles produced in $\sqrt{s_{NN}} = 5.02$ TeV Pb+Pb collisions with the ATLAS detector,” *Eur. Phys. J. C* **78**, 997 (2018), [arXiv:1808.03951 \[nucl-ex\]](#).
- [18] J. H. Putschke *et al.*, “The JETSCAPE framework,” (2019), [arXiv:1903.07706 \[nucl-th\]](#).
- [19] A. Kumar *et al.* (JETSCAPE), “JETSCAPE framework: $p+p$ results,” *Phys. Rev. C* **102**, 054906 (2020), [arXiv:1910.05481 \[nucl-th\]](#).
- [20] A. Kumar *et al.* (JETSCAPE), “Inclusive jet and hadron suppression in a multistage approach,” *Phys. Rev. C* **107**, 034911 (2023), [arXiv:2204.01163 \[hep-ph\]](#).
- [21] Chanwook Park (JETSCAPE), “Multi-stage jet evolution through QGP using the JETSCAPE framework: inclusive jets, correlations and leading hadrons,” *PoS HardProbes2018*, 072 (2019), [arXiv:1902.05934 \[nucl-th\]](#).
- [22] Eric Braaten and Robert D. Pisarski, “Simple effective Lagrangian for hard thermal loops,” *Phys. Rev. D* **45**, R1827 (1992).
- [23] Peter Brockway Arnold, Guy D. Moore, and Laurence G. Yaffe, “Effective kinetic theory for high temperature gauge theories,” *JHEP* **01**, 030 (2003), [arXiv:hep-ph/0209353](#).
- [24] Peter Brockway Arnold, Guy D. Moore, and Laurence G. Yaffe, “Photon emission from quark gluon plasma: Complete leading order results,” *JHEP* **12**, 009 (2001), [arXiv:hep-ph/0111107](#).
- [25] Jacopo Ghiglieri, Juhee Hong, Aleksi Kurkela, Egang Lu, Guy D. Moore, and Derek Teaney, “Next-to-leading order thermal photon production in a weakly coupled quark-gluon plasma,” *JHEP* **05**, 010 (2013), [arXiv:1302.5970 \[hep-ph\]](#).
- [26] Simon Caron-Huot, “O(g) plasma effects in jet quenching,” *Phys. Rev. D* **79**, 065039 (2009), [arXiv:0811.1603 \[hep-ph\]](#).
- [27] G. Jackson and M. Laine, “Testing thermal photon and dilepton rates,” *JHEP* **11**, 144 (2019), [arXiv:1910.09567 \[hep-ph\]](#).
- [28] Sajid Ali, Dibyendu Bala, Anthony Francis, Greg Jackson, Olaf Kaczmarek, Jonas Turnwald, Tristan Ueding, and Nicolas Wink (HotQCD), “Lattice QCD estimates of thermal photon production from the QGP,” *Phys. Rev. D* **110**, 054518 (2024), [arXiv:2403.11647 \[hep-lat\]](#).
- [29] Bjoern Schenke, Charles Gale, and Sangyong Jeon, “MARTINI: An Event generator for relativistic heavy-ion collisions,” *Phys. Rev. C* **80**, 054913 (2009), [arXiv:0909.2037 \[hep-ph\]](#).
- [30] Rouzbeh Modarresi Yazdi, Shuzhe Shi, Charles Gale, and Sangyong Jeon, “Jet-medium Photons as a Probe of Parton Dynamics,” *Acta Phys. Polon. Supp.* **16**, 1–A129 (2023), [arXiv:2207.12513 \[hep-ph\]](#).
- [31] Charles Gale, Jean-François Paquet, Björn Schenke, and Chun Shen, “Multimessenger heavy-ion collision physics,” *Phys. Rev. C* **105**, 014909 (2022), [arXiv:2106.11216 \[nucl-th\]](#).
- [32] Jean-François Paquet, Chun Shen, Gabriel S. Denicol, Matthew Luzum, Björn Schenke, Sangyong Jeon, and Charles Gale, “Production of photons in relativistic heavy-ion collisions,” *Phys. Rev. C* **93**, 044906 (2016), [arXiv:1509.06738](#)

- [hep-ph].
- [33] Niklas Götz, Anna Schäfer, Oscar Garcia-Montero, Jean-François Paquet, Hannah Elfner, and Charles Gale (SMASH), “Out-of-equilibrium photon production in the late stages of relativistic heavy-ion collisions,” *Phys. Rev. C* **105**, 044910 (2022), [Erratum: *Phys.Rev.C* 109, 049901 (2024)], [arXiv:2111.13603 \[hep-ph\]](#).
 - [34] Peter Brockway Arnold, Guy D. Moore, and Laurence G. Yaffe, “Transport coefficients in high temperature gauge theories. 1. Leading log results,” *JHEP* **11**, 001 (2000), [arXiv:hep-ph/0010177](#).
 - [35] Peter Brockway Arnold, Guy D Moore, and Laurence G. Yaffe, “Transport coefficients in high temperature gauge theories. 2. Beyond leading log,” *JHEP* **05**, 051 (2003), [arXiv:hep-ph/0302165](#).
 - [36] Raktim Abir and Abhijit Majumder, “Drag-induced radiative energy loss from semihard heavy quarks,” *Phys. Rev. C* **94**, 054902 (2016), [arXiv:1506.08648 \[nucl-th\]](#).
 - [37] Chathuranga Sirimanna, Shanshan Cao, and Abhijit Majumder, “Final-state gluon emission in deep-inelastic scattering at next-to-leading twist,” *Phys. Rev. C* **105**, 024908 (2022), [arXiv:2108.05329 \[hep-ph\]](#).
 - [38] Andreas Schafer, Xin-Nian Wang, and Ben-Wei Zhang, “Multiple Parton Scattering in Nuclei: Quark-quark Scattering,” *Nucl. Phys. A* **793**, 128–170 (2007), [arXiv:0704.0106 \[hep-ph\]](#).
 - [39] Xiao-feng Guo and Xin-Nian Wang, “Multiple scattering, parton energy loss and modified fragmentation functions in deeply inelastic e A scattering,” *Phys. Rev. Lett.* **85**, 3591–3594 (2000), [arXiv:hep-ph/0005044](#).
 - [40] Xin-Nian Wang and Xiao-feng Guo, “Multiple parton scattering in nuclei: Parton energy loss,” *Nucl. Phys. A* **696**, 788–832 (2001), [arXiv:hep-ph/0102230](#).
 - [41] R. E. Cutkosky, “Singularities and discontinuities of Feynman amplitudes,” *J. Math. Phys.* **1**, 429–433 (1960).
 - [42] <https://pdg.lbl.gov/2022/tables/rpp2022-sum-quarks.pdf>, (2022).